General Response:

We thank the Referees for their time to provide comments and feedback on the manuscript. We have edited the manuscript to address and incorporate their suggestions. In many cases, we realize that the clarity of our writing could be improved to address comments where the Reviewers had to make assumptions about technical details of our technique. We think that the manuscript contents are now clear, reflect the necessary corrections, and that the work is improved to a state we think meets the expectations for publication in Atmospheric Measurement Techniques. Our responses to specific comments from the Reviewers below are highlighted in yellow, while additions and alterations to our manuscript (or in cases where we are redirecting concerns to existing discussion) are highlighted in green with **added text bolded** below for additional clarity.

Anonymous Referee #1

In the manuscript by Lao et al. the development and characterisation of a portable calibration source of HONO is described. The generation of HONO is based on a former source developed by Febo et al. (1995) and which is based on a reaction of gaseous humidified HCl with solid sodium nitrite. In contrast to the former study HCl is produced by a modified custom-built permeation source and the sodium nitrite is simply deposited on a PFA reaction tube. Although the source produces lower HONO levels than demonstrated in the former study by Febo et al., I have several concerns with the manuscript.

We thank the Reviewer for their thorough and considered comments on our manuscript. Many of the major concerns seem to have arisen from a lack of clarity which we have attempted to rectify throughout the manuscript. In a number of instances, the Reviewer has overlooked significant sections of our submitted work that address the concerns expressed in their comments and we have made significant effort to draw their attention to our existing discussion below, with changes made to the manuscript where improved clarity was beneficial to resolving the expressed concerns.

Major Concerns:

1) Calibration source

While I realize that the source can produce more or less constant HONO levels under certain conditions (see below) this is not a calibration source. If you want to use this source e.g. to calibrate a new HONO instrument, you need another instrument to characterize the source before under fixed experimental conditions. Even the HCl concentration cannot be used to calculate the expected HONO level because of the parallel “H2O reaction”, see below. Thus a HONO source is described here but not a calibration source! A calibration source could be e.g. the HONO source by Taira and Kanda (1990) using known Henry’s law coefficients of HONO in the acidic bubble solutions and measured gas and liquid flows (NaNO2/H2SO4).

The point of the Reviewer regarding appropriate use of nomenclature is understandable and we are disappointed that they find our terminology misleading. However, first principles considerations suggest that the use of the word calibration in their example is also incorrect. Calibration refers to determining the response of an instrument when detecting a known quantity of an analyte. The method by which a given quantity of analyte is determined therefore must exist for all calibration approaches. The NaNO2 concentration and H2OS4 concentrations, in the example provided by the Reviewer, would have to be validated against a primary standard or be prepared as primary standards themselves, as evidenced in the report provided by the Reviewer below where they reported use of ion chromatography with UV-Vis detection for just such a purpose (Kleffmann et al., 2004). Further, uncertainty in the Henry's Law coefficient for HONO, and the flows of the NaNO2 and H2SO4 solutions would need to be propagated into determining the HONO quantity generated by the calibration approach suggested by the Reviewer. All calibrations are subject to uncertainty in the analyte quantity and require validation against some benchmark. Thus, validation of analyte concentrations completed in the laboratory by a NOx analyzer prior to use in the field for our HONO source, or the aqueous solutions the Reviewer suggests, are synonymous calibration approaches. Notably, without the need to quantify the emission rate of HCl from a permeation device (or to use a cylinder or thermostated bath of HCl in the field), generating HONO from water vapour and a coated NaNO2 reaction device in our work reduces the complexity of this task, as the NOx impurities can be ignored in the absence of requiring mass balance between HCl delivered versus HONO produced.

2) Stability of the source:
Already in the title the stability of the HONO source is high-lighted. However, when looking into detail to the study, I cannot see this stability, which is much lower than in the original study by Febo et al., but also lower than in several other studies.

The Reviewer is concerned with the claim that the presented HONO source output is stable, contending that it is not so. We feel that several sections of our manuscript (See Sections 3.5 and 3.6)) have been overlooked by the Reviewer to suggest our HONO source is not reliable. The section discussions are comprehensive in the manuscript to guide the community on how to achieve stable output, along with some advice on issues that may be easily overlooked (e.g. transient 'burbs' of HCl from permeation devices) when attempting high accuracy calibrations. We rebut these points in detail here and indicate changes where we believe clarity in the text can be improved.

We reiterate the stability statistics quantified by four separate research grade instruments all validated to measure HONO accurately to demonstrate the stability of our methodology, from Lines 471-481:

'Three trials using newly coated NaNO$_2$ reaction devices and PD-6a, once stabilized, generated an average HONO output of 2.28±0.58 ppbv, which corresponds to an RSD of 24 % between runs and an RSE of 3% (n = 2367; Figure 3). The noise observed in the stabilized HONO output in Figure 3 can be primarily attributed to the noise associated with the NO$_x$ analyzer detector (18 of the 24 %; DL = 0.4 ppbv; 1-minute average). This conclusion is supported by the lower noise in ~2.5 ppbv HONO mixing ratios observed by the CIMS (Fig. 2, RSD of 8.1%), ACES (RSD 8.2 %), and NO$_y$O$_3$ (RSD 1.9 %). In these added observations with higher sensitivity instrumentation, the stability was equal to instrumental precision. This represents a major improvement over our previously reported calibration sources with potential for 30 % variability at a minimum (VandenBoer et al., 2013; Zhou et al., 2018).'

Already the HCl production of the permeation source is not very stable and the variations are not well described, cf. e.g. Fig. 4a and Fig. S7. Also when you compare the HCl emission of the different PDs listed in Tab. 1, 2, 3 variations are observed which are much larger than the specified singles errors. E.g. In Tab. 1 the source PD-6a emits at 40 _C 0.21+-0.01 ppb HCl, whereas in Tab. 2 and Tab 3 0.08+-0.002 ppb and 0.33+-0.007 ppb are listed? What are the reasons for this variability?

We thank the Reviewer for bringing up these important points. The figures mentioned here are presenting HCl emissions where we are rapidly altering conditions, such as temperature (Fig. S7), to demonstrate the time required to regain stable output (e.g. see error bars on Fig. S6). In Figure 4a, we are showing transient issues in the use of permeation devices, which are not captured from standard certification practices for their emission rates and may affect calibration accuracy when using the permeation device approach to produce higher mixing ratios of HONO on the order of several ppbv. We did not present any plots of the stable output for our devices, as a straight line of 0.21+/-0.01 ppbv is not highlighting any issue of significance. For these reasons, it is understandable that the Reviewer feels that there is a conflict in the presentation of the use of the HCl permeation devices. It was indeed our intention to highlight some of the unexpected results we encountered using them, which we wish to present to the community transparently.

Overall, it is important to note the issues when using custom permeation devices in a HONO source. Their emission rates do change over time, such that they are not solely dependent on the concentration of solution used, the surface area and thickness of permeable polymer, and the temperature (O'Keeffe and Ortman, 1966; Susaya et al., 2012). Therefore, we do not expect every custom permeation device we make to always have the same emission. This is broadly true for commercial permeation devices and includes larger emission uncertainty (see excerpt from manuscript below). Reliance on certified commercial devices comes with both a large cost (~hundreds of dollars) and time investment (~6 weeks) so that emission rates can be determined by mass difference, with the emission rate values having much higher uncertainty due to the indirect nature of quantifying the active compound.

We addressed the variability in our custom HCl permeation device emission rates, including relevant context to commercial options, in detail in Section 3.3, including Table 1 and Lines 379-391:

'Two newly made 6 M HCl PDs (-6b and -6c) were found to emit different, yet highly stable (e.g. ±0.01 ppbv), mixing ratios at identical oven temperatures (Figure S6). This demonstrates potential variability with each new device due to inconsistent results during custom fabrication compared to commercial PDs. The most likely source of such differences in output is variability in our sealing of the PTFE plugs resulting in increased emission rates. In any case, the PDs remain stable with less than 10 % relative standard deviation. In comparison, commercial device emission rates are often certified within ±30 %. The emission rates of commercial PDs are certified through measurement by gravimetric weight loss over time (ng min^{-1}). A commercial ¼" (64 mm) Teflon HCl PDs of 6.55 M certified to emit 1905 ± 520 ppbv in 100 sccm flow at 40 ˚C (RSD = 27.3 %; VICI Metronics, Inc.; Poulsbo, WA), has this output variance due to the co-emission of water and propagated measurement uncertainties. A lower variance in the emitted HCl was observed from our custom-made PDs when we quantified HCl directly by either CRDS or IC-CD. Custom-built PDs were therefore chosen over commercial PDs due to their demonstrated stability and low cost.'

We have also highlighted the reasons for the variability in the output of a single permeation device in the manuscript, which the Reviewer seems to have missed. We discuss the observed decline in the output of PD-6a in detail, with reference to existing literature, at Lines 392-400:

'It was found that HCl outputs of the custom-PDs slowly diminished over time, which emphasizes the need for regular calibrations. For example, the HCl output from two-year-old PD-6a emitted 0.21±0.01 ppbv in 1.1 SLPM in comparison to 2.0±0.01 ppbv when it was newly made, which decreased the resulting HONO generation in the reaction device. Similar results have been observed in calibrations with PDs of aqueous NH_3 and HNO_3 solutions decreasing by ~30 % during two years of storage, as well as for carbonyl sulfide (Fried et al., 1998; Neuman et al., 2003). Despite the decreasing HCl output over a year or more of use, HCl PDs act as a stable acid source on the order of weeks, producing consistent HCl output to subsequently generate stable HONO, even when removed from the permeation oven or stored for up to two months.'

Therefore, we feel that further manuscript additions to explain that the same temporal decline in emissions accounts for the continued decrease in emission of HCl from PD-6a presented in Table 2 is not necessary. The emission rate quantified in Table 3 clearly pertains to the section of the manuscript presented above. We feel that this is clear in the main body of the manuscript and have not made modifications.

However, we have added additional text to the conclusions to highlight to the reader best practice when using custom-made HCl PDs at Lines 735-737:

‘**Custom-made HCl PDs are prone to variability in emission rates, both between similarly made PD and over time, and therefore require regular characterization, but can provide a stable output over the order of weeks**’.

Also the stability of the HONO source is very low. E.g., it takes more than 24 hours until the source produces stable HONO, see Run 1 in Fig. 3.

This comment is confusing as the Reviewer seems to have issue with the rate to which a stable output is reached, and not the stability characteristics of the HONO output itself, which we have already addressed above. The Reviewer has missed a clear explanation of the observation in our discussion at Lines 470-473:

‘The time required to achieve stable HONO signals was tested by inserting HCl PD-6a and new $NaNO_2$ PFA reaction device into the calibration system, followed by flow start up. Stable HONO signals were observed within 7 h of powering on the HONO calibration system. This is 5 h longer than required to reach stable mixing ratios for a previously stabilized $NaNO_2$ device.’

The device reached stable output within 7 hours, not 24 as the Reviewer suggests, and this is clearly stated in Section 3.5. We depict 24 hours of data in Fig. 3 to show the stability of the HONO produced and how an identical HONO output is rapidly reached with a number of freshly coated NaNO2 devices. In the best example, this is reached in 2 hours for Run 3. We also state here that when an NaNO2 device is stabilized once, that it can produce stable HONO output again within 2 hours of starting the system henceforth. There is an entire section of our manuscript devoted to this (Section 3.6) and it is clearly depicted in the 8 runs presented in Figure 5.

To improve clarity, we have changed our reference to the ‘runs’ presented in Figure 3 to now state ‘device’ and added a vertical dashed line to the figure to highlight where the output of all three coated NaNO2 devices are at the same stable HONO output (determined statistically), as described in the discussion, to improve the connection of our discussion to the figure. We present the revised figure and caption here:

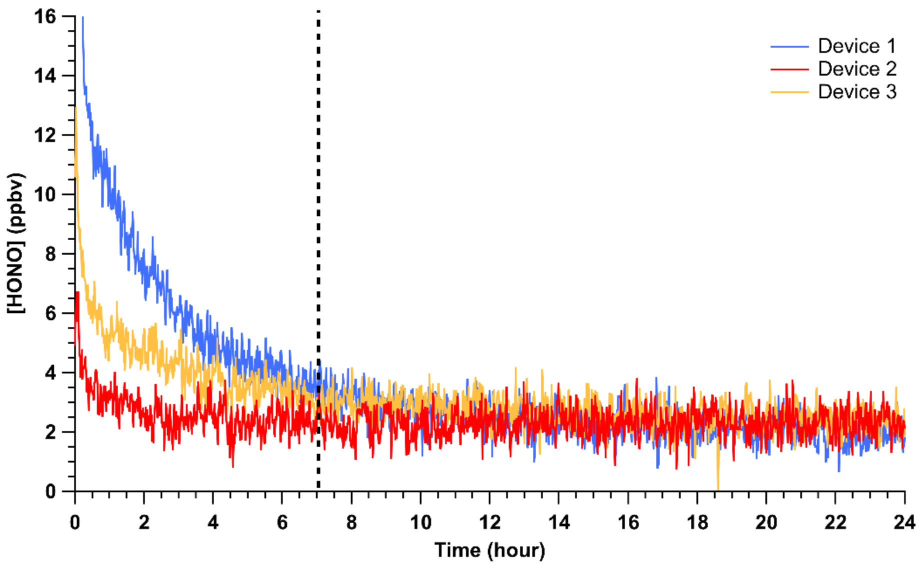

Figure 3. Mixing ratios of HONO observed using HCl PD-6a and three different, but freshly coated, $NaNO_2$ PFA reaction devices. Time zero indicates the start of HONO production in the calibration unit where no prior flow through the calibration unit existed, but all temperatures were stable at 40 °C. **The vertical dashed line denotes the time where the output of the three devices are no longer statistically different from each other.** Reported measurements are one-minute average data with a 30 s Kalman filter on the NO_x analyzer.

Or why is the HONO source so unstable over 90 hours in Fig. 4b? These spikes are not really well explained and do not completely disappear even after long running time (see Fig. S10, Run 2).

Here again, we cannot provide more information than the extensive section of the manuscript that has already been written to discuss this from Lines 492-498 and 508-517 (our emphasis added in bolded italics below):

‘However, when the HCl output from PDs is unstable, this can interfere with the stability of the HONO generated because it is dependent on acid displacement. A common characteristic of our custom-PDs monitored by real-time CRDS measurements are short-duration increases in output over min, up to 1 h, due to reduced emission of H_2O and increased emission of HCl, resulting in transient pulses from the device (Figure 4a). The anticorrelation between HCl and H_2O is expected for a constant mass emission to result from the contained aqueous solution. A corresponding rapid increase in HONO production results from such occurrences (Figure 4b).

Commercial PD manufacturers evaluate average mass emission rates by gravimetric weight loss over several weeks at 40 °C for certification, which could include such short-term events. The HONO output from a newly made custom-HCl PD (PD-6c) over four consecutive observation periods upon insertion of a new $NaNO_2$ reaction device (Runs 1 – 4) at constant temperature (40 °C) show that the new custom-PD requires about 1 week of operation before its output is stable (Figure 4b-c). Therefore, careful preparation of PDs and $NaNO_2$ reaction devices in advance of extensive use will yield a HONO calibration source with the fastest stabilization times possible for continuous operation over a period of months. ***Note again, that the HONO measurements for Figures 5b-c were performed several months before the HCl emission rate for PD-6c presented in Table 1 were obtained, resulting in high HONO mixing ratios produced in these experiments.’***

The comment regarding Figure S10 is explained, from the newly prepared nature of the custom permeation device, in the main body of the manuscript from Lines 577-584, where it is referenced:

‘We next tested the reproducibility for newly made HCl PDs. Two experiments used PD-6b, containing 6 M HCl (Figure S10). After a period of stabilization, the two experiments generated similar HONO mixing ratios (2.58±0.43 ppbv after 25 hrs, RSD = 16.5 %, RSE = 1.43 %, n = 792). The spikes in HONO output at 15 h and 21 h in the second experiment (green trace, Fig. S10) were likely due to pulses of HCl which we commonly observed with new PDs (e.g. Fig. 4a-b). This emphasizes our recommendation that new custom-HCl PDs should be used for an extended period prior to use for acid displacement to ensure the emission rate has stabilized.’

And even when the source is running for long time a variability of the HONO emission of 24 % is specified (see Figure 5b and line 525). This means that even when the HONO source is calibrated with very high accuracy by an independent method before (e.g. by precise NOy-measurement using chemiluminescence and a carbonate denuder) than the uncertainty of a field calibration using the source is only +-25 %. This is not sufficient for many applications, when e.g. daytime levels of HONO are compared with calculated PSS levels under urban conditions, when the PSS is only a factor of two lower than measured values (in this case the uncertainty of the “unknown daytime source” would be +-50 %!).

We have already addressed this comment above. As we demonstrate in the manuscript it is quite possible to achieve less than 10 % variance between restarts of the instrument, yet we report 24 % as a lower limit of the system performance based on our experience and the use of a low precision instrument (NOx analyzer, DL = 0.4 ppbv). We note here, and throughout the manuscript, that no field-deployed gaseous HONO calibration sources from the recent literature have achieved such performance; they all rely on laboratory calibrations that have similar uncertainties on the order of 25 % when validated against an external orthogonal method (McGrath et al., 2019; Peng et al., 2020; VandenBoer et al., 2013; Young et al., 2012; Zhou et al., 2018). The use of aqueous nitrite standards has long been the method of wet chemical instrumentation, resulting in high precision, but these do not represent overall method accuracy. The total instrument accuracy would necessarily include an inlet addition of HONO, which is not standard practice (Afif et al., 2016; Crilley et al., 2019; Pinto et al., 2014; Ren et al., 2011; VandenBoer et al., 2014). Even the gold standard of differential optical absorption spectroscopy relies on a calibrated cross-section determined using long-duration observations of HONO from the Febo *et al.* (1995) calibration source at high mixing ratios, to minimize error (Stutz et al., 2000). To our knowledge, there are no reports of HONO calibration sources in the literature that achieve better than 25 % accuracy performance at environmentally relevant levels. We note that most reports HONO measurements report variance in the measurements without including the accuracy of the measurements themselves. This is certainly a concern for the HONO community in assessing the HONO PSS.

Regarding stability of HONO production we note here, prior to the additional comments from the Reviewer below, that Febo et al. (1995) do not specify the averaging time for their reported stability numbers. Based on the instrumentation used, the mixing ratios (e.g. Fig 3 at ~ 7 ppmv!), and the presented data, we have concluded that the reported variance is most likely based on 1 minute measurements averaged over at least 12 hours, for which our % RSE values of 3 % on similar timescales compare very well given the >3 orders of magnitude lower mixing ratios we measured. Thus, the system presented in this work not only provides stable HONO mixing ratios but does so at considerably lower levels of environmental relevance.

The original source by Febo was much more stable and could also in theory be tuned to lower HONO concentrations by using more dilute HCl solutions (not tested in Febo et al., but works). Also the simple source by Taira and Kanda is much more stable and shows precisions of a few percent. This source was further modified by using a temperature controlled stripping coil and also shows much higher stability (see https://qumashop.de/images/LOPAP%2003%20HONO%20Source%20short_v2.pdf). I used this source during the FIONA intercomparison (http://euphore.es/fiona/fiona.html), which is a 19" instrument producing stable low HONO levels (ca. 1 % precision in the low ppb range) in a few tens of minutes which can be quickly and exactly tuned in a few minutes simply by changing the nitrite solution.

We note that as we are using permeation devices, which always require calibration or certification, that the resulting system is much safer and simpler to use over mixing liquid solutions of acid. We choose to use permeation devices as they are portable and easy to use in the field and have been successfully used for field calibrations of numerous other compounds (Veres et al., 2010; Washenfelder et al., 2003). Neither the method of Taira and Kanda (1990), nor the modified version published by the Reviewer below (Kleffmann et al., 2004), (1995) has achieved wide use in the atmospheric chemistry community (compared to that of Febo *et al.* (1995)), presumably due to the need for a peristaltic pump and custom glassware or the cost of the commercial unit from QUMA mentioned. Further, the mixing ratios of HONO generated by the Taira and Kanda (1990), Kleffman *et al.* (2004), and the Febo *et al.* (1995) approaches are often much higher than found in the ambient environment. These require several expensive and power-demanding gas pumps, mass flow controllers, and dilution to reach single parts per billion mixing ratios and have not been demonstrated to reach sub-ppbv levels except by us (VandenBoer et al., 2013). From our personal experience with our own sources, the output was not stable within 25 % across multiple days and also required independent verification of the output by a gold catalyst NOy instrument (calibrated for NO and NO2 conversion independently with a certified cylinder) or ion chromatograph in order to accurately calibrate instrumentation to better than 10 % for use in either the lab or the field (McGrath et al., 2019; VandenBoer et al., 2013, 2015; Zhou et al., 2018). We emphasize again our goal of developing robust instrumentation, which means that all instances of moving parts should be avoided, chemical safety hazards minimized (i.e. no bulk solutions), and the resulting system should be easily assembled and operated by users with a wide range of expertise.

Since the QUMA calibration source performance is a personal statement on observations that have not been subject to peer-review, we can only congratulate the Reviewer on their modified source performance and encourage them to publish this work and the results of the FIONA intercomparison. We have investigated the published work referenced by the Reviewer below that is related to this major concern, which reports a modified source that was capable of generating 30-770 ppbv of HONO. However, the rapidity of the transitions, precision, and accuracy of the output are not provided in the manuscript (Kleffmann et al., 2004). The output of the reported source in the work of the Reviewer was quantified by ion chromatography, a technique used in nearly all our prior work with HONO calibration sources (e.g. VandenBoer *et al.* (2015)), from which the accuracy is regularly on the order of 15 % when robustly assessed. Given that our source is stable to the precision of all instruments that measure its output at ~2 ppbv with a relative standard error of 3 % within 2 hours (120 minutes, comparable to 'tens of minutes') of being turned on, as stated above, perhaps analysis of our source output with higher precision instrumentation will be the subject of a future intercomparison, as we suggest in the Conclusions. We note here that adjusting the calibration mixing ratios with mass flow controllers in this system respond on the order of seconds, as has been well-established in our prior work (Roberts et al., 2010; VandenBoer et al., 2013). The versatility in changing output by orders of magnitude that the Reviewer is concerned with requiring a few hours is not a major trade-off. Our source inherently produces HONO at much lower mixing ratios than any others to date, such that the need for such adjustments is an infrequent demand. In response to further comments from the Reviewer below, we have made an addition to the Conclusions of the manuscript to note that the four channels in the Al-block of the permeation oven can be used to operate parallel HONO source channels and addressing the 'tunability' concern further.

We have added this excellent point to our discussion at Lines 723-725:

'**The HONO calibration source was designed to facilitate multiple calibrant concentrations, as the four holes in the aluminium heating block (Fig. S3) allows for the operation of parallel HONO sources if desired.**'

We would like to emphasize a formal point regarding peer review: existing published literature should be used to support concerns in our work submitted for review in Atmospheric Measurement Techniques over the Reviewer's opinion or unpublished results on their preferred calibration source, where a conflict of interest with a commercial product not widely used by the HONO community seems to also exist.

3) Purity of the source: In the present study a purity of >90 % is mentioned and impurities of NO of 5.5%/6 % are specified (lines 656 and 658). Typically NO impurities are formed by the bimolecular decomposition of HONO on surfaces producing equal amounts of NO and NO2 (R3). Thus for me at least the NOx impurities are higher than 10 %, which is much higher than in the original paper by Febo et al. where NOx impurities of <0.5 % were determined at <20 ppm.

As the Reviewer rightly mentioned, Febo *et al.* (1995) found that <0.5% of the HONO signal (<20 ppmv) was a NOx impurity and was attributed to R3. In our system, R3 cannot account for the observations of NOx. In Section 3.7.3, where we specifically address the purity of the HONO source, the HONO output was 770 pptv. If we assume that the impurity from R3 is linear at these lower mixing ratios, i.e. that 0.5% of the HONO signal is NOx due to R3 (as an upper limit), we would expect a NOx impurity of 3.85 pptv due to R3. This is notably lower than what we measured. If we take the high sensitivity NO measurements (Rollins et al., 2020), as this was the instrument with the lowest detection limit, we observed 42 pptv of NO, or 5.5% of the total HONO, well above that predicted due to R3 from Febo *et al*. The bimolecular decomposition reaction (R3) requires sufficient levels of HONO to be able to react with itself. We note that the HONO mixing ratios in the current work are 2-3 orders of magnitude lower than previous work (e.g. Febo *et al.* (1995)). Due to the second-order nature of this reaction, it may be that the levels of HONO are so low that R3 is not significant due to the square dependence on the number density of HONO, making our concentration-independent scaling for the upper-limit estimate presented above a very conservative estimate. As we observed higher levels of NO than expected from the upper limit calculation, it points to additional chemical pathways affecting the purity of the HONO output sources capable of reaching the sub-ppbv range, as stated at Lines 685-690.

Thus, the best way to constrain the NOx impurity is through measurements. Using multiple instruments, no NO2 impurities were observed in any of our experiments, even where NO was above the NOx analyzer detection limits (e.g. NaNO2-coated denuder tests). Despite these observations, we again provided a conservative perspective on our assessment of source purity by utilizing the measurements of the ACES platform which has higher precision and accuracy than our NOx analyzer. Thus, the potential NO2 and NO impurities from our source were found to be less than or equal to 10 % of the total HONO, with the limit set by the precision of our instruments at the low mixing ratios generated, see Lines 668-673:

'The I^- TOF CIMS is not sensitive to NO or NO_2, so further measurements were made with our Mo-catalyst NO_x analyzer, a cavity-enhanced absorption spectrometer (Min et al., 2016), and a gold-catalyst NO_y instrument (Fahey et al., 1985; Fontijn et al., 1970; Ridley and Grahek, 1990; Ridley and Howlett, 1974; Ryerson et al., 1999), which determined that NO_2 impurities were at or below 10 % of the generated HONO based on the detection precisions of the latter two instruments.'

We acknowledge that the stated purity of the system described in the current work is lower than stated in Febo *et al.* (1995), but as we were aiming to build a field portable and robust HONO source at atmospherically relevant concentrations (i.e. sub-ppbv), we feel that the trade-off in potentially higher NOx impurities is more than compensated for by the ease of using this instrument in the field.

To clarify this point, we have added the following text to the conclusions at Lines 729-732:

'**The purity of HONO source was determined to be >90%, and while lower than previous work (99.5%, Febo *et al.* (1995)) this may be a consequence of previously unseen side reactions of increasing importance at the low HONO mixing ratios generated. We consider this an acceptable trade-off for a robust field deployable HONO source unit.**'

And we have changed the description of our purity spanning 90-99 % at Lines 21-22 in the abstract to read:

'The calibration source developed in this work can generate HONO across the atmospherically relevant range and has high purity **(>90 %)'**

Also the loss of HCl is not negligible. There is a clear small Cl- signal in Figure 2 with the source on (I expect this is of the order of few percent of the HONO level, please expand the Cl- signal). In contrast the simpler source by Taira and Kanda will not show HCl emission, since non-volatile H2SO4 can be used.

With regard to the loss of HCl, from Fig 2, the Cl (m/z 35) counts were 37 ± 12 compared to 1100 ± 135 ncps for the HONO signal when the gas exiting the source was sampled, and so the Cl signal represents 3±1 % as an average breakthrough using the one sigma uncertainties to arrive at a worst-case estimate. The m/z 35 counts during the HONO measurement were indistinguishable from the zero measurement, which gives a 3-sigma detection limit of 39 ncps at m/z 35. We concluded that no detectable, let alone quantifiable, HCl was exiting the calibration source.

This is further supported in the mass balance experiments discussed in our work in Section 3.4.1, where we observed no HCl exiting the source when using the CRDS which has a superior sensitivity (3 sigma detection limit of 5 pptv) compared to the CIMS. See Lines 437-438:

'No HCl was observed to exit the devices, indicating unit acid displacement efficiency and reaching mass balance.'

In order to avoid confusion from other readers, we have modified the discussion in Section 3.4.2 from Lines 454-457, which initially stated:

'The signal of Cl^- at m/z 35 remained constant near zero throughout this period, confirming again that the HCl from the PD was entirely consumed by the $NaNO_2$ reaction device throughout the measurement period, consistent with the experiments presented above where no HCl was measured by the CRDS.'

This section now states more clearly:

'The signal of Cl^- at m/z 35 **was below the detection limit** throughout this period, confirming again that the HCl from the PD was entirely consumed by the $NaNO_2$ reaction device throughout the measurement period, consistent with the experiments presented above where no HCl was measured by the CRDS.'

We also note also that the approach/reaction mechanism described by Taira and Kanda (1990) is not applicable to the approach presented the current work, as we used permeation devices to deliver the gas-phase acid required for the acid displacement reaction and therefore need a volatile compound (i.e. one cannot use dilute sulphuric acid in a PD). Even so, if HCl were to pass through the reaction bed it does not bias the ability to quantify the HONO output or the stability so long as the kinetics are constant. In addition, we have shown that the H20 mechanism is not possible to ignore at low HONO mixing ratio production and requires more attention to detail than the 'HCl in equals HONO out' strategy used in high-output HONO sources (Febo et al., 1995; Gingerysty and Osthoff, 2020; Taira and Kanda, 1990). We challenge the Reviewer's assertion that the source based on acid displacement of H2SO4 is simpler, as it requires a peristaltic pump, glass components to mix the liquid reagents and a solution of H2SO4, which all represent added complexity/hazard and reduce the portability and robustness of that calibration source for field use, particularly on mobile platforms.

4) Formation mechanisms: In the present study two formation mechanisms are identified, the "HCl-" and the "H2O-mechanism". While the acid displacement mechanism of HONO by the strong acid HCl is clear (see Febo et al.) the H2O-mechanism should be better characterised (see line 406: "beyond the scope of this work.") since this is the main reason for the low stability of the HONO source for the initial phase when the source is started (e.g. first 24 hours for Run 1 in Figure 3, or »40 hours in Figure 6, the final steady state level will be 5 ppb in Fig. 6, see HCl emission of PD-6c in Table 1). The authors propose that NaOH is formed when H2O reacts with the sodium nitrite (see line 405). However, I expect that they still have CO2 from their zero air generator which decrease the pH in the adsorbed water surface layers on the NaNO2 to pH = 5.5 at which the fraction of HONO to nitrite is ca. 0.5 % (see pKa of HONO) making small HONO emissions possible in the absence of HCl. With extended operation of the source the increasing amount of NaHCO3 and Na2CO3 formed on the surface will decrease the pH leading to lower HONO formation. This mechanism could also explain the much higher HONO emissions of the annular denuder compared to the PFA-tubes when using the same HCl permeation source (see the 6.2 ppb in Table 2 compared to the 24.5 ppb, see line 626, or the 400 -> 25 ppb in Fig. 6, when using PD-6c).
Only when this non-stable side reaction can be minimized there is a chance for a really stable and predictable (by [HCl]g) HONO source!

We did not use a zero air generator for generation of HONO in the calibration source, we used either zero air or nitrogen cylinders (at >99.998% purity). The zero air generator was used to provide dilution flow prior to instrument sampling.

We have clarified the description in the text from Lines 176-180, which now reads:

‘Carrier gas flow through the permeation oven **was** provided by a compressed cylinder of zero air or nitrogen (Praxair; Air Ultra Zero, 99.999%, AI 0.0UZ-K; High Purity Nitrogen, 99.998 %, NI 4.8, Toronto, ON) **but an in-situ zero air generator could also be used** (e.g. Aadco Instruments Model 747-10, Cleves, OH**; used only for dilution flows here**) providing 20 psi of pressure to control the flow entering a four-way ¼” (64 mm) Swagelok cross fitting.’

Furthermore, the water in the bubbler originates from a heated reservoir on our deionised water system, which is engineered with the explicit purpose of minimizing uptake of CO2. The deionised water was replenished regularly and would have been rapidly purged of CO2/CO3-/CO32- by the high purity gases used to generate HONO. Therefore, we expect that there should be very transient, but more often an absence of, CO2 entering the source. In either case, the amount would be insufficient for the pH to decrease with use. It is worth noting that the Reviewer is relying on the concept of bulk solution pH in this argument, which does not apply so readily to surface films and we caution them from making this extrapolation. Consequently, we do not think that a decrease in pH in the reaction device due to CO2 uptake is a viable alternative hypothesis to explain the mechanism we ascribe to H2O, nor does CO2 affect the stability of our source. We do not think the H2O mechanism is the cause of the instability of the HONO source when initially turned on, but rather due to the emissions from the PD stabilizing, which is typical for these devices.

We did think long and hard about the actual mechanism for the H2O mechanism but could not come up with anything plausible. Despite this, as the experimental evidence was strong, we wanted to share this finding with the community as this may negate the need for HCl (or indeed any acid) in a HONO source. Future work will explore the chemistry underlying the H2O mechanism.

Specific Concerns:
The following concerns are listed in the order how they appear in the manuscript.

Line 22: while 90% purity is possible, I do not see the 99% (see above)!

Please see our earlier response, we have edited this to read (>90 %)

Lines 42-43: HONO levels of up to 18 ppb have been determined in the Po-valley (Milan) in Los Angles and in Santiago de Chile.

We thank the Reviewer for the added locations where high HONO mixing ratios have been reported and have located the references we suspect they are aware of, but without the provision of the actual citations by the Reviewer. We apologize if a specific measurement they had in mind is not in the list. Regardless, this sentence is to provide an example – hence our use of ‘such as’ here - on the observed HONO levels in polluted environments, not to perform an exhaustive review of such observations.

We have updated the text to include the references we have found at Lines 42-45:

‘…to **18** parts per billion by volume (ppbv) in polluted megacities such as Milan, Los Angeles, and Beijing **(Elshorbany et al., 2009; Febo et al., 1996; Harris et al., 1982; Tong et al., 2016; Zhang et al., 2019)**.’

Line 46: Start with 2010a when using references by Veres et al. for the first time (and 2010b in line 113).

This is a known issue with the reference template for AMT used in the Mendeley software and is subject to correction during typesetting. We thank the Reviewer for their attention to detail.

Line 66: The study by Villena et al., 2011 is not on HONO?

Our apologies, we meant to reference the identification of HONO partitioning to fog and dew water to form nitrite, as observed by Rubio et al. (2009) where Villena was a co-author on that work, which would result in a particulate nitrite interference.

Line 80: A modified HONO source of the one by Taira and Kanda is missing (Kleffmann et al., J. Phys. Chem. A, 2004, 108, 5793-5799, see also link above).

We have not added the modified Taira and Kanda (1990) HONO source at this point in the manuscript as there is inadequate description of the modifications and performance of the system to make it suitable to include here. We have also not referenced the web links provided above as they are not peer reviewed materials.

Line 85: The advantage of the source by Taira and Kanda is that non-volatile dilute H2SO4 can be used bearing no risk of HCl emissions for incomplete acid displacement.

We have added a comment in the introduction to this effect when discussing this paper and the subsequent modification by Kleffmann et al. (2004) at Lines 96-101:

‘**An alternative approach that utilised dilute H_2SO_4 for the acid displacement reaction with aqueous $NaNO_2$ was outlined by Taira and Kanda (1990). While this approach was shown to generate a stable and tunable HONO output at hundreds of ppbv, it has not been widely adapted, likely due to the need for complex custom glassware and liquid flow control in the calibration apparatus and significant dilution to reach single digit ppbv mixing ratios (Kleffmann et al., 2004).**’

Line 104: The reason why the nitrite was stirred in Febo et al. is a) to minimize concentration peaks of HONO in channels in the nitrite powder to reduce the quadratic reaction kinetics of R3 and b) to increase the assessable surface area for complete acid displacement.

We have clarified this, and included the point on decomposition kinetics from the Reviewer, at Lines 109-112:

‘Further, to reduce the variability in HONO output over time, the powdered $NaNO_2$ bed requires continuous mixing to maintain equilibrium **between the adsorbed HONO and carrier gas flowing over the salt bed minimize the production of NO_x by R3**, as well as a Teflon filter to prevent loss of $NaNO_2$ powder by entrainment in the gas flow.’

Line 109-110: The stabilization of the original HONO source by Febo et al. takes much shorter than the present source (see Febo et al., 1995). When I used that source several years ago it took only ca. 1 hour to get stable HONO levels, e.g. when the temperature of the HCl bath was changed. And other sources are even faster (see major concerns).

The literature we are referencing here are ‘other systems using dispersed NaNO2’ which are not stirred (McGrath et al., 2019; Roberts et al., 2010; VandenBoer et al., 2013; Zhou et al., 2018). We have already addressed the issue about the stabilization time of our system being 2 hours above and refer the Reviewer back to our responses on their major concerns above.

Section 2.1 and 3.1: The coating procedure of the PFA tubes is not clear for me. In section 2.1 it seems that all the nitrite added by the 3 ml coating solution stay inside the tube until the solvents are completely evaporated. However in Section 3.1 only a small fraction of the nitrite is recovered. Where is the rest? Or is the solution decanted similar to the procedure used for the annular denuder (see line 158)?

We have carefully stated where we believe the losses of the nitrite from the coating solution are in our procedure in both of these sections and refer the Reviewer to our statements in these sections. The solution is not decanted. The nitrite from the applied solution is partly lost during the coating process due to the highly hydrophobic nature of the PFA tubing which we have stated in Section 2.1 (Lines 154: ‘to reduce solution loss while evaporating solvent’) and Section 3.1 (Lines 287: ‘… and the loss of liquid solution during the drying procedure…’). Some of the nitrite may also be lost as NO, NO2 or HONO during the drying procedure, but an experiment was not conducted to explore this as we only required sufficient nitrite to be available on the surface to facilitate HONO production.

Figure 1 and S3: Are each two holes (1/2”) in the aluminium block (see S3) used for one HONO source (1x HCl and 1x NaNO2, see Figure 1), i.e. can two parallel HONO source lines by used here?

Yes! As discussed in Section 3.7 of the manuscript, we have evaluated various combined options for adaptable HONO source outputs, either by increasing the available HCl (we tried temperature, but multiple permeation devices are also an implicit option; Section 3.7.1), and multiple NaNO2 devices (Section 3.7.2).

This is already stated at Lines 611-612:

‘The use of multiple HCl permeation tubes in a single oven, in series, or in parallel are additional options to control the HONO mixing ratio generated in the calibration system.’

Operating parallel calibration channels, as the Reviewer suggests, at 1-2 orders of magnitude higher or lower mixing ratios could be easily accomplished and using a larger Al-block with more holes could increase the versatility further.

We have added this excellent point to our discussion at Lines 723-725:

‘The HONO calibration source was designed to facilitate multiple calibrant concentrations, as the four holes in the aluminium heating block (Fig. S3) allows for the operation of parallel HONO sources if desired.’

Section 2.3 and S2: The set-up of the HCl permeation source is not clear for me. Is the 1/4” tube filled with liquid HCl inserted into a 1/2” PFA tube which is temperature controlled in the Al-block and flushed by the zero air? Is the smaller tube fixed in the middle of the larger PFA tube (how?) or is it simply lying on the ground of the larger tube? Please show a more detailed figure of the HCl permeation source.

The Reviewer has correctly identified how the HCl permeation source operates. This is the same as any commercial permeation source operates and does not warrant a more detailed figure.

However, for readers who are not familiar with commercial permeation ovens, we have clarified these specific details at Lines 205-207:

“During operation the HCl PD is placed within the ½” tubing in the heating block, through which the carrier gas is flushed.”

Line 209 and Fig.1: Why is the low HONO source flow rate of only 100 sccm used and later diluted to 1.1 slm? If the source should be tuned to high HONO levels (ppms, see line 664), the HONO concentration in these 100 sccm are 11 times higher leading to stronger decomposition of HONO by R3. Why not using 1.1 slm for the reaction?

The reaction to produce HONO relies on the complete heterogeneous uptake of HCl by the coated NaNO2 reaction device. Increasing the flow will potentially decrease the reaction efficiency. The mixing ratios in our HONO source are lower by a factor of 2000 compared to all other sources presented in the literature (Febo et al., 1995; Gingerysty and Osthoff, 2020; Taira and Kanda, 1990), and is therefore the least susceptible to the decomposition of HONO by R3. The HONO calibration community has widely used percentages of impurities to market the quality of their sources. However, we note that this leads to biased perspective as the absolute quantities of impurities scale with the amount of HONO produced. Regardless, we have addressed this issue in other responses to the major comments from the Reviewer above.

Line 214: Typically also 1 % glycerol is added to a coating solution of a denuder (see coating of the NaNO2 reaction devices, see line139)?

This is explicitly detailed in Section 2.1, which is titled ‘Coated NaNO2 Reaction Devices’ and specifies our approach. From Lines 145-150:

‘A $NaNO_2$ (EMSURE®; ACS Reag. Ph Eur, Germany) coating solution was made as a 20 g L^{-1} $NaNO_2$ solution. The coating solution solvent was composed of equal volumes of methanol (HPLC Grade; Fisher Chemicals, Ottawa, ON) and 18.2 MΩ·cm deionised water with 1.0 g L^{-1} glycerol (Sigma Chemical Company, St. Louis, MO, USA) to facilitate a uniform salt coating. The solution was made by dissolving the $NaNO_2$ in the water first, followed by the addition of the glycerol and then methanol.’

Section 3.2: caused by the non stable reaction by “H2O” (or CO2?) this side reaction should be minimized, see major concern. I cannot follow the statement in lines 335-337 – HONO production by this reaction is not defined and not constant, see Figure 6!

We acknowledge that more work needs to be done to understand this potential water-driven mechanism. We do not believe the reaction is caused by the presence of CO2. As stated in our response to the major concern of the Reviewer above, our compressed gases were ultrapure cylinders and our deionised water system minimizes the uptake of CO2. Figure 6 was produced using an NaNO2 coated annular denuder in the presence of HCl and it is not clear why the Reviewer is conflating this Figure, presented 10 pages later in the manuscript, with the results of the water reaction investigated in isolation with water vapour alone in Section 3.2.

We were able to isolate the water effect using the denuders, yet we also stated that these devices had unstable ouput which was not observed with the PFA devices. We have presented a robust mass balance analysis of the stability of this side reaction within PFA devices in Table 2, although the HONO quantities generated challenged our instrumental detection limits, leading to the denuder-based experiments.

Regardless, at Lines 646-648 we clearly state that the denuders generated very drift-prone HONO outputs when attempting to generate higher HONO mixing ratios:

'The major drawback of using an annular denuder is that the output drifted to lower mixing ratios continuously at a rate of a few ppbv per hour, which was not a feature of the PFA devices (Figure 6).'

Lines 350-353. For me the source is already unstable at 40 C, see peaks at 2 PM in Figure S7.

The Reviewer is incorrect that the variance in the output increases at 40 C. The time period they are referring to corresponds to 50 C. At this time off-gassing of HCl from the interior walls and fittings of the permeation oven is occurring. This has been described in the manuscript.

We refer the Reviewer to the following statements from the manuscript at Lines 362-367:

'The HCl output was found to be temperature-dependent and increased exponentially with temperature, as expected from theory (Section S2). However, as the PD was ramped to higher temperatures (> 50 °C) the permeation rate became more unstable, with a resulting settling time of about an hour as the materials from the permeation oven apparatus re-equilibrated (Figure S7). Since the HCl PDs were observed to be most stable at 30 °C and 40 °C, these temperatures were considered optimal to generate the stable HONO mixing ratios.'

To clarify the temperatures being used in Figure S7, we have added additional windows demarking the stable regions:

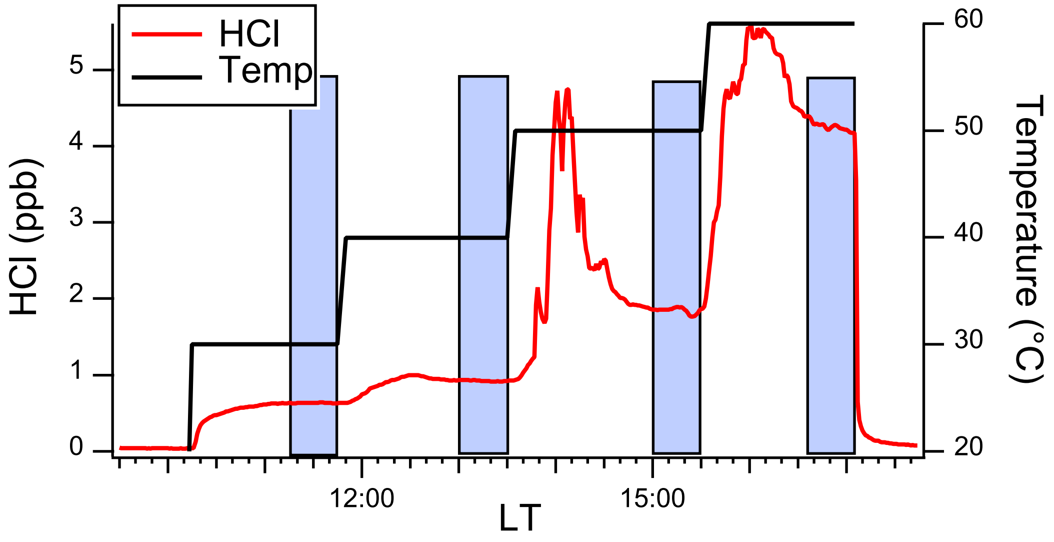

'**Figure S7**: Time series of the measured HCl output from PD-6b using CRDS**, as well as temperature of the oven**. The blue-shaded bars indicate the region where HCl output was considered stable and this data was used to calculate the variance shown in Figure S6.'

Table 1 and section S2: The production of the HCl tubes seems to be really “tricky” since similar tubes produce variable HCl emission by one order of magnitude! In addition the given errors of 0.01 ppb for the first three HCl concentrations are only a short term precision but not for longer time, compare data in Tables 2+3.

Yes, there is an art to sealing the PTFE rods in the end of the permeation tubes that can result in large variability. We have addressed these nuances in the manuscript and in detail to the HCl permeation device stability raised by the Reviewer in their major concerns above. We have also proposed an alternative method to potentially obtain reproducible emission results, in line with commercially available permeation devices, to encourage continued use of economical custom-built permeation devices.

Line 380-384: Why are the HCl emissions decreasing by one order of magnitude for a time period of 2 years? Is this in accordance with the expected decrease of the liquid HCl concentration (e.g. 6 M) from the loss of gaseous HCl? In addition, a 30 % decrease is not similar to an order of magnitude (2 -> 0.21).

Permeation device emissions are well known to decrease over time. The actual amount it decreases will depend on use, the quantity of the chemical species, and how well it is made. The 30 % came from another study using permeation devices ¼” in diameter compared to ours which are 1/8” and it may be that this particular PD decreased faster as they contain much less solution. We advise regular check on the permeation device outputs, which is standard practice for this equipment.

To clarify this point we have included additional text in the Conclusions:

‘**Custom-made HCl PDs are prone to variability in emission rates, both between similarly made PD and over time, and therefore require regular characterization, but can provide a stable output over the order of weeks**’.

Table 2: ADEs of only >55% and >84 % can be determined based on the given errors of HONO (e.g. 0.14/0.31: : :) and not >99%.

We measured the HCl exiting the reaction devices and could not detect it by our high sensitivity cavity ringdown system (Line 258: DL = 5 pptv; Lines 437-438: ‘No HCl was observed to exit the devices, indicating unit acid displacement efficiency and reaching mass balance.’) . The error of the HONO measurement is not required to then calculate the >99 % ADE values. Lines 437-438 noted above immediately precede this table and it is not clear how our approach can be clarified further.

Figure 2: The red shaded area is almost invisible during zero. In addition I do not see any blue shaded area?

The shaded blue region is rightfully difficult to discern as it is nearly the same width as the line. Numerically, it is 37+/-12 counts, and not above the CIMS detection limits for m/z 35, which we have presented above in response to another comment from the Reviewer.

We have increased the saturation intensity of the red shaded region in Figure 2 to make it easier to see in the zero regions and amended the Figure caption regarding the variance in the HCl trace:

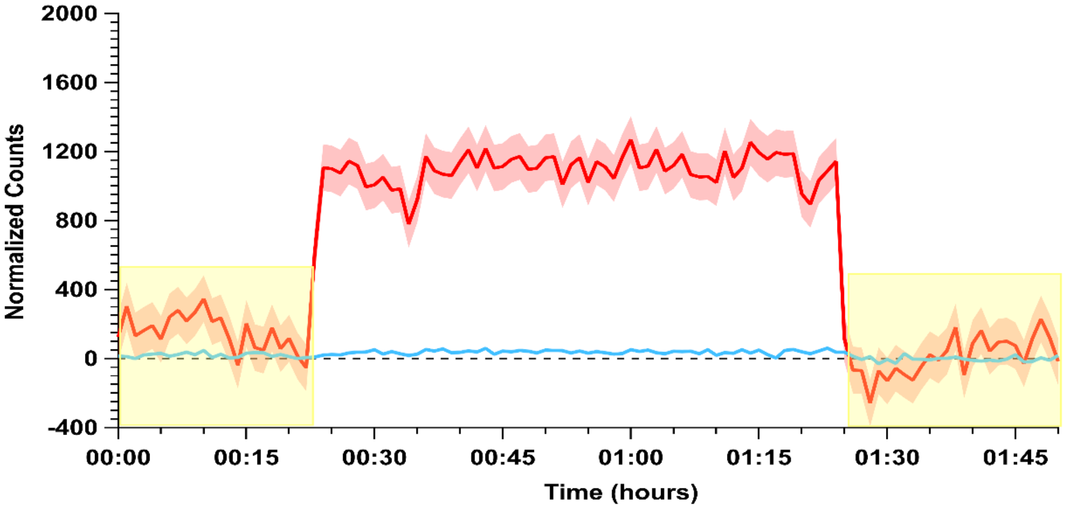

‘**Figure 2.** Conversion efficiency of HCl (blue) to HONO (red) via the acid displacement reaction on a $NaNO_2$ reaction device. The HCl PD-6a and one coated PFA device were used and measured following two hours of stabilization. The acids were observed by acetate quadrupole CIMS with time resolution of 0.50 s and averaged to 60 s. Yellow shaded regions indicate the addition of zero air to the instrument inlet for background correction, while red and blue shaded regions correspond to 1σ variance in the observations. **Note that the variance in the HCl trace is similar to the width of the line**.’

Line 458-459: That is not true for Run1 in Figure 3 (>24 h)

We have already addressed this misperception in a previous comment from the Reviewer and have revised the figure that was creating confusion.

Figure 3, 5, S9, S10, S12: Why do the authors not use a more precise HONO instrument or higher HONO levels? The precision of 0.4 ppb of the NOy monitor is too low to determine any dependencies at HONO levels of ca. 2 ppb. Typically the concentrations should be more than 10 times higher than the precision of the instrument used

We used a standard commercial NOx monitor for two reasons: 1) this is what we had available in the lab for quantification, and 2) we wanted to keep the system to be as low-cost as possible and use instruments that are widely available. Previous work has demonstrated that using a NOx monitor can give reliable measurements of HONO (Febo et al., 1995; McGrath et al., 2019; Zhou et al., 2018) but we do agree that we are limited by the precision of the NOx monitor. However, we note that we did use more precise instruments: BBCEAS, CIMS, and a gold catalyst NOy in this work to already address this limitation explicitly. In all cases, the uncertainty in the measured HONO from the source was equal to the instrument noise, which demonstrates that the uncertainty in the HONO source output was related more to the instrument than to the stability of the source (see first paragraph Section 3.5). We also note that we have applied statistical evaluation of the source output, consistent with the original work of Febo *et al.* (1995), by averaging the measurements over longer durations to get a more representative picture of the HONO stability.

Our approach is specifically designed to generated atmospherically relevant mixing ratios. It does not translate well to higher HONO levels, because we are limited by the concentration outputs of the permeation devices.

Line 477 and Figure 4: I do not understand the low stability of the HCl/HONO production (variability by factors, see Figure 4b: : :)? From where are these peaks coming even after 15 days of use, see Figure S10?

We have addressed this issue above in response to numerous comments from the Reviewer. We point out here that Figure S10 has time units of hours, not days, as the Reviewer states.

Line 501: should be "after" and not "before" or "Figure 4b-c"? In Fig 5 the output is more or less stable (+-25%...).

The Reviewer is correct that this should be 'Figure 4b-c' and we have corrected the typo.

Line 505-506: I cannot follow that statement, see major concerns.

We have addressed the major concerns and hope that the Reviewer can now follow these statements.

Line 563-565: Both data shown in Figure S10 are not stable (+- factor of 2) and I cannot follow the RSD of only 16.5%? Cf. the red data at 5, 10 and 37 h.

We addressed this concern in the responses above and do so again here. We refer the Reviewer to Lines 576-584:

'We next tested the reproducibility for newly made HCl PDs. Two experiments used PD-6b, containing 6 M HCl (Figure S10). After a period of stabilization, the two experiments generated similar HONO mixing ratios (2.58±0.43 ppbv after 25 hrs, RSD = 16.5 %, RSE = 1.43 %, n = 792). The spikes in HONO output at 15 h and 21 h in the second experiment (green trace, Fig. S10) were likely due to pulses of HCl which we commonly observed with new PDs (e.g. Fig. 4a-b). This emphasizes our recommendation that new custom-HCl PDs should be used for an extended period prior to use for acid displacement to ensure the emission rate has stabilized.'

Stability of the output was measured after 25 hours of operation in both runs, each with a new permeation device. We have already explained in the manuscript the source of the transient emissions of HCl from newly prepared permeation tubes as well.

Line 592: The relative stability of the HONO source is lower at 40 _C compared to 50_C see Table 3 (1+-0.5 = +-50% and 2+-0.5 = +-25 %). So I do not understand that statement?

We have rephrased to improve clarity:

'**Part of the** observed variability in HONO emissions at 50 ˚C was **contributed by the increasingly** unstable emissions of HCl at this temperature (e.g. see Fig. S6).'

Line 606-607 and Table 4: I do not understand the lower output of the quartz tubing? Normally quartz is hydrophilic and can be much better wetted by aqueous solutions than the very hydrophobic PFA, leading to higher expected nitrite levels for the quartz?

We agree that quartz is normally more hydrophilic than PFA, but we believe that this result was due to the poor coating of nitrite solution as was observed visually when making this device.

We are not sure why and we have adjusted the text at Lines 624-625 to read:

"The quartz tubing gave a notably lower HONO output compared to other materials. This may have been due to a poor coating efficiency on the surface**, as observed visually when making this device. This is an unexpected outcome given that quartz is more hydrophilic than PFA."**

Lines 624-630: The reason for the unstable and much higher HONO emissions (»[HCl]) is the higher surface area and the unwanted side reaction by "H2O" (or CO2?), see above

We agree that the higher HONO emissions with the annular denuder were due to the higher surface area and this is already stated in the first sentence of the last paragraph in Section 3.7.2, Lines 642-644:

'More HONO can be generated using the same PDs in conjunction with an annular denuder, which has a larger internal surface area of 3063 cm^2 compared to 388 cm^2 for the PFA device.'

Line 643-644: The source by Febo et al. was much more pure (>99.5%) than the present one (see 6 % NO = 12 % NOx, see R3 => purity 88%...).

This comment has already been addressed in detail in prior responses. The measurement of impurities at these very low levels is not trivial. For example, it is important to consider relative versus absolute purity of the gases measured when comparing techniques. The Febo source generated tens of ppmv, whereas our source generated a few ppbv of HONO. This means observing impurities in our source is i) more challenging to perform and ii) likely to arise from pathways other than HONO self-reaction (R3). For this reason, we used the highest sensitivity NO instrument developed to date to pursue this task, a pair of world-class NO2 instruments, and compared the observations from those instruments to our extensive NOx analyzer dataset to reach our conclusions. Given that all HONO sources must be validated for their output, the issue of purity was explored more for comparison to the literature rather than to verify the acid displacement assumption (i.e. moles of HCl in equal the moles of HONO out).

Line 662-664: While the former study showed impurities in the 10 % range at 4 ppm, this source shows similar impurities already below 1 ppb (see line 657), which is very untypical with respect to the quadratic reaction kinetics of reaction R3. And again in Febo et al. the purity was higher than 90% even in the ppm range.

We do not posit the HONO self-reaction of R3 to be the mechanism by which the observed NOx species are produced at the much lower HONO mixing ratios generated in our source. The mechanism must be something else. See prior responses for expanded details above.

Line 675: Should be <25 % see line 560?

The error here was writing RSD, which should have been RSE. This has been corrected in the manuscript.

Line 858: Processes

This suggestion is incorrect. The abbreviated notation we have applied is correct.

Line 887 and 902 Res. Atmos.

Corrected.

Line 988: 10155-10171

This is a formatting issue in the AMT template for Mendeley. The correction has been entered manually.

Line 993: 9093-9106

This is a formatting issue in the AMT template for Mendeley. The correction has been entered manually.

Line 999: delete the second Vecera, Z.

Corrected.

Line 1010: D23302

Corrected.

Line 1061: L15820

Corrected.

Line 1074: 1681

Corrected.

Supplement Section S1, second paragraph, line 5: should be 47 and 51 sccm, see Figure 1?

We have corrected this to read ~50 sccm.

Section S1, last paragraph before Figure S1: The temperature should be electronically limited to 150 _C (see harmful degradation products for PFA in the case of a malfunction).

We have added a note here regarding this advice:

‘An upper limit on the temperature controller should be set at 150 °C to prevent thermal degradation of PFA tubing in the Al-block during use.’

Figure S3: Why are larger hole diameters (0.6”) used in the Al block for the 0.5” PFA permeation source tubes? There would be better heat transfer, if the holes would be only slightly larger than the PFA tubes (e.g. 0.51”) getting them into direct contact with the aluminium.

The 0.5” for the PFA tubes in the permeation oven is their inner diameter and the external diameter is 0.6”. They fit very tightly in the machined holes to ensure firm contact for heat transfer.

We have added a statement to clarify this:

'The machined holes are the exact size of the outer diameter of the ½" PFA tubes, resulting in firm contact between the polymer and Al.'

Figure S7. From where do the peaks during the temperature ramps (40-50_C and 50- 60_C) result? There should be constant increases of HCl similar to the ramp between 30-40 _C?

See our response to prior comments above. The HCl is adsorbed on and in the PFA polymer, as well as the permeation oven fittings. When the temperature is raised, the HCl desorbs from the surfaces, while the permeation device emissions adjust slowly, resulting in the observed peaks.

Anonymous Referee #2

Lao et al. present the design of a HONO calibration source suitable for field use. The manuscript gives a detailed description of the design of the source and extensive information on its performance. The paper solves a challenge that the community currently faces, the lack of reliable HONO calibrations of in-situ instrument. It is thus timely and highly relevant.

Overall the paper is very well written and informative. It provides all the details needed for the community to reproduce the study and, most importantly, build their own HONO calibration source. I did not find any real issues with the manuscript, and my more detailed comments below are just requests for some minor clarifications. Overall, the manuscript is well suited for publication in AMT, and I recommend for publication after a few minor clarifications.

We thank the Reviewer for their comments and have addressed their requests for clarifications in our responses below and in the main manuscript.

- As water bath operates at 40C producing a RH of 50%, I am wondering if there is an issue with condensation once the air flow cools down while exiting the oven and/or instrument. This may be especially relevant if the system is used in cold climates. Could you please comment on this in the manuscript?

The impinger/bubbler to control the RH at 50 % operates at room temperature, not 40 °C (see depiction in Figure 1).

We recognize that this is not clearly stated in the description in Section 2.2 and we have clarified the text from Lines 185-189:

'The first critical orifice connects to the HCl PD channel within the heated Al block and the second connects to a 25 mL glass impinger (EMD Millipore Corporation, Billerica, MA, USA) containing deionised water **at room temperature**. The flows are combined and mixed to a **resultant** relative humidity (RH) of 50 %, which then enters the coated $NaNO_2$ reaction device **in the temperature-controlled Al block**.'

We appreciate the Reviewer's point about condensation and have also added text to caution against condensation at Lines 193-194:

‘If operating in cold environments, care should be taken to ensure the 50 % RH exiting the calibration system does not generated condensation in the lines.’

• Could you explain in the manuscript how you determined relative humidity? Was it measured or calculated from the saturation vapor pressure and the gas flows? In the latter case, did you check that the calculated RH is in fact correct?

We calculated the RH using saturated vapour pressure. We have clarified that it is the saturation vapour pressure and mixing of equal flows in the modified text at Lines 185-189 noted in the prior response by adding ‘**resultant**’.

We have measured this numerous times in the past for producing 50 % RH in HONO sources with loose salt beds, and given the reproducibility of this approach across several years of experimental work (MacInnis et al., 2016; McGrath et al., 2019; Roberts et al., 2010; VandenBoer et al., 2015; Zhou et al., 2018), did not repeat the measurements as part of this work.

• You mention that the system has been found to be stable for approximately one month. Could you clarify if this means that it yielded a constant HONO concentration for this time period, or was there a drift in the concentration due to aging of the NaNO2 reaction device?

Could you comment on whether the length of the tubing between the source and the HONO instrument (or NOx instrument) has an impact?

We thank the Reviewer for these comments. For the stability, at Lines 539-540 we report a constant HONO mixing ratio of 2.07 +/- 0.48 ppbv for the time period of a month. After 5 weeks, we observed the mixing ratios started to decline from the depletion of NaNO2 in one coated device.

We have added a comment on this at Lines 540-542:
‘These measurements used a single $NaNO_2$ reaction device over 5 weeks of continuous operation, after which the depletion of $NaNO_2$ resulted in a decline of HONO mixing ratios.’

From the range of NaNO2 mass coated on each device, we conservatively estimated that these would be stable for a month, using our observations with many additional coated devices producing stable HONO over periods of 4 weeks as a second justification that this was a sound estimate.

We have clarified this point in the manuscript at Lines 312-315:

‘In practice, **we observed** a PFA device generating **approximately** 2 ppbv min^{-1} of HONO to be reliable **for over four weeks** during experiments performed to test the stability and reproducibility of the PFA devices (Sections 3.5, 3.6).’

We are happy to comment on the impact of tubing length for the Reviewer. In general, adsorption effects in the very clean PFA lines of the calibration source are not an issue and are minimal on glass surfaces as well (VandenBoer et al., 2015). We cannot comment on losses to other tubing materials and HONO losses to inlets sampling ambient air have been noted previously (Zhou et al., 2002). The impact of the length of PFA tubing between the source and instrument depends on the temperature of the lines, residence time of the HONO, and the surface area to volume ratio. With decreasing temperature and increasing SA/V for a given residence time, adsorption losses of HONO to the surface would increase, but eventually equilibrate (likely on the timescale of minutes or less under most relevant operating conditions). Decreasing residence time of the HONO in the lines is the easiest approach to mitigate any potential losses and we suggest using the shortest lines possible leaving the calibration source prior to being diluted into a low residence time flow to deliver to instruments. If the calibration lines can be heated to > 30 °C, then line effects can be effectively nullified (VandenBoer et al., 2013).

Anonymous Referee #3

Lao et al. presented the design and detailed test results of a system capable of producing a wide range of concentrations of gas-phase HONO. The system is a modification to that by Febo et al (1995), based on displacement of nitrous acid from solid sodium nitrite by gaseous hydrochloric acid. The modifications include the uses of a custom built HCl permeation source and a NaNO2-coated tube (or denuder) for the HONO displacement to take place. These modifications indeed make the system more compact in size and easier to transport. The tests are comprehensive, the results are well presented, and manuscript is well prepared. The manuscript can be helpful for laboratories in constructing a portable HONO generation system for calibrating field HONO instruments and for atmospheric HONO chemistry research in the laboratory. However, I find following major issues with the manuscript:

1. Compared to the original design by Febo (1995), the system described in this manuscript offers more compact in size and is capable of generating lower HONO source at concentrations (sub ppb vs 5 ppb). However, there are no improvements in stability and reproducibility (∼24% vs <0.4%), and purity (>90% vs 99.5%) of the HONO source generation. The NOx analyzer used to quantify HONO output has a lower detection limit of ∼0.4 ppb. The poor signal stability of the NOx analyzer near its detection limit may in part be responsible for the not-so-great performance of the system.

We have previously addressed in detail the stability and purity of our source relative to the design from Febo et al. (1995) in our response to Reviewer 1, major comments 2 and 3.

We agree that we were limited by the precision and detection limit of our NOx analyser, and much of the apparent noise that we see from the calibration source we believe is due to the noise on the instrument used for quantification. The lack of comparability when using percentages is not surprising. Febo *et al.* (1995) measured their output stability with a NOx analyzer from a source generating dramatically higher HONO mixing ratios (on the order of ppmv). Thus, the relative variance can easily be lower than in our report as the absolute variance from the prior work is many ppbv. In terms of stability, as we note in our manuscript it is difficult to make a solid comparison to the prior work as the statistical handling of the data (i.e. averaging period) and measurement parameters (i.e. measurement rate, use of active filters) were not reported, but the stabilities are comparable using some reasonable assumptions. The stability of our source may even be better and this is demonstrated by the fact that the noise from the calibration source corresponded to the instrument precision of all devices that measured the HONO output rather than actual fluctuations in the output of the calibration source, as stated at Lines 476-481:

'The noise observed in the stabilized HONO output in Figure 3 can be primarily attributed to the noise associated with the NOx analyzer detector (18 of the 24 %; DL =465 0.4 ppbv; 1-minute average). This conclusion is supported by the lower noise in ~2.5 ppbv HONO mixing ratios observed by the CIMS (Fig. 2, RSD of 8.1%), ACES (RSD 8.2 %), and NOyO3 (RSD 1.9 %). In these added observations with higher sensitivity instrumentation, the stability was equal to instrumental precision.'

2. The HONO gas stream generated by this system must be calibrated by a primary instrument before it could be used as a HONO calibration source. Therefore, the system itself is not a tunable calibration source for HONO as the authors claimed in the title. A better HONO measurement will be needed to calibration the HONO source at low concentrations; the NOx analyzer described in the manuscript is not adequate for this purpose.

We were referring to the output of the calibration source as tunable, as the output can be changed through adjustments in oven temperature, different HCl PDs, and dilution flows. Simply put, the tunability of previously published approaches by changing liquid flows or solution concentrations as in Taira and Kanda (1990), or operating additional pumps to reduce the HONO concentrations as in Gingerysty and Osthoff (2020) are cumbersome and expensive compared to simple changes to dilution flows on our source, which produces substantially lower mixing ratios of HONO to reach an environmentally-relevant work range. Gas phase dilutions are abundantly described for HONO in the literature, often being 'tuned' on the order of seconds or, more often, dictated by the instrument response time. If the Reviewer's point is that our calibration source cannot adjust the output across orders of magnitude in a systematic fashion quickly, that is also incorrect, but could require 1 or 2 hours should such large changes be needed. This is done by changing the temperature of the heating block, swapping permeation devices, or operating multiple channels in parallel. However, we have addressed this apparent need for instantaneous tunability in response to Reviewer 1 by noting that the heating block can simply house multiple parallel calibration channels that cover the necessary range.

The remainder of the calibration work is rapidly achieved by modifying the dilution flow, as stated in the abstract at Lines 22-23:

'Mixing ratios at the tens of pptv level are easily reached with reasonable dilution flows.'

Please see the added text in the conclusions to emphasize this point at Lines 723-725:

'The HONO calibration source was designed to facilitate multiple calibrant concentrations, as the four holes in the aluminium heating block (Fig. S3) allows for the operation of parallel HONO sources if desired.'

The versatility of multiple permeation devices and parallel channels for tunability are already stated at Lines 611-612:

'The use of multiple HCl permeation tubes in a single oven, in series, or in parallel are additional options to control the HONO mixing ratio generated in the calibration system.'

We have previously addressed in detail the issue of using a commercial NOx analyser to calibrate the output of our HONO source in an earlier response to Reviewer 1. Briefly, we choose to use a commercial NOx analyser as this was available and also we wanted to keep the total system as low-cost as possible.

3. A commercial HONO source is available, based on the reaction of NaNO2 with diluted H2SO4 solution in a stripping coil (Taira and Kanda, 1990; Kleffmannet al., 2004) (https://qumashop.de/images/LOPAP%2003%20HONO%20Source%20short_v2.pdf). A unit was used during the FIONA intercomparison in 2010 in Valencia, Spain, to generate a HONO source being distributed to and shared by the collaborating groups. Based on my own experience from this intercomparison, the system appeared to perform significantly better than the system described in the manuscript. Specifically, it offered high precision and stability (~ 1% at low-ppb concentrations) and is truly tunable (stabilized within minutes after switching to a different concentration). Of course, the commercial unit could be much pricier than the home-build system described in this manuscript.

As we stated in our response to Reviewer 1, the unit used in the FIONA inter-comparison has not been described in the peer-reviewed literature and so we are unable to compare our source to the results mentioned by Reviewer 3. We also note that low ppbv concentrations are not sub-ppbv mixing ratios, which are typically observed in the daytime troposphere. This means that the modified source used during FIONA was not readily reaching environmentally-relevant mixing ratios, particularly near the daytime minima of 10-100 pptv of HONO. Our source can reach these mixing ratios with simple gas phase dilutions and this means it is far more easily tuned in this range. We have added more text to clarify the lower purity of our source relative to previous work, please see our response to Reviewer 1, major comment 4.

As the Reviewer rightly points out, the HONO calibration source presented in the current work is likely cheaper than the commercially available system mentioned from QUMA, as one of our project goals was to keep the system as low-cost as possible.

References

Afif, C., Jambert, C., Michoud, V., Colomb, A., Eyglunent, G., Borbon, A., Daële, V., Doussin, J. F. and Perros, P.: NitroMAC: An instrument for the measurement of HONO and intercomparison with a long-path absorption photometer, J. Environ. Sci. (China), 40, 105–113, doi:10.1016/j.jes.2015.10.024, 2016.

Crilley, L. R., Kramer, L. J., Ouyang, B., Duan, J., Zhang, W., Tong, S., Ge, M., Tang, K., Qin, M., Xie, P., Shaw, M. D., Lewis, A. C., Mehra, A., Bannan, T. J., Worrall, S. D., Priestley, M., Bacak, A., Coe, H., Allan, J., Percival, C. J., Popoola, O. A. M., Jones, R. L. and Bloss, W. J.: Intercomparison of nitrous acid (HONO) measurement techniques in a megacity (Beijing), Atmos. Meas. Tech., 12, 6449–6463, doi:10.5194/amt-12-6449-2019, 2019.

Elshorbany, Y. F., Kurtenbach, R., Wiesen, P., Lissi, E., Rubio, M., Villena, G., Gramsch, E., Rickard, A. R., Pilling, M. J. and Kleffmann, J.: Oxidation capacity of the city air of Santiago, Chile, Atmos. Chem. Phys., 9(6), 2257–2273, doi:10.5194/acp-9-2257-2009, 2009.

Fahey, D. W., Eubank, C. S., Hübler, G. and Fehsenfeld, F. C.: Evaluation of a catalytic reduction technique for the measurement of total reactive odd-nitrogen NOy in the atmosphere, J. Atmos. Chem., 3(4), 435–468, doi:10.1007/BF00053871, 1985.

Febo, A., Perrino, C., Gherardi, M. and Sparapani, R.: Evaluation of a high-purity and high-stability continuous generation system for nitrous acid, Environ. Sci. Technol., 29(9), 2390–2395, doi:10.1021/es00009a035, 1995.

Febo, A., Perrino, C. and Allegrini, I.: Measurement of nitrous acid in Milan, Italy, by DOAS and diffusion denuders, Atmos. Environ., 30(21), 3599–3609, doi:10.1016/1352-2310(96)00069-6, 1996.

Fontijn, A., Sabadell, A. J. and Ronco, R. J.: Homogeneous chemiluminescent measurement of nitric oxide with ozone: Implications for continuous selective monitoring of gaseous air pollutants, Anal. Chem., 42(6), 575–579, doi:10.1021/ac60288a034, 1970.

Fried, A., Henry, B. and Sewell, S.: Potential calibration errors in carbonyl sulfide permeation devices: Implications for atmospheric studies, J. Geophys. Res. Atmos., 103(D15), 18895–18906, doi:10.1029/98JD00620, 1998.

Gingerysty, N. J. and Osthoff, H. D.: A compact , high-purity source of HONO validated by Fourier transform infrared and thermal dissociation cavity ring-down spectroscopy, Atmos. Meas. Tech. Discuss., 1–20, doi:10.5194/amt-2020-92, 2020.

Harris, G. W., Carter, W. P. L., Winer, A. M., Pitts, J. N., Platt, U. and Perner, D.: Observations of Nitrous Acid in the Los Angeles Atmosphere and Implications for Predictions of Ozone—Precursor Relationships, Environ. Sci. Technol., 16(7), 414–419, doi:10.1021/es00101a009, 1982.

Kleffmann, J., Benter, T. and Wiesen, P.: Heterogeneous reaction of nitric acid with nitric oxide on glass surfaces under simulated atmospheric conditions, J. Phys. Chem. A, 108(27), 5793–5799, doi:10.1021/jp040184u, 2004.

MacInnis, J. J., VandenBoer, T. C. and Young, C. J.: Development of a gas phase source for perfluoroalkyl acids to examine atmospheric sampling methods, Analyst, 141(12), doi:10.1039/c6an00313c, 2016.

McGrath, D. T., Ryan, M. D., Macinnis, J. J., Vandenboer, T. C., Young, C. J. and Katz, M. J.: Selective decontamination of the reactive air pollutant nitrous acid via node-linker cooperativity in a metal-organic framework, Chem. Sci., 10(21), 5576–5581, doi:10.1039/c9sc01357a, 2019.

Min, K. E., Washenfelder, R. A., Dubé, W. P., Langford, A. O., Edwards, P. M., Zarzana, K. J., Stutz, J., Lu, K., Rohrer, F., Zhang, Y. and Brown, S. S.: A broadband cavity enhanced absorption spectrometer for aircraft measurements of glyoxal, methylglyoxal, nitrous acid, nitrogen dioxide, and water vapor, Atmos. Meas. Tech., 9(2), 423–440, doi:10.5194/amt-9-423-2016, 2016.

Neuman, J. A., Ryerson, T. B., Huey, L. G., Jakoubek, R., Nowak, J. B., Simons, C. and Fehsenfeld, F. C.: Calibration and evaluation of nitric acid and ammonia permeation tubes by UV optical absorption, Environ. Sci. Technol., 37(13), 2975–2981, doi:10.1021/es026422l, 2003.

Peng, Q., Palm, B. B., Melander, K. E., Lee, B. H., Hall, S. R., Ullmann, K., Campos, T., Weinheimer, A. J., Apel, E. C., Hornbrook, R. S., Hills, A. J., Montzka, D. D., Flocke, F., Hu, L., Permar, W., Wielgasz, C., Lindaas, J., Pollack, I. B., Fischer, E. V., Bertram, T. H. and Thornton, J. A.: HONO Emissions from Western U.S. Wildfires Provide Dominant Radical Source in Fresh Wildfire Smoke, Environ. Sci. Technol., 54(10), 5954–5963, doi:10.1021/acs.est.0c00126, 2020.

Pinto, J. P., Dibb, J., Lee, B. H., Rappenglück, B., Wood, E. C., Levy, M., Zhang, R. Y., Lefer, B., Ren, X. R., Stutz, J., Tsai, C., Ackermann, L., Golovko, J., Herndon, S. C., Oakes, M., Meng, Q. Y., Munger, J. W., Zahniser, M. and Zheng, J.: Intercomparison of field measurements of nitrous acid (HONO) during the

SHARP campaign, J. Geophys. Res. Atmos., 119(9), 5583–5601, doi:10.1002/2013JD020287, 2014.

Ren, X., Sanders, J. E., Rajendran, A., Weber, R. J., Goldstein, A. H., Pusede, S. E., Browne, E. C., Min, K. E. and Cohen, R. C.: A relaxed eddy accumulation system for measuring vertical fluxes of nitrous acid, Atmos. Meas. Tech., 4(10), 2093–2103, doi:10.5194/amt-4-2093-2011, 2011.

Ridley, B. A. and Grahek, F. E.: A small, low flow, high sensitivity reaction vessel for NO chemiluminescence detectors, J. Am. Meteorol. Soc., 7, 307–311, 1990.

Ridley, B. A. and Howlett, L. C.: An instrument for nitric oxide measurements in the stratosphere, Rev. Sci. Instrum., 45(6), 742–746, 1974.

Roberts, J. M., Veres, P., Warneke, C., Neuman, J. A., Washenfelder, R. A., Brown, S. S., Baasandorj, M., Burkholder, J. B., Burling, I. R., Johnson, T. J., Yokelson, R. J. and De Gouw, J.: Measurement of HONO, HNCO, and other inorganic acids by negative-ion proton-transfer chemical-ionization mass spectrometry (NI-PT-CIMS): Application to biomass burning emissions, Atmos. Meas. Tech., 3(4), 981–990, doi:10.5194/amt-3-981-2010, 2010.

Rollins, A. W., Rickly, P. S., Gao, R.-S., Ryerson, T. B., Brown, S. S., Peischl, J. and Bourgeois, I.: Single-photon laser-induced fluorescence detection of nitric oxide at sub-parts per trillion mixing ratios, Atmos. Meas. Tech., 13, 2425–2439, doi:10.5194/amt-13-2425-2020, 2020.

Rubio, M. A., Lissi, E., Villena, G., Elshorbany, Y. F., Kleffmann, J., Kurtenbach, R. and Wiesen, P.: Simultaneous measurements of formaldehyde and nitrous acid in dews and gas phase in the atmosphere of Santiago, Chile, Atmos. Environ., 43(38), 6106–6109, doi:10.1016/j.atmosenv.2009.09.017, 2009.

Ryerson, T. B., Huey, L. G., Knapp, K., Neuman, J. A., Parrish, D. D., Sueper, D. T. and Fehsenfeld, F. C.: Design and initial characterization of an inlet for gas-phase NOy measurements from aircraft, J. Geophys. Res., 104(D5), 5483–5492, 1999.

Stutz, J., Kim, E. S., Platt, U., Bruno, P., Perrino, C. and Febo, A.: UV-visible absorption cross sections of nitrous acid, J. Geophys. Res. Atmos., 105(D11), 14585–14592, doi:10.1029/2000JD900003, 2000.
Taira, M. and Kanda, Y.: Continuous generation system for low-concentration gaseous nitrous acid, Anal. Chem., 62(6), 630–633, doi:10.1021/ac00205a018, 1990.

Tong, S., Hou, S., Zhang, Y., Chu, B., Liu, Y., He, H., Zhao, P. and Ge, M.: Exploring the nitrous acid (HONO) formation mechanism in winter Beijing: Direct emissions and heterogeneous production in urban and suburban areas, Faraday Discuss., 189, 213–230, doi:10.1039/c5fd00163c, 2016.

VandenBoer, T. C., Brown, S. S., Murphy, J. G., Keene, W. C., Young, C. J., Pszenny, A. A. P., Kim, S., Warneke, C., De Gouw, J. A., Maben, J. R., Wagner, N. L., Riedel, T. P., Thornton, J. A., Wolfe, D. E., Dubé, W. P., Öztürk, F., Brock, C. A., Grossberg, N., Lefer, B., Lerner, B., Middlebrook, A. M. and Roberts, J. M.: Understanding the role of the ground surface in HONO vertical structure: High resolution vertical profiles during NACHTT-11, J. Geophys. Res. Atmos., 118(17), 10155–10171, doi:10.1002/jgrd.50721, 2013.

VandenBoer, T. C., Markovic, M. Z., Sanders, J. E., Ren, X., Pusede, S. E., Browne, E. C., Cohen, R. C., Zhang, L., Thomas, J., Brune, W. H. and Murphy, J. G.: Evidence for a nitrous acid (HONO) reservoir at the ground surface in Bakersfield, CA, during CalNex 2010, J. Geophys. Res. Atmos., 119, 1–14, doi:10.1002/2013JD020971, 2014.

VandenBoer, T. C., Young, C. J., Talukdar, R. K., Markovic, M. Z., Brown, S. S., Roberts, J. M. and Murphy, J. G.: Nocturnal loss and daytime source of nitrous acid through reactive uptake and displacement, Nat. Geosci., 8(1), 55–60, doi:10.1038/ngeo2298, 2015.

Veres, P., Gilman, J. B., Roberts, J. M., Kuster, W. C., Warneke, C., Burling, I. R. and De Gouw, J.: Development and validation of a portable gas phase standard generation and calibration system for volatile organic compounds, Atmos. Meas. Tech., 3(3), 683–691, doi:10.5194/amt-3-683-2010, 2010.

Washenfelder, R. A., Roehl, C. M., McKinney, K. A., Julian, R. R. and Wennberg, P. O.: A compact, lightweight gas standards generator for permeation tubes, Rev. Sci. Instrum., 74(6), 3151–3154, doi:10.1063/1.1570949, 2003.

Young, C. J., Washenfelder, R. A., Roberts, J. M., Mielke, L. H., Osthoff, H. D., Tsai, C., Pikelnaya, O., Stutz, J., Veres, P. R., Cochran, A. K., Vandenboer, T. C., Flynn, J., Grossberg, N., Haman, C. L., Lefer, B., Stark, H., Graus, M., De Gouw, J., Gilman, J. B., Kuster, W. C. and Brown, S. S.: Vertically resolved measurements of nighttime radical reservoirs in Los Angeles and their contribution to the urban radical budget, Environ. Sci. Technol., 46(20), 10965–10973, doi:10.1021/es302206a, 2012.

Zhang, W., Tong, S., Ge, M., An, J., Shi, Z., Hou, S., Xia, K., Qu, Y., Zhang, H., Chu, B., Sun, Y. and He, H.: Variations and sources of nitrous acid (HONO) during a severe pollution episode in Beijing in winter 2016, Sci. Total Environ., 648, 253–262, doi:10.1016/j.scitotenv.2018.08.133, 2019.

Zhou, S., Young, C. J., Vandenboer, T. C., Kowal, S. F. and Kahan, T. F.: Time-resolved measurements of nitric oxide, nitrogen dioxide, and nitrous acid in an occupied New York home, Environ. Sci. Technol., 52(15), 8355–8364, doi:10.1021/acs.est.8b01792, 2018.

Zhou, X., He, Y., Huang, G., Thornberry, T. D., Carroll, M. A. and Bertman, S. B.: Photochemical production of nitrous acid on glass sample manifold surface, Geophys. Res. Lett., 29(14), 1681, doi:10.1029/2002gl015080, 2002.

A portable, robust, stable and tunable calibration source for gas-phase nitrous acid (HONO)

Melodie Lao[1], Leigh R. Crilley[1], Leyla Salehpoor[1], Teles C. Furlani[1], Ilann Bourgeois[2,3], J. Andrew Neuman[2,3], Andrew W. Rollins[2], Patrick R. Veres[2], Rebecca A. Washenfelder[2], Caroline C. Womack[2,3], Cora J. Young[1], and Trevor C. VandenBoer[1, *]

[1] *Department of Chemistry, York University, Toronto, ON*
[2] *NOAA Chemical Sciences Laboratory, Boulder, CO*
[3] *Cooperative Institute for Research in Environmental Sciences, University of Colorado, Boulder, CO*

[*] *Communicating Author:* tvandenb@yorku.ca

Abstract

Atmospheric HONO mixing ratios in indoor and outdoor environments span a range of less than a few parts per trillion by volume (pptv) up to tens of parts per billion by volume (ppbv) in combustion plumes. Previous HONO calibration sources have utilized proton transfer acid displacement from nitrite salts or solutions, with output that ranges from tens to thousands of ppbv. Instrument calibrations have thus required large dilution flows to obtain atmospherically relevant mixing ratios. Here we present a simple universal source to reach very low HONO calibration mixing ratios using a nitrite-coated reaction device with the addition of humid air and/or HCl from a permeation device. The calibration source developed in this work can generate HONO across the atmospherically relevant range and has high purity (>90 %), reproducibility, and tunability. Mixing ratios at the tens of pptv level are easily reached with reasonable dilution flows. The calibration source can be assembled to start producing stable HONO mixing ratios (RSE ≤ 2 %) within two hours, with output concentrations varying ≤ 25 % following simulated transport or complete disassembly of the instrument, and ≤ 10 % under ideal conditions. The simplicity of this source makes it highly versatile for field and lab experiments. The platform facilitates a new level of accuracy in established instrumentation, as well as intercomparison studies to identify systematic HONO measurement bias and interferences.

1. Introduction

In the lower troposphere, the hydroxyl radical (OH) is the principal daytime gas-phase oxidant, and will react with volatile organic compounds (VOC) to form secondary pollutants such as ozone (O_3) and secondary organic aerosols (Spataro and Ianniello, 2014; Ye et al., 2018). Photolysis of nitrous acid (HONO) is a direct source of the hydroxyl radical (OH) (R1). Consequently, this can be a significant contributor to the integrated daily OH budget, ranging from 4-56 % in urban areas (Lee et al., 2013; Volkamer et al., 2010), up to 80% in semi-rural areas in the winter (Kim et al., 2014), along with additional vertical and temporal variability (Crilley et al., 2016; Young et al., 2012; Zhang et al., 2009).

$$HONO_{(g)} + h\nu\ (\lambda<405\ nm) \rightarrow OH_{(g)} + NO_{(g)} \qquad \text{(R1)}$$

The reported daytime mixing ratios of ambient HONO outdoors can vary considerably for different environments, ranging from a few parts per trillion by volume (pptv) in the clean remote marine and Arctic boundary layers (Honrath et al., 2002; Kasibhatla et al., 2018; Reed et al., 2017) to 18 parts per billion by volume (ppbv) in polluted megacities such as Milan, Los Angeles, and Beijing (Elshorbany et al., 2009; Febo et al., 1996; Harris et al., 1982; Tong et al., 2016; Zhang et al., 2019). Measurements within biomass burning plumes from forest fires have shown very high HONO levels, often up to 60 ppbv (Chai et al., 2019; Neuman et al., 2016; Veres et al., 2010b). There is a growing body of evidence that HONO concentrations can be significant in indoor environments, with levels up to 50 ppbv reported from gas stove cooking emissions (Collins et al., 2018; Gligorovski, 2016; Gómez Alvarez et al., 2012; Liu et al., 2019; Young et al., 2019; Zhou et al., 2018). There are a number of atmospheric HONO sources that have been reported: direct emissions (e.g. vehicles and biomass burning); gas-phase homogenous reaction of NO and OH, biological production in soils (Mushinski et al., 2019), and a number of heterogeneous surface reactions ((Spataro and Ianniello, 2014) and references therein). Despite the importance of HONO to atmospheric photochemistry and radical budgets, the contribution of these sources to observed HONO levels is still poorly constrained, particularly during the daytime (Gall et al., 2016; Kleffmann, 2007; Lee et al., 2016; Oswald et al., 2013; Pusede et al., 2015; Sörgel et al., 2015; Tsai et al., 2018; Ye et al., 2016).

Due to the importance of HONO in our understanding of tropospheric photochemical oxidation and indoor atmospheric oxidation chemistry, accurate and precise quantitative measurements are required. However, gas-phase HONO has remained a challenging compound to measure due to several instrument artefacts and interferences. Within inlet lines, positive artefacts can occur as a result of heterogenous HONO formation on wet surfaces (Kleffmann and Wiesen, 2008; Zhou et al., 2002), while the reactive nature of HONO can also lead to negative artefacts due to wall losses (Pinto et al., 2014). Furthermore, there can be interferences from ambient components in the atmospheric matrix, such as the reduction of NO_2 by numerous compounds, as well as particulate nitrite (Kleffmann et al., 2006; Kleffmann and Wiesen, 2008; Rubio et al., 2009; Sörgel et al., 2011; VandenBoer et al., 2014). Recent intercomparison studies have shown substantial differences between various HONO measurement techniques (Cheng et al., 2013; Crilley et al., 2019; Pinto et al., 2014; Stutz et al., 2010). Crilley et al. (2019) observed that while different HONO measurement techniques agreed on the temporal trends in HONO concentrations, the reported absolute concentrations displayed systematic variation. Most studies are unable to pinpoint the exact cause of the observed divergence between instruments; it may be due to spatial heterogeneity in ambient HONO concentration, unknown chemical interference(s), and/or differences in the accuracy and precision of calibration approaches. A portable calibration unit compatible with all instruments/techniques could assist in ruling out systematic bias and identifying interferences between instruments during intercomparison studies.

A variety of approaches have been used in the past to generate gaseous HONO standards. Most of these depend on acid displacement from a solution containing nitrite (NO_2^-) or from solid sodium nitrite ($NaNO_2$). Acids used have included sulfuric acid, hydrochloric acid, and oxalic acid, with evaporation of NH_4NO_2 also reported (Braman and de la Cantera, 1986; Febo et al., 1995; Taira and Kanda, 1990; Večeřa and Dasgupta, 1991). By far the most widely employed modern HONO calibration methods stem from the report of Febo et al. (1995) who presented a system for generating a continuous source of stable gas-phase HONO in the tens of ppbv to parts per million by volume (ppmv) range. This system utilised the reaction between gas-phase hydrochloric acid (HCl) and $NaNO_2$ powder to generate gas-phase HONO, as described in R2:

$$NaNO_{2(s)} + HCl_{(g)} \rightarrow HONO_{(g)} + NaCl_{(s)} \qquad \text{(R2)}$$

However, this calibration source requires a gas-tight vessel of HCl solution contained in a thermostatic bath that presents considerable difficulty for many field measurement applications. Adaptations include immersing thin-wall Teflon tubing in concentrated HCl, high concentration HCl cylinders, and HCl permeation devices. Gaseous HCl generated by these methods then mixes with loose $NaNO_2$ crystals in a stirred reactor (Stutz et al., 2000), dispersed using 3 mm glass beads packed in PFA tubing to increase porosity (Roberts et al., 2010), or pieces of PFA tubing (McGrath et al., 2019; VandenBoer et al., 2015; Zhou et al., 2018). These adapted approaches have been used to calibrate many atmospheric HONO instruments (Crilley et al., 2019; Heland et al., 2001; Ren et al., 2010; Roberts et al., 2010; Stutz et al., 2000; VandenBoer et al., 2013, 2015; Wang and Zhang, 2000; Young et al., 2012). An alternative approach that utilised dilute H_2SO_4 for the acid displacement reaction with aqueous $NaNO_2$ was outlined by Taira and Kanda (1990). While this approach was shown to generate a stable and tunable HONO output at hundreds of ppbv, it has not been widely adapted, likely due to the need for complex custom glassware and liquid flow control in the calibration apparatus and significant dilution to reach single digit ppbv mixing ratios (Kleffmann et al., 2004).

While widely used, the method described by Febo et al. (1995) presents several practical challenges. The typically high HONO mixing ratios generated by this approach (up to 20 ppmv) are challenging to dilute to atmospherically relevant mixing ratios. The high quantities also lead to auto-dissociation of HONO (R3), resulting in the production of nitrogen oxide impurities of NO and NO_2 (Febo et al., 1995; Neuman et al., 2016), and ClNO in the presence of HCl at ppmv levels (Gingerysty and Osthoff, 2020).

$$HONO_{(g)} + HONO_{(ads)} \rightarrow NO_{(g)} + NO_{2(g)} + H_2O \qquad \text{(R3)}$$

Further, to reduce the variability in HONO output over time, the powdered $NaNO_2$ bed requires continuous mixing to maintain equilibrium between the adsorbed HONO and carrier gas flowing over the salt bed minimize the production of NO_x by R3, as well as a Teflon filter to prevent loss of $NaNO_2$ powder by entrainment in the gas flow. The degradation of the powdered $NaNO_2$ structure can limit the lifetime of the source and results in unstable HONO production rates (Febo et al., 1995; Gingerysty and Osthoff, 2020). Other systems using dispersed $NaNO_2$ suffer from sensitivity to vibration, causing changes in HONO output and limiting calibration accuracy (Zhou et al., 2018). Once operational, the original or modified methods require up to a day to stabilize and these systems must be kept continuously operating and stationary to preserve the HONO output stability.

One solution for producing gaseous HCl for acid displacement is to use a temperature-controlled permeation device (PD). A permeation oven is a simple instrument that can be used for the preparation of low mixing ratios of gases from ppbv to ppmv levels (Veres et al., 2010a; Washenfelder et al., 2003). This approach has been used to generate a consistent quantity of gaseous analytes for over 400 compounds because it is low-cost, portable, and robust (Mitchell, 2000). Permeation devices are typically made of inert polymer tube of known permeability filled with a (semi-)volatile liquid. Both ends of the device are sealed either with caps or permeable plugs and the emission is determined by the surface area and thickness of permeable polymer, the concentration of the contained solution, and the temperature (O'Keeffe and Ortman, 1966; Susaya et al., 2012).

The aim of the current work was to make a portable and easy to assemble HONO calibration instrument compatible with HONO-measuring instruments commonly used within the atmospheric research community. We developed coated devices to facilitate reactions of sodium nitrite ($NaNO_2$) which release HONO when exposed to water vapour and HCl (R2). Herein we demonstrate that the $NaNO_2$-coated reaction devices produce a stable and continuous supply of high-purity gaseous HONO. The output of this HONO calibration source spans the range of environmentally relevant mixing ratios, up to tens of ppbv. The emission quantities, mass balance, and purity of gaseous HONO were determined through a series of control tests with various instruments. We present evidence of its robustness, reproducibility, and stability in HONO output. Finally, we evaluated methods to control the mixing ratio output of the calibration source and provide several approaches and recommendations on its use.

2. Experimental Methods

2.1 Coated $NaNO_2$ reaction devices

Reactions of $NaNO_2$ on humidified surfaces produce HONO. A large and consistent surface area is required to reproducibly produce HONO at the desired levels.

A $NaNO_2$ (EMSURE®; ACS Reag. Ph Eur, Germany) coating solution was made as a 20 g L^{-1} $NaNO_2$ solution. The coating solution solvent was composed of equal volumes of methanol (HPLC Grade; Fisher Chemicals, Ottawa, ON) and 18.2 MΩ·cm deionised water with 1.0 g L^{-1} glycerol

(Sigma Chemical Company, St. Louis, MO, USA) to facilitate a uniform salt coating. The solution was made by dissolving the $NaNO_2$ in the water first, followed by the addition of the glycerol and then methanol. The coating solution was stored in an HDPE bottle wrapped in aluminum foil at 4 °C until needed and remade every three months. To coat a reaction device, 3 mL of coating solution was first transferred into a heat-straightened ½" (1.27 cm) PFA tube with a length of 14.4 cm and surface area of 86.2 cm^2. Rubber stoppers with centred 4.5 mm holes were inserted into both ends of the PFA tube to reduce solution loss while evaporating the solvent. The PFA reaction device was repeatedly inverted and rotated while covering both stopper holes to coat the inner surface completely. The reaction device was then dried by insertion into an 8" (20 cm) length of aluminum pipe (1-¼"/3.18 cm I.D.) and placed onto heated stainless steel rollers to evenly coat the PFA reaction device surface as the solution evaporates over a few hours (Nostalgia Electrics, RHD800 Retro Series; or Great Northern Popcorn Company, 4078 GNP Hotdog 7 Roller Machine). Until their experimental use, prepared $NaNO_2$ PFA reaction devices were sealed with Parafilm or vinyl end caps (McMaster-Carr; P/N: 40005K14) and kept in a dark box at room temperature.

Teflon-coated aluminum annular denuders (URG-2000-30x150-3CSS, URG Corporation, Chapel Hill, NC) were also used in some experiments in place of the $NaNO_2$ device (Figure 1). To coat these denuders, 3.0 mL of the $NaNO_2$ coating solution was transferred to the device, followed by capping, inversion, rotation and shaking to ensure all concentric etched glass surfaces were coated. The excess $NaNO_2$ coating was decanted and the denuder dried with zero air at a flow of 1.0 standard litre per minute (SLPM) for about 10 min at room temperature.

2.2 Gas flows

The calibration source, which uses a permeation oven and $NaNO_2$ reaction device to generate HONO, was designed to be cost-effective, lightweight, and robust for use with dry compressed air as the carrier gas (Figure 1). Full technical details of the design rationale and assembly of the custom-built permeation oven can be found in the Supporting Information (SI, Sections S1-2, Figures S1-5), with only a brief description given below. A NO_x analyzer was used to characterize the output from the HONO source. A single cylinder or zero air generator provided the separate carrier gas flows required for the PD, a humidifier, and a dilution flow.

Carrier gas flow through the permeation oven was provided by a compressed cylinder of zero air or nitrogen (Praxair; Air Ultra Zero, 99.999%, AI 0.0UZ-K; High Purity Nitrogen, 99.998 %, NI 4.8, Toronto, ON) but an in-situ zero air generator could also be used (e.g. Aadco Instruments Model 747-10, Cleves, OH; used only for dilution flows here) providing 20 psi of pressure to control the flow entering a four-way ¼" (64 mm) Swagelok cross fitting. The zero air flows through two critical orifices setting flows of ~50 sccm (Lenox Laser, Glen Arm, MD; SS-4-VCR-2-50) and a mass flow controller (MFC; MKS Instruments, Inc.; M100B00814CS1BV, 10 SLPM, gas; AIR, Kanata, Canada) set to deliver a dilution flow of 1.0 SLPM. A proportional-integral-differential (PID) temperature controller (Omega™; CN 7823, St-Eustache, QC) was used to regulate the temperature of a machined aluminum (Al) block. The first critical orifice connects to the HCl PD channel within the heated Al block and the second connects to a 25 mL glass impinger (EMD Millipore Corporation, Billerica, MA, USA) containing deionised water at room temperature. The flows are combined and mixed to a resultant relative humidity (RH) of 50 %, which then enters the coated $NaNO_2$ reaction device in the temperature-controlled Al block. The HCl drives the acid displacement reaction in the $NaNO_2$-coated PFA device, releasing HONO into the gas phase. The flow exits the oven into the dilution flow being delivered to an instrument or experimental system. If operating in cold environments, care should be taken to ensure the 50 % RH exiting the calibration system does not generated condensation in the lines.

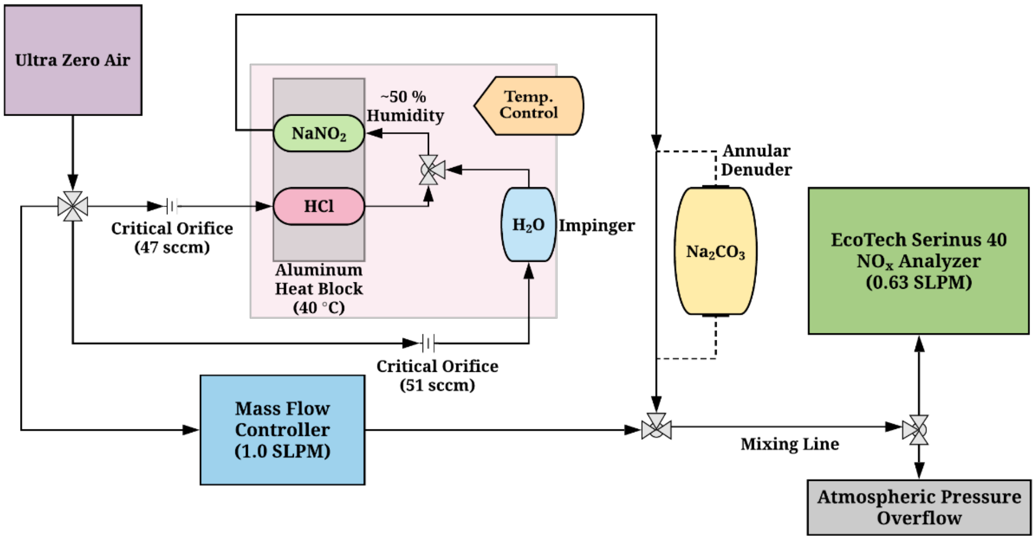

Figure 1. Flow and component schematic of the HONO calibration system (pink shaded region) interfaced with a NO_x analyzer (green), dilution mass flow controller (blue), and an exchangeable Na_2CO_3 annular denuder (yellow). Lines with black arrows denote the direction of gas flow through system components. Tee and cross fittings are denoted by arrays of grey triangles.

2.3 Custom-built HCl permeation devices (PDs)

Although PDs are available from commercial suppliers, they are custom made here to reduce costs, as described in detail in the Supporting Information (Section S2, Figure S5). Briefly, custom PDs are made from PFA tubing (3.2 mm ID with 5 mm OD, P/N: 5733K73; McMaster-Carr, Aurora, OH) fitted with PTFE plugs (3.2 mm diameter, P/N: 84935K64; McMaster-Carr). A series of HCl PDs were made as aqueous solutions to obtain PDs containing 1.2 M and 6 M HCl solutions (OmniTrace®; 34-37 %, HX0607-1, SigmaAldrich, Oakville, ON; Table 1). During operation the HCl PD is placed within the ½'' tubing in the heating block, through which the carrier gas is flushed.

2.4 NO_x analyzer for HONO detection

The output from the HONO calibration source was monitored using a commercial chemiluminescent NO_x analyzer fitted with a Mo catalytic converter, set to 325 ˚C (Serinus 40, American Ecotech, Warren, RI). The conversion efficiency of NO_2 to NO was calculated by combining known concentrations of NO from a standard cylinder (Praxair; NI NO5MC-A3, 4.88 (±5 %) ppmv, Toronto, ON) and O_3 using a gas calibration instrument (Gascal 1100TS, American Ecotech, Warren, RI). The conversion efficiency was determined according to the manufacturer specifications at 98.84 (±0.38 %) for NO_2 mixing ratios delivered to the system spanning 100 to 400 ppbv. While the Mo catalyst is meant to convert NO_2 to NO for detection by the analyzer, it is well known that HONO is also quantitatively converted to NO (Febo et al., 1995), and the conversion efficiency was determined experimentally (Section 2.6). A NO_x analyzer was preferred to other independent calibration methods such as ion chromatography with conductivity detection (IC-CD), as it is capable of continuous real-time measurement of HONO, allowing rapid frequent checks on the calibration source output stability.

During experiments, ~100 sccm from the HONO source was diluted into an additional 1.0 SLPM of zero air from which the NO_x instrument sampled 0.63 SLPM (Fig. 1). The NO_x analyzer measured NO on either the NO or NO_x channels for an averaging period of 1 minute with the Kalman filter set to 60 s or 300 s. To correct for instrument drift or NO_x contamination in the zero air, the analyzer was flushed for at least 15 min at the beginning and end of each experiment. An annular denuder coated with 20 g L^{-1} sodium carbonate in 50:50 methanol and water solution (Na_2CO_3; ACS reagent >99.7%; SigmaAldrich, St. Louis, MO) – similar to that used here for $NaNO_2$ - was inserted during some experiments to scrub HONO from the experimental flow (Fig. 1). The denuder was prepared by transferring 10 mL of Na_2CO_3-coating solution, capping, then inverting and rotating to distribute the solution evenly. The remainder of the coating solution was decanted and the denuder surfaces dried under a flow of 1.0 SLPM of zero air until completely dry (~10 min). The denuder was inserted into experimental flows for at least one hour as a second check on sources of background NO and NO_2 as impurities being emitted from the calibration source or carrier gas. A Na_2CO_3 denuder can also be used as a robust alternative to provide the NO_x analyzer inlet overflow instead of a cylinder of zero air. The enables corrections of HONO measurements or calibrations for NO_x present in the sample air or calibration source carrier gas, respectively.

2.5 Conversion efficiency of the NO_x analyzer Mo-catalyst for HONO

A Mo catalyst at 325 °C will reduce HONO to NO, though reports have shown that this conversion may vary between NO_x analyzers (McGrath et al., 2019; Zhou et al., 2018). We measured the HONO generated by the calibration source with the NO_x analyzer, then directed the HONO to a scrubbing solution of 1 mM NaOH in two glass impingers connected in series for several hours to days to collect NO_2^- to a level that could be quantified by IC-CD. The second bubbler was used to determine the extent that HONO was quantitatively collected in the first bubbler (i.e. to capture any breakthrough). The HONO generated by the calibration source and quantified by IC was compared to the NO_x analyzer measurement, using the introduction of a Na_2CO_3 annular denuder to perform background correction. The HONO conversion efficiency determined by comparison to the IC was found to be 104 ± 4 % (n = 3), confirming unit conversion efficiency, with the associated error set by the 4 % accuracy of the IC-CD method for NO_2^- ($R^2 > 0.999$) when employing our previously developed separation method (Place et al., 2018). The IC precision near the analyzed concentrations for NO_2^- was measured to be 3 %. All data presented in this manuscript therefore uses a conversion efficiency of unity for the Mo-catalyst.

2.6 Supporting Instrumentation

In our mass balance experiments for the production mechanisms governing HONO generation in the calibration system, we used two additional tools to monitor experimental gas flows. Mixing ratios of HCl were measured at 0.5 Hz using a cavity ring down spectrometer (CRDS) (G2108 HCl Gas Concentration Analyzer, Picarro, Santa Clara, CA) with a 5 pptv detection limit for 1-minute averaged data. Further details on the performance of this instrumentation can be found in Dawe et al. (2019). Measurements of HCl and HONO to investigate acid displacement efficiency of the calibration system were measured at 2 Hz using a quadrupole chemical ionisation mass spectrometer (CIMS, THS Instruments LLC, Atlanta, GA) using acetate reagent ions to facilitate proton transfer and detection of negative ions at m/z 35 and 46, respectively. Observed ions were normalized to the detected quantity of the acetate reagent ion and multiplied by $8x10^5$, resulting in signal units of normalized counts, as we have previously reported for the detection of these analytes (VandenBoer et al., 2013). Signal from the CIMS was averaged to a 1-minute time base to compare to other measurements.

In our purity and stability experiments, additional instrumentation was used to detect HONO, NO_y, and other reactive gases. A time-of-flight chemical ionisation mass spectrometer utilising iodide adduct reagent ions (I^- ToF-CIMS; Aerodyne Research Inc., Billerica, MA) was used to measure HONO and detect a wide array of other analytes (e.g. $ClNO_2$, HNO_3, N_2O_5, etc.) in experimental gas flows. Specific operational details of the I^- ToF-CIMS for these atmospheric species are presented elsewhere (Neuman et al., 2016; Veres et al., 2020). A broadband cavity enhanced absorption spectrometer (ACES) was used to measure HONO and NO_2 (Min et al., 2016) and a single-photon laser induced fluorescence (LIF) instrument was used to measure NO (Rollins et al., 2020). A high sensitivity chemiluminescent NO instrument fitted with a gold catalyst (NO_yO_3) was used to quantify NO and NO_y (Fahey et al., 1985; Fontijn et al., 1970; Ridley and Grahek, 1990; Ridley and Howlett, 1974; Ryerson et al., 1999).

3 HONO calibration source characterization

3.1 $NaNO_2$-coated reaction device

Previous calibration methods required a 1-2 g bed of loose crystalline $NaNO_2$ to generate high mixing ratios of HONO, but only consumed a minimal amount of $NaNO_2$ from the total supply before being thrown away (Febo et al., 1995; Roberts et al., 2010). At maximum, our $NaNO_2$ coated PFA reaction devices could contain up to 60 mg of $NaNO_2$ (3.0 mL x 20 g L^{-1} $NaNO_2$ coating solution) or 40 mg of NO_2^- if there was 100 % coating efficiency. Due to the hydrophobic nature of PFA and the loss of liquid solution from the drying procedure, however, the reaction device retained only a fraction of the applied $NaNO_2$. The amount of NO_2^- present after coating the PFA devices (n = 3) was determined by rinsing with deionised water and analysis by IC-CD. An average mass of 0.53±0.27 mg NO_2^- was deposited on the surface of the PFA device, 1.3 % of the total NO_2^- applied. The quantity coated on the PFA devices was sufficient to generate stable, low mixing ratios of HONO for extended periods. To efficiently use most of the salt, we calculated how long the $NaNO_2$ coating could provide a specific calibration mixing ratio of HONO (E1). Thus, we designed and operated our coated devices based on their calculated capacity to generate a specific mixing ratio of HONO (C_{HONO}) continuously over time based on the number of moles of $NaNO_2$ deposited in the coating (n_{NaNO2}) and the total dilution flow in moles of air for that same duration (F_{air}).

$$C_{HONO} = n_{NaNO2} / F_{air} \tag{E1}$$

To generate higher mixing ratios of HONO, more $NaNO_2$ mass and/or coated surface area are required. The higher surface area of a coated glass annular denuder housed in Teflon-coated aluminum tubing was explored for use as an alternative to PFA tubing. To test this, three annular denuders were prepared using the same volume of coating solution. An average mass of 7.26±1.80 mg of $NaNO_2$ on the denuder surface was determined, 18 % of the total applied. Thus, the coated annular denuder resulted in about eighteen times more deposited $NaNO_2$ than the PFA devices, due to the higher available surface area of pattern-etched glass. Unfortunately, these devices proved unstable, as discussed below, and are expensive. The HONO output from other tubing materials were also tested (Section 3.7.2).

The lifetime of the $NaNO_2$ devices can be approximated using E1, under the assumption that a stable output of HONO is generated from the start of the experiment. At standard room temperature and pressure a device generating 2 ppbv of HONO and containing the average 0.53 mg of NO_2^- observed for the PFA device could last for up to 88 days. In practice, we observed a PFA device generating approximately 2 ppbv min^{-1} of HONO to be reliable for over four weeks during experiments performed to test the stability and reproducibility of the PFA devices (Sections 3.5, 3.6). The lifetime of the device is expected to decrease proportionally if a higher output of HONO for a given mass of $NaNO_2$ coating is required. Decreasing HONO mixing ratios on the order of a hundred pptv on hourly timescales (for an initial few ppbv of output) was used as a metric to indicate that coated reaction devices were depleted since their output was no longer stable.

3.2 HONO generation with water vapour

Prior calibration sources have exclusively reported HONO production via the acid displacement mechanism. In the mass balance experiments reported below, where we employ this mechanism, it was discovered that water vapour alone was responsible for a measurable amount of the generated HONO in the ppbv regime. Mixing ratios of HONO produced using our coated PFA reaction devices exposed to water vapour were too low to accurately measure using our NO_x analyzer (≤ 0.6 ppbv). To explore the influence of water vapour (i.e. humid air) on HONO output, we performed a series of experiments at different RH using an $NaNO_2$ coated annular denuder. The denuder generated higher HONO mixing ratios, on the order of several ppbv in 1.1 SLPM. Prior to the experiments, the calibration source unit was flushed with zero air for at least 12 hours. The absence of HCl (< 5 pptv) was confirmed with the CRDS. When the RH passing through the denuder was 0 % we observed no HONO, with signal near the detection limit of the NO_x analyzer (0.50 ± 0.48 ppbv, n = 43). When we increased the RH of the carrier gas, we observed the production of HONO, but the variation was not monotonic. At a RH of 25 % HONO output increased to 11.73 ± 0.39 ppbv (n = 35) followed by a decrease at an RH of 50 % to 8.60 ± 0.63 ppbv (n = 38). This trend is likely due to the effective Henry's Law constant of HONO in the aqueous film on the surface of the $NaNO_2$ device, due to the weak acid nature of HONO ($pK_a = 3.4$). When the humidity is higher, less HONO may be released from the surface due to the increased presence of water in which a larger equilibrium concentration of aqueous nitrite can be sustained. This contrasts with HCl (pK_a of -8), which completely dissociates in aqueous solution on the surface of the $NaNO_2$ device and facilitates the acid displacement mechanism (R2).

This is the first observation of water vapour-produced HONO. Prior calibration sources typically generated very high HONO mixing ratios from 100 ppbv up to tens of ppmv in the displacement vessel, resulting in the contribution from humid air being undetected (Febo et al., 1995; Gingerysty and Osthoff, 2020; McGrath et al., 2019; Roberts et al., 2010; VandenBoer et al., 2015; Zhou et al., 2018). The observed HONO mixing ratios from this mechanism in our experiments would likely be within error of the mass balance calculations, or indistinguishable from noise in the analytical instrumentation in prior reports. Our results suggest that the use of water vapour passed over a $NaNO_2$ coated PFA reaction device produces sub-ppbv mixing ratios of HONO for calibration of instruments making ambient observations in remote environments. Using water vapour alone, the only way to increase the HONO mixing ratios from the calibration system is to increase the available amount of $NaNO_2$, which is challenging (Sections 3.1 and 3.7.2). A more controlled approach to reach higher mixing ratios is through the acid displacement technique.

3.3 HCl emissions from custom-built PDs

To generate stable HONO mixing ratios using an $NaNO_2$ reaction device on the order of a few to tens of ppbv, a stable source of HCl is required. The HCl generated from custom-made PDs was therefore evaluated as a function of solution concentration contained (1.2 – 6 M), temperature (30 – 60 °C), and stability by CRDS (Table 1, Figure S6). Custom-made PDs of different concentration and lengths were tested for their ability to produce a range of HONO mixing ratios. Custom-made

PDs have been previously demonstrated in our work to provide a stable emission source of HCl (MacInnis et al., 2016). The HCl output was found to be temperature-dependent and increased exponentially with temperature, as expected from theory (Section S2). However, as the PD was ramped to higher temperatures (> 50 °C) the permeation rate became more unstable, with a resulting settling time of about an hour as the materials from the permeation oven apparatus re-equilibrated (Figure S7). Since the HCl PDs were observed to be most stable at 30 °C and 40 °C, these temperatures were considered optimal to generate the stable HONO mixing ratios. Note that the HONO mixing ratios in the 100 sccm flow exiting the reaction device range from 9.7 to 72 ppbv (Table 1), which are much lower than all prior calibration sources, enabling easy dilution to reach environmentally relevant HONO mixing ratios for instrument calibration or experimental applications.

Table 1. Description of custom-made HCl permeation devices used to generate HONO. Zero air-corrected mixing ratios of emitted HCl and generated HONO using a single $NaNO_2$-coated PFA reaction device were measured with the heated Al-block at 40 °C in 1.1. SLPM. The variability reported for each observation represents one standard deviation from the mean (n = 30 to 60 using 1-minute averaged data).

PD	HCl (M)	Date of Manufacture (YYYY/MM)	PFA Device (cm)	PTFE Plug (cm)	HCl (ppbv)	HONO (ppbv)	Measured Date (YYYY/MM)
PD-1	1.2	2017/04	9.92	0.60	0.58 ±0.01	0.95 ±0.51	2019/10
PD-6a	6	2017/04	9.41	0.70	0.21 ±0.01	0.88 ±0.4	2019/10
PD-6b	6	2019/04	9.11	0.75	2.0 ±0.01	2.8 ±0.41	2019/11
PD-6c	6	2019/04	9.65	0.70	5.0 ±0.3	6.2 ±0.5	2019/11

Two newly made 6 M HCl PDs (-6b and -6c) were found to emit different, yet highly stable (e.g. ±0.01 ppbv), mixing ratios at identical oven temperatures (Figure S6). This demonstrates potential variability with each new device due to inconsistent results during custom fabrication compared to commercial PDs. The most likely source of such differences in output is variability in our sealing of the PTFE plugs resulting in increased emission rates. In any case, the PDs remain stable with less than 10 % relative standard deviation. In comparison, commercial device emission rates are often certified within ±30 %. The emission rates of commercial PDs are certified through measurement by gravimetric weight loss over time (ng min^{-1}). A commercial ¼" (64 mm) Teflon HCl PDs of 6.55 M certified to emit 1905 ± 520 ppbv in 100 sccm flow at 40 ˚C (RSD = 27.3 %; VICI Metronics, Inc.; Poulsbo, WA), has this output variance due to the co-emission of water and propagated measurement uncertainties. A lower variance in the emitted HCl was observed from our custom-made PDs when we quantified HCl directly by either CRDS or IC-CD. Custom-built PDs were therefore chosen over commercial PDs due to their demonstrated stability and low cost. It was found that HCl outputs of the custom-PDs slowly diminished over time, which emphasizes the need for regular calibrations. For example, the HCl output from two-year-old PD-6a emitted

0.21±0.01 ppbv in 1.1 SLPM in comparison to 2.0±0.01 ppbv when it was newly made, which decreased the resulting HONO generation in the reaction device. Similar results have been observed in calibrations with PDs of aqueous NH_3 and HNO_3 solutions decreasing by ~30 % during two years of storage, as well as for carbonyl sulfide (Fried et al., 1998; Neuman et al., 2003). Despite the decreasing HCl output over a year or more of use, HCl PDs act as a stable acid source on the order of weeks, producing consistent HCl output to subsequently generate stable HONO, even when removed from the permeation oven or stored for up to two months. Overall, it is difficult to replicate PD emission rates using the same HCl concentration and material dimensions for a custom-PD. The custom-built PD seals can be altered by replacing the PTFE plug by crimping the ends of heated-to-pliability PFA tubing to form welded polymer ends (Section S2). Such an approach is expected to improve the reproducibility of the custom-device emission rates but is beyond the scope of this work to explore in more detail.

3.4 Acid displacement to generate HONO

Two techniques were used to assess the reaction completion between HCl and $NaNO_2$ in the calibration system. We applied a mass balance approach that combined the CRDS measurement of HCl, our NO_x analyzer HONO measurement, and IC-CD quantitation of these acids scrubbed into 1 mM NaOH. The displacement efficiency was further confirmed by simultaneous observation of HCl and HONO by acetate quadrupole CIMS.

3.4.1 Mass balance of HONO generated

Experiments were conducted to confirm that HONO can be generated by introducing only humid air (50 % RH) within the $NaNO_2$ devices without the presence of HCl. In humid air, we observed HONO levels above the detection limit (DL) of the NO_x analyzer. A single PFA device exposed to humid air (50 % RH) released up to 0.61 ppbv of HONO – equivalent to 77 % of the total HONO generated when coupled with an HCl PD (Table 2). The reaction of the humidified $NaNO_2$-coated device, resulting in the release of HONO, implies formation of NaOH. Further speculation on the reaction mechanism is beyond the scope of this work. Given the existing challenge in producing low mixing ratios of HONO in the pptv range, it appears that these can be reached most easily without the use of an HCl PD in our calibration system, while higher mixing ratios necessitate the addition of HCl (Section 3.7). The NO_x analyzer signal was indistinguishable from zero when the $NaNO_2$ reaction device was absent, but all other conditions were matched. This demonstrates that HONO was generated only within the $NaNO_2$ reaction device.

The total flow for all mass balance experiments was 1.1 SLPM (Fig. 1) with zero air flows replacing those typically carrying reagents when they were removed. We observed that the HONO output from the reaction devices was greater than the HCl input from the PDs, confirming that another chemical reaction was generating the remaining HONO (Table 2). Mass balance could only be achieved when accounting for the HONO generated by the $NaNO_2$ exposed to humid air (~50 % RH). No other acidic or ionic contaminants were present in $NaNO_2$ reaction devices or the HCl PDs when scrubbed solutions were analyzed by IC-CD. Therefore, other NO_y species that could have biased the NO_x analyzer measurement high were judged to be absent and pure HONO was generated (i.e. only NO_2^- was enhanced in calibration system flows scrubbed into 1 mM NaOH). Further investigation of the system HONO purity is presented in Section 3.7.3 which further supports this conclusion. The remainder of the HONO output from $NaNO_2$ devices quantitatively matched the HCl input to the reaction device in dry air after accounting for the water vapour production route. No HCl was observed to exit the devices, indicating unit acid displacement efficiency and reaching mass balance.

Table 2. Mass balance of measured mixing ratios of HCl entering and HONO exiting the calibration source to determine acid displacement efficiency (ADE) at 50 % RH and 40 °C. Uncertainties represent 1σ standard deviation from the mean for ≥30 min of measurements and 1σ propagated error for calculated values.

PD	HCl_{IN} (ppbv)	HONO from HCl+H_2O (ppbv)	HONO from H_2O (ppbv)	HONO from H_2O (%)	ADE (%)
PD-6a	0.08 ±0.002	0.31 ±0.15	0.24 ±0.14	77 ±45	>99
PD-6b	2.2 ±0.011	2.78 ±0.41	0.61 ±0.44	22 ±16	>99

3.4.2 CIMS Measurements

Confirmation of these observations with the quadrupole CIMS provided higher time resolution observations of HONO and HCl simultaneously. The ions monitored were m/z 35 (Cl^-) for HCl and 46 (NO_2^-) for HONO (Figure 2). The instrumental sensitivity to these two analytes is similar under this ionisation scheme (VandenBoer et al., 2013). The HONO calibration source was stabilized for 2 h before the gas stream was introduced to the CIMS. Zero measurements were taken for 15 min before and after the measurements to correct for background drift in the m/z 46 signal. Upon sampling the output of the HONO calibration source the signal at m/z 46 rapidly increased (Fig. 2). The signal of Cl^- at m/z 35 was below the detection limit throughout this period, confirming again that the HCl from the PD was entirely consumed by the $NaNO_2$ reaction device throughout the measurement period, consistent with the experiments presented above where no HCl was measured by the CRDS. Overall, the results from these assessments indicate that the HONO calibration source is generating HONO with a one to one displacement efficiency by HCl, consistent with this observation from other HONO calibration sources using higher quantities of HCl in a salt bed (Febo et al., 1995; Roberts et al., 2010), and the remainder originating from the water vapour reaction.

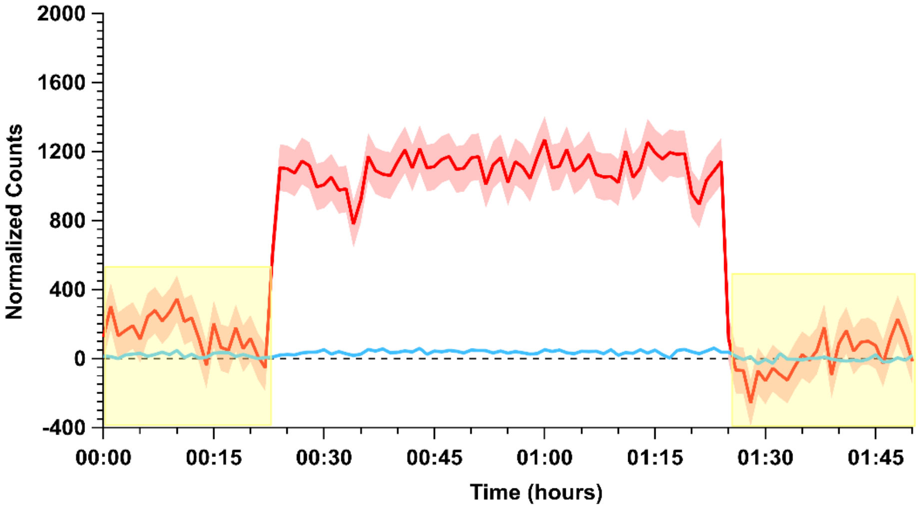

Figure 2. Conversion efficiency of HCl (blue) to HONO (red) via the acid displacement reaction on a $NaNO_2$ reaction device. The HCl PD-6a and one coated PFA device were used and measured following two hours of stabilization. The acids were observed by acetate quadrupole CIMS with time resolution of 0.50 s and averaged to 60 s. Yellow shaded regions indicate the addition of zero air to the instrument inlet for background correction, while red and blue shaded regions correspond to 1σ variance in the observations. Note that the variance in the HCl trace is similar to the width of the line.

3.5 Stability of HONO production

The time required to achieve stable HONO signals was tested by inserting HCl PD-6a and new $NaNO_2$ PFA reaction device into the calibration system, followed by flow start up. Stable HONO signals were observed within 7 h of powering on the HONO calibration system. This is 5 h longer than required to reach stable mixing ratios for a previously stabilized $NaNO_2$ device. Three trials using newly coated $NaNO_2$ reaction devices and PD-6a, once stabilized, generated an average HONO output of 2.28±0.58 ppbv, which corresponds to an RSD of 24 % between runs and an RSE of 3% (n = 2367; Figure 3). The noise observed in the stabilized HONO output in Figure 3 can be primarily attributed to the noise associated with the NO_x analyzer detector (18 of the 24 %; DL = 0.4 ppbv; 1-minute average). This conclusion is supported by the lower noise in ~2.5 ppbv HONO mixing ratios observed by the CIMS (Fig. 2, RSD of 8.1%), ACES (RSD 8.2 %), and NO_yO_3 (RSD 1.9 %). In these added observations with higher sensitivity instrumentation, the stability was equal to instrumental precision. This represents a major improvement over our previously reported calibration sources with potential for 30 % variability at a minimum (VandenBoer et al., 2013; Zhou et al., 2018).

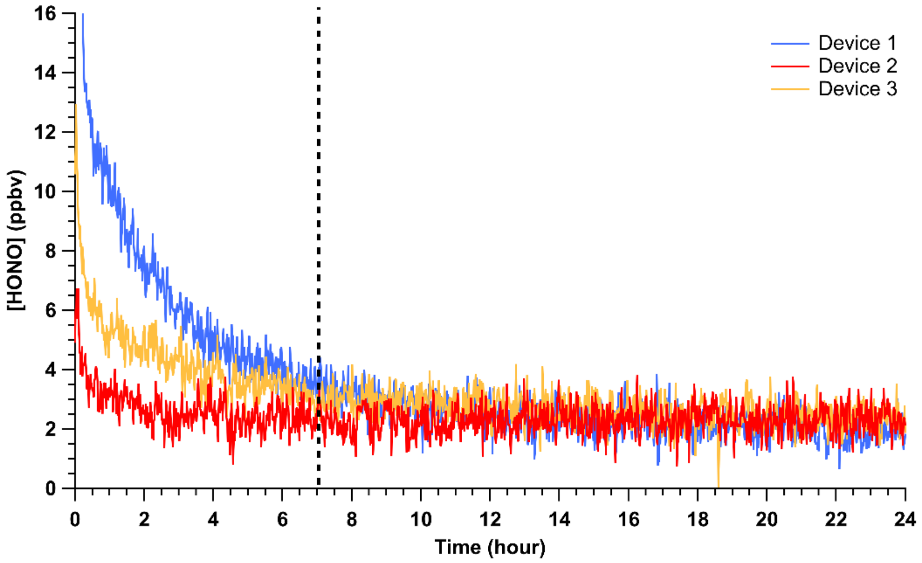

Figure 3. Mixing ratios of HONO observed using HCl PD-6a and three different, but freshly coated, $NaNO_2$ PFA reaction devices. Time zero indicates the start of HONO production in the calibration unit where no prior flow through the calibration unit existed, but all temperatures were stable at 40 °C. The vertical dashed line denotes the time where the output of the three devices are no longer statistically different from each other. Reported measurements are one-minute average data with a 30 s Kalman filter on the NO_x analyzer.

However, when the HCl output from PDs is unstable, this can interfere with the stability of the HONO generated because it is dependent on acid displacement. A common characteristic of our custom-PDs monitored by real-time CRDS measurements are short-duration increases in output over min, up to 1 h, due to reduced emission of H_2O and increased emission of HCl, resulting in transient pulses from the device (Figure 4a). The anticorrelation between HCl and H_2O is expected for a constant mass emission to result from the contained aqueous solution. A corresponding rapid increase in HONO production results from such occurrences (Figure 4b).

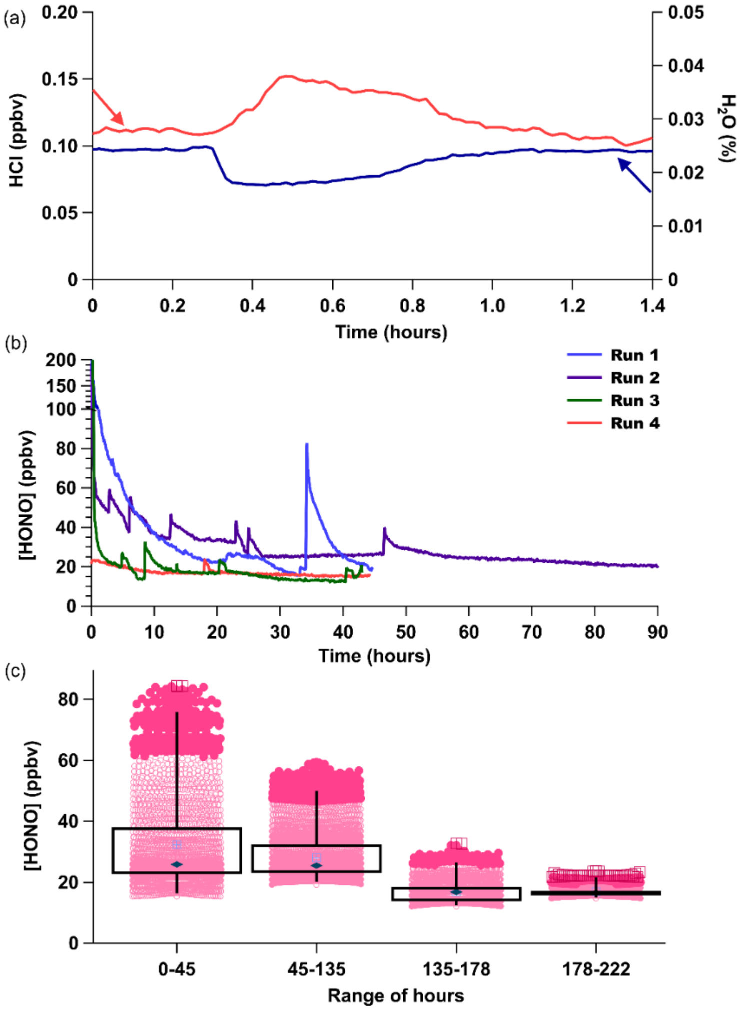

Figure 4. (a) CRDS high-resolution observation an HCl emission pulse (red) and H_2O decrease (blue) from PD-6a resulting in 50 % increase of the HCl mixing ratio emitted. (b) Time series of four consecutive measurement periods of HONO production, using only PD-6c and a new $NaNO_2$ coated reaction device in each run. (c) Box (1st and 3rd quartile) and whiskers (3σ from the mean) of HONO mixing ratios observed for the four runs are binned by duration of use for each new reaction device in hours. Mean values are indicated with a filled dark blue diamond marker, median values by the light blue crossed box marker, dark pink circles are 2σ outliers and dark red squares 3σ outliers

Commercial PD manufacturers evaluate average mass emission rates by gravimetric weight loss over several weeks at 40 °C for certification, which could include such short-term events. The HONO output from a newly made custom-HCl PD (PD-6c) over four consecutive observation periods upon insertion of a new $NaNO_2$ reaction device (Runs 1 – 4) at constant temperature (40 °C) show that the new custom-PD requires about 1 week of operation before its output is stable (Figure 4b-c). Therefore, careful preparation of PDs and $NaNO_2$ reaction devices in advance of extensive use will yield a HONO calibration source with the fastest stabilization times possible for continuous operation over a period of months. Note again, that the HONO measurements for Figures 4b-c were performed several months before the HCl emission rate for PD-6c presented in Table 1 were obtained, resulting in high HONO mixing ratios produced in these experiments.

3.6 Reproducibility and robustness

The HONO calibration system was designed to not only be stable, but reproducible in its output of HONO for a given PD and any $NaNO_2$ reaction device, resulting in robust portability. We tested the reproducibility, and therefore robustness, of the HONO calibration system by putting it through a series of experiments designed to simulate transport to, and use in, the field. Further assessment of its reproducibility by measuring the output with different $NaNO_2$ reaction devices and HCl PDs were also made.

3.6.1 Field transport simulations

Simulations of field transportation subjected the system to full disassembly and reassembly of the acid displacement and permeation oven setup. In addition, for some experiments the calibration unit was transported on a lab cart over very rough flooring to simulate vibrations experienced for real use when transported using rolling carts, mobile labs, or aircraft. For the first eight simulations PD-6a and one $NaNO_2$ coated reaction device were used over several weeks (see Table S1 for further detail). Following reassembly after the field transport simulations, the HONO calibration source was restarted, the system was equilibrated for 2 hours, and then its output measured by the NO_x analyzer (Figure 5). An Na_2CO_3 coated annular denuder was incorporated into the middle of five of the eight trial experiments for an hour to determine whether any NO_x was being generated between restarts and its associated variability (FS1-FS5; Table S1). No measurable NO_x was detected in any of these experiments.

The average HONO mixing ratio within the eight field transport simulations (FS) ranged from 1.68 to 2.51 ppbv. The HONO output across all eight field simulations had an average of 2.07±0.48 ppbv (RSD = 24 %; RSE = 2 % (n = 218)). These measurements used a single $NaNO_2$ reaction device over 5 weeks of continuous operation, after which the depletion of $NaNO_2$ resulted in a decline of HONO mixing ratios. These HONO mixing ratios are similar to the average HONO output of 2.28±0.58 ppbv (RSD of 24 %; RSE of 3 % (n = 2367) from the previous measurements with PD-6a (Figure 3), which were not subject to field simulations but did use freshly coated $NaNO_2$ reaction devices. The generated HONO mixing ratios varied most between our early experiments (FS1-FS4; RSD ≥ 24 %), when first gaining experience in ensuring gas-tight connections throughout the calibration system, with improvement clearly emerging over time (FS4-FS8; RSD ≤ 10 %). The RSE values of field transport simulations had a lower RSE of 1 % compared to 3 % for the experiments that were stationary (Fig. 5), likely due to the reuse of the same $NaNO_2$ reaction device. This demonstrates that the HONO calibration source can robustly generate a reproducible mixing ratio output within 25 % of the mean during each system reconstruction if the same HCl PD is used. It is worth noting here again that most of the variance observed in HONO mixing ratio output within any of the presented trials derives from the precision of our NO_x analyzer detector (Section 3.5).

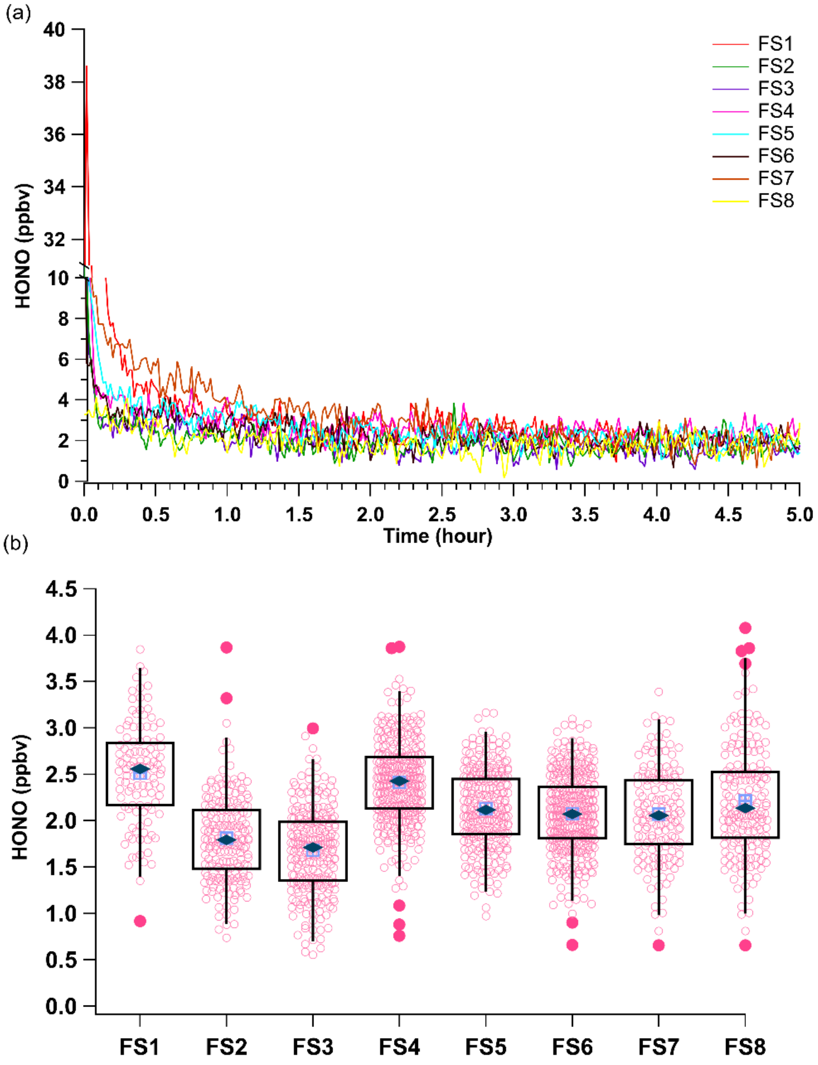

Figure 5. (a) Mixing ratios of HONO for the eight field transport simulations (FS, Table S1). All observations were background corrected by linear interpolation across the experiments using zero air before and after HONO observations and an Na_2CO_3 coated annular during (Fig. S4). (b) Box and whiskers plot of the HONO output using measurements collected after two hours of calibration source stabilization. The light blue crossed box represents the median, the dark blue diamond the mean, light pink circles the data points, dark pink circles the 3σ outliers, and the black box the 1st and 3rd quartiles of observed HONO mixing ratios. The whiskers denote the 3σ standard deviation.

3.6.2 Factors affecting reproducibility of HCl input

As shown in Table 1, PDs made with the same HCl concentration (6 M) and similar dimensions did not lead to the same HONO output, due to variability in the HCl emission rates. While it is possible for custom-made PDs to have similar HCl emissions and therefore HONO output (when using the same $NaNO_2$ device), it is difficult to achieve in practice. When making a new PD as per the methods described in Section S2, it can be difficult to replicate because the emission rate depends on the effectiveness of the plug seal. For this reason, one cannot simply make a HCl PD with plugs using the same concentration and material dimensions and necessarily expect the same output. We present an alternative Teflon welding method to overcome this limitation in Section S2 which has been successfully used for generation of VOC PDs. Regardless, the output of new HCl PDs should be quantified prior to use and not subject to extreme conditions to ensure the polymer permeability is retained.

The reproducibility of HONO output using a stable HCl PD is shown in Figure 5. The observed HONO output ranged from 1.68-2.51 ppbv (n=8, RSD = 24 %). We next tested the reproducibility for newly made HCl PDs. Two experiments used PD-6b, containing 6 M HCl (Figure S10). After a period of stabilization, the two experiments generated similar HONO mixing ratios (2.58±0.43 ppbv after 25 hrs, RSD = 16.5 %, RSE = 1.43 %, n = 792). The spikes in HONO output at 15 h and 21 h in the second experiment (green trace, Fig. S10) were likely due to pulses of HCl which we commonly observed with new PDs (e.g. Fig. 4a-b). This emphasizes our recommendation that new custom-HCl PDs should be used for an extended period prior to use for acid displacement to ensure the emission rate has stabilized.

We made another PD with 1.2 M HCl, as it emits less HCl in comparison to a PD made with 6 M HCl (Table 1), to determine the reproducibility in HONO output at lower mixing ratios. Across three experiments using a previously stabilized $NaNO_2$ device, an output of 0.69-1.12 ppbv (RSD = 53.7 %, RSE = 4.52 %, n = 143) was observed (Fig. S11). The high RSD is due to instrument noise as the HONO output approached the detection limit of the NO_x analyzer (0.4 ppbv). Nonetheless, a stable output of HONO was achieved within two hours after starting the calibration system, similar to our previous results (Fig. 5). As long as a new custom-HCl PD has been allowed adequate time to stabilize under a gas flow at constant temperature (ideally 7 days), a stable HONO output can be easily replicated within two hours of starting the resulting HONO calibration system. We recommend quantifying the HCl emissions prior to use if the PD has been stored for a long period or been subjected to extreme conditions.

3.7 Adjusting and controlling HONO mixing ratios

Increasing the mixing ratio of HCl, and the type and quantity of $NaNO_2$ reaction devices connected in series were explored as methods to adjust the HONO mixing ratio exiting the calibration system.

3.7.1 Temperature control

The HONO calibration system was designed to be tunable by adjusting the oven temperature. HCl emissions increased with increasing temperatures (30 ˚C – 60 ˚C, Fig. S6), The HONO mixing ratios increased exponentially with increasing oven temperatures (Table 3 and Fig. S12). Very low levels of HCl exited the $NaNO_2$ device (≤ 3% of HCl input), which demonstrated that there was continued near-unity acid displacement efficiency. With increasing temperature of the $NaNO_2$ reaction device in the presence of water vapour, a similar increase in HONO mixing ratio was observed, roughly doubling for every increase of 10 °C. Thus, the HONO mixing ratio output can be adjusted by changing the temperature of the Al-block with either water vapour alone or in combination with an HCl PD. Part of the observed variability in HONO emissions at 50 ˚C was contributed by the increasingly unstable emissions of HCl at this temperature (e.g. see Fig. S6). The use of multiple HCl permeation tubes in a single oven, in series, or in parallel are additional options to control the HONO mixing ratio generated in the calibration system.

Table 3. Average mixing ratios of HCl input (PD-6a), and HONO emitted from reaction with water vapour and with both reagents as function of temperature. Uncertainty denotes 1σ standard deviation from the mean of measured values.

Temperature (°C)	HCl (ppbv)	HONO from H_2O (ppbv)	Total HONO (ppbv)
30	0.230 ±0.003	0.3	0.5 ±0.4
40	0.330 ±0.007	0.7	1.0 ±0.5
50	0.660 ±0.037	1.3	2.0 ±0.5

3.7.2 HONO output with different types of $NaNO_2$-coated devices

The produced HONO mixing ratios were tested using different materials coated with $NaNO_2$ via the same methodology as the PFA devices (Section 2.1) to see if there was an improvement in output stability or increased emissions of HONO. The materials used were all cylindrical tubing with ½" (1.27 cm) inner diameters and were of similar lengths and surface area. The different materials that were tested showed similar HONO outputs (within variability), except for quartz (Table 4). The quartz tubing gave a notably lower HONO output compared to other materials. This may have been due to a poor coating efficiency on the surface, as observed visually when making this device. This is an unexpected outcome given that quartz is more hydrophilic than PFA. That we observed similar HONO outputs for the other materials could be due to the devices having the same internal surface area coated with $NaNO_2$, implying that HONO output is proportional to surface-available $NaNO_2$.The inside of a PFA device was etched manually every few mm in concentric circles in an attempt to increase the surface availability of $NaNO_2$, but no change HONO output was observed compared to the unetched device.

Table 4. Average measured HONO mixing ratios (ppbv) using different ½" inner diameter tubing. All results at 40 ˚C and using same HCl PD (PD-6c). Variability shown is 1σ from the mean.

Device material	HONO (ppbv)
PFA	6.20 ±0.50

Etched PFA	5.68 ±0.71
Stainless Steel	6.75 ±0.83
Nylon	6.06 ±0.61
Quartz	3.72 ±0.55

Two additional methods were tested to increase the available surface area in the $NaNO_2$ device: increasing the number of coated PFA reaction devices in series and using an annular denuder. The HONO output with two PFA devices connected in series increased when using either 2.0 ppbv (PD-6b) or 5.0 ppbv of HCl (PD-6c) at 40 ˚C and 50 % RH. We did not observe HCl breakthrough at the exit of the first PFA device, indicating that the increased HONO mixing ratio is the result of the water vapour reaction. We observed variability in the amount of HONO produced between the four PFA devices, ranging from 0.8 to 1.3 ppbv per device.

More HONO can be generated using the same PDs in conjunction with an annular denuder, which has a larger internal surface area of 3063 cm^2 compared to 388 cm^2 for the PFA device. HONO emissions using PD-6c and an annular denuder produced a factor of four higher mixing ratio 24.5 ±1.0 ppbv compared to 6.2 ±0.5 ppbv with a single PFA device, but it required 45 hours to stabilize. Again, the increase is due to promotion of the water vapour reaction. The major drawback of using an annular denuder is that the output drifted to lower mixing ratios continuously at a rate of a few ppbv per hour, which was not a feature of the PFA devices (Figure 6). The HONO output over any 4 hour period was reasonably stable (within 0.5 ppbv) following the first 24 hours of stabilization time, which suggests that a $NaNO_2$ coated annular denuder could be viable for short duration HONO calibrations if a secondary quantitative method is available to confirm its output (e.g. a NO_x analyzer with a quantified HONO conversion efficiency). Overall, using a $NaNO_2$ coated annular denuder can provide higher HONO outputs than using PFA devices but requires at least daily independent verification.

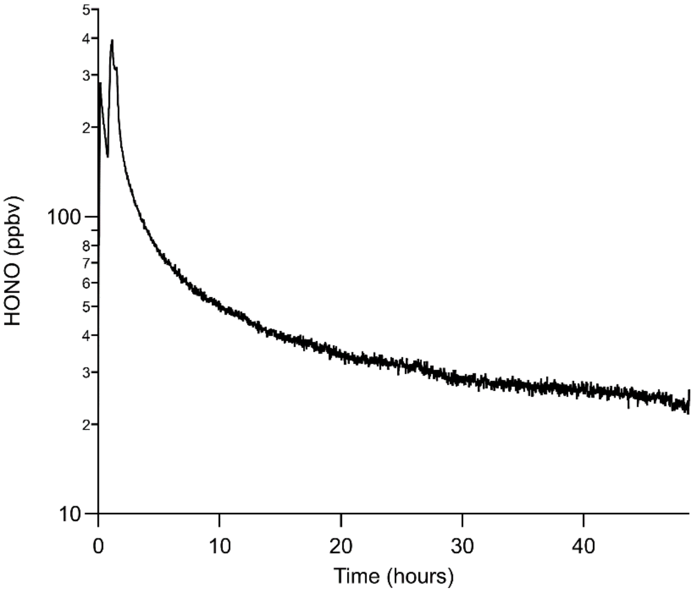

Figure 6. Mixing ratio of HONO produced from a $NaNO_2$ coated annular denuder using PD-6c. Time zero is when HCl was first introduced to the annular denuder at 50 % RH. Note that HONO mixing ratios are on a log scale.

3.7.3 Purity of the HONO output

Previous work has demonstrated that there can be a notable NO_x impurity when generating HONO via the acid displacement method (Febo et al., 1995). To test the purity of the calibration source, the HONO output was analysed by additional reactive nitrogen, NO_x, and NO_y instrumentation. For these experiments, we used a 6 M HCl PD and two PFA devices in series in a 40 °C calibration system, which was determined to have an output of 770 pptv of HONO. First, the output was analysed by an I^- ToF CIMS and found no evidence for any detectable amounts of other nitrogen containing species (e.g. $ClNO_2$, ClNO, HNO_3; Figure S13) except for HONO (Neuman et al., 2016; Veres et al., 2020). The I^- TOF CIMS is not sensitive to NO or NO_2, so further measurements were made with our Mo-catalyst NO_x analyzer, a cavity-enhanced absorption spectrometer (Min et al., 2016), and a gold-catalyst NO_y instrument (Fahey et al., 1985; Fontijn et al., 1970; Ridley and Grahek, 1990; Ridley and Howlett, 1974; Ryerson et al., 1999), which determined that NO_2 impurities were at or below 10 % of the generated HONO based on the detection precisions of the latter two instruments. Finally, we quantified NO impurities using a single-photon LIF instrument, which is sensitive to sub-pptv levels of NO (Rollins et al., 2020). We observed NO at 5.5 % of the measured HONO signal (42 versus 770 pptv). Examination of our modified NO_x analyzer experiments using the same calibration system configuration revealed 6 % NO on average compared to the observed HONO (ca. 6-9 ppbv), consistent with the LIF measurements. In contrast, when using a $NaNO_2$-coated annular denuder with the same HCl PD, our modified NO_x analyzer observed NO/HONO to decrease to 2%.

Recent work, using an analogous HONO calibration system, has found high production of NO, NO_2 and ClNO (> 10 %) when HCl input to loose $NaNO_2$ was > 4 ppmv (Gingerysty and Osthoff, 2020). We observed similarly high output of NO when the HCl input was increased to 2.4 ppmv through the $NaNO_2$-coated devices. Under these conditions, the impurity may be due to self-reactions of HONO at high mixing ratios, as seen in other packed or stirred $NaNO_2$ salt beds (Febo et al., 1995). NO impurities at HONO mixing ratios below 100 ppbv in the salt bed may result from other heterogeneous processes generating NO in the lower HONO production regime. It may be that such small absolute quantities of NO have been produced in all prior calibration sources, but as the mixing ratio of HONO produced has been reduced in our calibration system, that this impurity increases in a relative sense. The purity of the calibration source when generating < 100 ppbv in the salt bed is ≥ 90 % HONO, with the remainder accounted for as NO and/or NO_2.

3.8 Context and application

The RSE of our stable HONO output is < 2.5% and less than previous HCl acid displacement calibration source adaptations (VandenBoer et al., 2013; Zhou et al., 2018). Potential reasons for the improved stability in HONO output are the stable production of HCl from custom-PDs and that the calibration system presented in the current work eliminated the need for solid $NaNO_2$ powder, which is prone to disturbance of equilibrated emissions through vibrations that can result in changes up to a factor of two in mixing ratio output (VandenBoer et al., 2013; Zhou et al., 2018). The RSD at the low HONO mixing ratios in this work are larger than reported by Febo et al. (1995), who generated much larger mixing ratios, but did not specify the measurement details of their NO_x analyzer to facilitate true comparison. The greatest accuracy possible for this calibration source requires quantitation of the HONO output by a separate analytical method (e.g. IC-CD) and should not rely on the assumption that the HONO generated is equivalent to the HCl delivered into the reaction device due to the additional production mechanism driven by water vapour. While the output of this system is demonstrated to be highly reproducible with a given HCl PD, we recommend regular calibration.

4 Conclusions

We present a cost-effective, portable, stable, tunable, and robust gas-phase HONO calibration source. We utilised both a water vapour only, as well as its combination with the acid displacement reaction of HCl, with sodium nitrite ($NaNO_2$) coated on the inner wall of a short length of PFA tubing within a machined Al-block permeation oven to produce a stable and continuous supply of high purity gaseous HONO. We demonstrated for the first time that HONO was produced by humid air in the $NaNO_2$ reaction device, such that the HONO output was consistently higher than the HCl input. If a HONO calibration source in the pptv range was desired, it could be achieved easily by using only humid air flowing through an $NaNO_2$ coated reaction device. The output of this HONO calibration source spans the range of environmentally relevant mixing ratios - from pptv levels to tens of ppbv. This will allow instruments to be calibrated and/or intercompared using their standard atmospheric sampling parameters, without the need for excessive - or impossible – dilution; nor additional pumps, valves, and mass flow controllers.

We demonstrated that our HONO calibration system mixing ratio was tunable by adjusting the temperature of the permeation oven to control the water vapour reaction, as well as HCl emission rates from PDs. The HONO calibration source was designed to facilitate multiple calibrant concentrations, as the four holes in the aluminium heating block (Fig. S3) allows for the operation of parallel HONO sources if desired. The most stable HONO output was achieved using $NaNO_2$ coated PFA devices at 40 °C, with HONO mixing ratios of 2.28±0.58 ppbv (RSD of 24 % and RSE of 3%, n = 8) that were reliably reproduced following complete assembly of the system. From our wide range of instrumental observations, the output of the source appears to be constant within ±10 % or better. The purity of HONO source was determined to be >90%, and while lower than previous work (99.5%, Febo *et al.* (1995)) this may be a consequence of previously unseen side reactions of increasing importance at the low HONO mixing ratios generated. We consider this an acceptable trade-off for a robust field deployable HONO source unit. The resulting system can be disassembled, transported, and reassembled to produce the same HONO mixing ratios reproducibly, without the need for regular maintenance – where the same PD is retained between rebuilds. Custom-made HCl PDs are prone to variability in emission rates, both between similarly made PDs and over time, and therefore require regular characterization, but can provide a stable output over the order of weeks. While higher HONO outputs were possible to generate using an $NaNO_2$ coated annular denuder for any given HCl PD, the outputs were unstable over time.

This HONO calibration instrument provides a universal solution to gas-phase HONO calibrations suitable for the full range of atmospheric instrumentation used for outdoor or indoor field measurements or laboratory experiments. This calibration unit could be used to intercompare the responses/measurements between HONO instruments to investigate and validate accuracy and precision of their ambient measurements in addition to identifying and isolating potential interferences (Crilley et al., 2019). We anticipate it will also find utility in the generation of isotopically-labelled HONO for the emerging exploration of stable-isotopic composition of HONO and its relation to the wide variety of suspected atmospheric HONO sources (Chai et al., 2019).

Author Contributions

TV, CY, and RW conceptualized the calibration source. TV and CY supervised the experiments, acquired the funding, and provided the resources to support this work. TV designed the experiments, guided the investigations, and managed the project. ML constructed the custom PDs under the guidance of TF and LS. ML and LS built the custom permeation oven and analyzed IC-CD samples. LC and ML performed the mass balance, reaction device, and purity experiments. LC and ML established and validated the methodologies. IB, AN, DR, PV, RW and CW provided instrumental resources, and performed measurements included in the stability and purity experiments. LS created the schematics and wrote the detailed description of the custom permeation oven. ML constructed the reaction devices, performed part - or the entirety - of the experiments, and prepared the manuscript with contributions from all authors. All authors participated in data analysis, and the review and editing of the manuscript.

The authors declare that they have no conflict of interest.

Acknowledgments

The Authors thank E Gaona-Colman for help in collecting the CIMS data, as well as J Liggio and J Wentzell for enabling the use of and training on the quadrupole CIMS. ML acknowledges research support from an NSERC Undergraduate Student Research Award, and travel support through a York University Fieldwork Cost Fund award, respectively. LS acknowledges research support from the Harold I Schiff graduate award in Atmospheric Chemistry. LC and TV acknowledge travel support from the York University Faculty of Science Junior Faculty Fund. CY acknowledges support for this project through an NSERC Discovery Grant. TV and CY acknowledge funding for the instrumentation developed and used in this work provided by the Alfred P. Sloan Foundation Chemistry of Indoor Environments program (G-2018-11051).

Data Availability

Datasets are presented in figures and summarized in tables throughout the main manuscript and supporting information. Raw data from these resources are available from the corresponding author upon request.

References

Braman, R. S. and de la Cantera, M. A.: Sublimation sources for nitrous acid and other nitrogen compounds in air, Anal. Chem., 58(7), 1533–1537, doi:10.1021/ac00298a059, 1986.

Chai, J., Miller, D. J., Scheuer, E., Dibb, J., Selimovic, V., Yokelson, R., Zarzana, K. J., Brown, S. S., Koss, A. R., Warneke, C. and Hastings, M.: Isotopic characterization of nitrogen oxides (NO_x), nitrous acid (HONO), and nitrate (pNO_3^-) from laboratory biomass burning during FIREX, Atmos. Meas. Tech., 12, 6303–6317, doi:10.5194/amt-2019-229, 2019.

Cheng, P., Cheng, Y., Lu, K., Su, H., Yang, Q., Zou, Y., Zhao, Y., Dong, H., Zeng, L. and Zhang, Y.: An online monitoring system for atmospheric nitrous acid (HONO) based on stripping coil and ion chromatography, J. Environ. Sci. (China), 25(5), 895–907, doi:10.1016/S1001-0742(12)60251-4, 2013.

Collins, D. B., Hems, R. F., Zhou, S., Wang, C., Grignon, E., Alavy, M., Siegel, J. A. and Abbatt, J. P. D.: Evidence for gas-surface equilibrium control of indoor nitrous acid, Environ. Sci. Technol., 52(21), 12419–12427, doi:10.1021/acs.est.8b04512, 2018.

Crilley, L. R., Kramer, L., Pope, F. D., Whalley, L. K., Cryer, D. R., Heard, D. E., Lee, J. D., Reed, C. and Bloss, W. J.: On the interpretation of in situ HONO observations via photochemical steady state, Faraday Discuss., 189, 191–212, doi:10.1039/c5fd00224a, 2016.

Crilley, L. R., Kramer, L. J., Ouyang, B., Duan, J., Zhang, W., Tong, S., Ge, M., Tang, K., Qin, M., Xie, P., Shaw, M. D., Lewis, A. C., Mehra, A., Bannan, T. J., Worrall, S. D., Priestley, M., Bacak, A., Coe, H., Allan, J., Percival, C. J., Popoola, O. A. M., Jones, R. L. and Bloss, W. J.: Intercomparison of nitrous acid (HONO) measurement techniques in a megacity (Beijing), Atmos. Meas. Tech., 12, 6449–6463, doi:10.5194/amt-12-6449-2019, 2019.

Dawe, K. E. R., Furlani, T. C., Kowal, S. F., Kahan, T. F., VandenBoer, T. C. and Young, C. J.: Formation and emission of hydrogen chloride in indoor air, Indoor Air, 29(1), doi:10.1111/ina.12509, 2019.

Elshorbany, Y. F., Kurtenbach, R., Wiesen, P., Lissi, E., Rubio, M., Villena, G., Gramsch, E., Rickard, A. R., Pilling, M. J. and Kleffmann, J.: Oxidation capacity of the city air of Santiago, Chile, Atmos. Chem. Phys., 9(6), 2257–2273, doi:10.5194/acp-9-2257-2009, 2009.

Fahey, D. W., Eubank, C. S., Hübler, G. and Fehsenfeld, F. C.: Evaluation of a catalytic reduction technique for the measurement of total reactive odd-nitrogen NO_y in the atmosphere, J. Atmos. Chem., 3(4), 435–468, doi:10.1007/BF00053871, 1985.

Febo, A., Perrino, C., Gherardi, M. and Sparapani, R.: Evaluation of a high-purity and high-stability continuous generation system for nitrous acid, Environ. Sci. Technol., 29(9), 2390–2395, doi:10.1021/es00009a035, 1995.

Febo, A., Perrino, C. and Allegrini, I.: Measurement of nitrous acid in Milan, Italy, by DOAS and diffusion denuders, Atmos. Environ., 30(21), 3599–3609, doi:10.1016/1352-2310(96)00069-6, 1996.

Fontijn, A., Sabadell, A. J. and Ronco, R. J.: Homogeneous chemiluminescent measurement of nitric oxide with ozone: Implications for continuous selective monitoring of gaseous air pollutants, Anal. Chem., 42(6), 575–579, doi:10.1021/ac60288a034, 1970.

Fried, A., Henry, B. and Sewell, S.: Potential calibration errors in carbonyl sulfide permeation devices: Implications for atmospheric studies, J. Geophys. Res. Atmos., 103(D15), 18895–18906, doi:10.1029/98JD00620, 1998.

Gall, E. T., Griffin, R. J., Steiner, A. L., Dibb, J., Scheuer, E., Gong, L., Rutter, A. P., Cevik, B. K., Kim, S., Lefer, B. and Flynn, J.: Evaluation of nitrous acid sources and sinks in urban outflow, Atmos. Environ., 127, 272–282, doi:10.1016/j.atmosenv.2015.12.044, 2016.

Gingerysty, N. J. and Osthoff, H. D.: A compact , high-purity source of HONO validated by Fourier transform infrared and thermal dissociation cavity ring-down spectroscopy, Atmos. Meas. Tech. Discuss., 1–20, doi:10.5194/amt-2020-92, 2020.

Gligorovski, S.: Nitrous acid (HONO): An emerging indoor pollutant, J. Photochem. Photobiol. A Chem., 314, 1–5, doi:10.1016/j.jphotochem.2015.06.008, 2016.

Gómez Alvarez, E., Wortham, H., Strekowski, R., Zetzsch, C. and Gligorovski, S.: Atmospheric photosensitized heterogeneous and multiphase reactions: From outdoors to indoors, Environ. Sci. Technol., 46(4), 1955–1963, doi:10.1021/es2019675, 2012.

Harris, G. W., Carter, W. P. L., Winer, A. M., Pitts, J. N., Platt, U. and Perner, D.: Observations of Nitrous Acid in the Los Angeles Atmosphere and Implications for Predictions of Ozone—Precursor Relationships, Environ. Sci. Technol., 16(7), 414–419, doi:10.1021/es00101a009, 1982.

Heland, J., Kleffmann, J., Kurtenbach, R. and Wiesen, P.: A new instrument to measure gaseous nitrous acid (HONO) in the atmosphere, Environ. Sci. Technol., 35(15), 3207–3212, doi:10.1021/es000303t, 2001.

Honrath, R. E., Lu, Y., Peterson, M. C., Dibb, J. E., Arsenault, M. A., Cullen, N. J. and Steffen, K.: Vertical fluxes of NOx, HONO, and HNO_3 above the snowpack at Summit, Greenland, Atmos.

Environ., 36(15–16), 2629–2640, doi:10.1016/S1352-2310(02)00132-2, 2002.

Kasibhatla, P., Sherwen, T., Evans, M. J., Carpenter, L. J., Reed, C., Alexander, B., Chen, Q., Sulprizio, M. P., Lee, J. D., Read, K. A., Bloss, W., Crilley, L. R., Keene, W. C., Pszenny, A. A. P. and Hodzic, A.: Global impact of nitrate photolysis in sea-salt aerosol on NO_x, OH, and O_3 in the marine boundary layer, Atmos. Chem. Phys., 18(15), 11185–11203, doi:10.5194/acp-18-11185-2018, 2018.

Kim, S., VandenBoer, T. C., Young, C. J., Riedel, T. P., Thornton, J. A., Swarthout, B., Sive, B., Lerner, B., Gilman, J. B., Warneke, C., Roberts, J. M., Guenther, A., Wagner, N. L., Dubé, W. P., Williams, E. and Brown, S. S.: The primary and recyling source of OH during the NACHTT-2011 campaign: HONO as an important OH primary source in the wintertime, J. Geophys. Res. Atmos., 119, 6886–6896, doi:10.1002/2013JD021186, 2014.

Kleffmann, J.: Daytime sources of nitrous acid (HONO) in the atmospheric boundary layer, ChemPhysChem, 8(8), 1137–1144, doi:10.1002/cphc.200700016, 2007.

Kleffmann, J. and Wiesen, P.: Technical Note: Quantification of interferences of wet chemical HONO LOPAP measurements under simulated polar conditions, Atmos. Chem. Phys., 8(22), 6813–6822, doi:10.5194/acp-8-6813-2008, 2008.

Kleffmann, J., Benter, T. and Wiesen, P.: Heterogeneous reaction of nitric acid with nitric oxide on glass surfaces under simulated atmospheric conditions, J. Phys. Chem. A, 108(27), 5793–5799, doi:10.1021/jp040184u, 2004.

Kleffmann, J., Lörzer, J. C., Wiesen, P., Kern, C., Trick, S., Volkamer, R., Rodenas, M. and Wirtz, K.: Intercomparison of the DOAS and LOPAP techniques for the detection of nitrous acid (HONO), Atmos. Environ., 40(20), 3640–3652, doi:10.1016/j.atmosenv.2006.03.027, 2006.

Lee, B. H., Wood, E. C., Herndon, S. C., Lefer, B. L., Luke, W. T., Brune, W. H., Nelson, D. D., Zahniser, M. S. and Munger, J. W.: Urban measurements of atmospheric nitrous acid: A caveat on the interpretation of the HONO photostationary state, J. Geophys. Res. Atmos., 118(21), 12274–12281, doi:10.1002/2013JD020341, 2013.

Lee, J. D., Whalley, L. K., Heard, D. E., Stone, D., Dunmore, R. E., Hamilton, J. F., Young, D. E., Allan, J. D., Laufs, S. and Kleffmann, J.: Detailed budget analysis of HONO in central London reveals a missing daytime source, Atmos. Chem. Phys., 16(5), 2747–2764, doi:10.5194/acp-16-2747-2016, 2016.

Liu, J., Li, S., Zeng, J., Mekic, M., Yu, Z., Zhou, W., Loisel, G., Gandolfo, A., Song, W., Wang, X., Zhou, Z., Herrmann, H., Li, X. and Gligorovski, S.: Assessing indoor gas phase oxidation capacity through real-time measurements of HONO and NO_x in Guangzhou, China, Environ. Sci. Process. Impacts, 21(8), 1393–1402, doi:10.1039/c9em00194h, 2019.

MacInnis, J. J., VandenBoer, T. C. and Young, C. J.: Development of a gas phase source for perfluoroalkyl acids to examine atmospheric sampling methods, Analyst, 141(12), doi:10.1039/c6an00313c, 2016.

McGrath, D. T., Ryan, M. D., Macinnis, J. J., Vandenboer, T. C., Young, C. J. and Katz, M. J.: Selective decontamination of the reactive air pollutant nitrous acid via node-linker cooperativity in a metal-organic framework, Chem. Sci., 10(21), 5576–5581, doi:10.1039/c9sc01357a, 2019.

Min, K. E., Washenfelder, R. A., Dubé, W. P., Langford, A. O., Edwards, P. M., Zarzana, K. J., Stutz, J., Lu, K., Rohrer, F., Zhang, Y. and Brown, S. S.: A broadband cavity enhanced absorption spectrometer for aircraft measurements of glyoxal, methylglyoxal, nitrous acid, nitrogen dioxide, and water vapor, Atmos. Meas. Tech., 9(2), 423–440, doi:10.5194/amt-9-423-2016, 2016.

Mitchell, G. D.: A review of permeation tubes and permeators, Sep. Purif. Methods, 29(1), 119–128, doi:10.1081/SPM-100100005, 2000.

Mushinski, R. M., Phillips, R. P., Payne, Z. C., Abney, R. B., Jo, I., Fei, S., Pusede, S. E., White, J. R., Rusch, D. B. and Raff, J. D.: Microbial mechanisms and ecosystem flux estimation for aerobic NO_y emissions from deciduous forest soils, Proc. Natl. Acad. Sci. U. S. A., 116(6), 2138–2145, doi:10.1073/pnas.1814632116, 2019.

Neuman, J. A., Ryerson, T. B., Huey, L. G., Jakoubek, R., Nowak, J. B., Simons, C. and Fehsenfeld, F. C.: Calibration and evaluation of nitric acid and ammonia permeation tubes by UV optical absorption, Environ. Sci. Technol., 37(13), 2975–2981, doi:10.1021/es026422l, 2003.

Neuman, J. A., Trainer, M., Brown, S. S., Min, K. E., Nowak, J. B., Parrish, D. D., Peischl, J., Pollack, I. B., Roberts, J. M., Ryerson, T. B. and Veres, P. R.: HONO emission and production determined from airborne measurements over the Southeast U.S., J. Geophys. Res. Atmos., 121(15), 9237–9250, doi:10.1002/2016JD025197, 2016.

O'Keeffe, A. E. and Ortman, G. C.: Primary standards for trace gas analysis, Anal. Chem., 38(6), 760–763, doi:10.1021/ac60238a022, 1966.

Oswald, R., Behrendt, T., Ermel, M., Wu, D., Su, H., Cheng, Y., Breuninger, C., Moravek, A., Mougin, E., Delon, C., Loubet, B., Pommerening-Röser, A., Sörgel, M., Pöschl, U., Hoffmann, T., Andreae, M. O., Meixner, F. X. and Trebs, I.: HONO emissions from soil bacteria as a major source of atmospheric reactive nitrogen, Science (80-.)., 341(6151), 1233–1235, doi:10.1126/science.1242266, 2013.

Pinto, J. P., Dibb, J., Lee, B. H., Rappenglück, B., Wood, E. C., Levy, M., Zhang, R. Y., Lefer, B., Ren, X. R., Stutz, J., Tsai, C., Ackermann, L., Golovko, J., Herndon, S. C., Oakes, M., Meng, Q. Y., Munger, J. W., Zahniser, M. and Zheng, J.: Intercomparison of field measurements of nitrous acid (HONO) during the SHARP campaign, J. Geophys. Res. Atmos., 119(9), 5583–5601, doi:10.1002/2013JD020287, 2014.

Place, B. K., Young, C. J., Ziegler, S. E., Edwards, K. A., Salehpoor, L. and VandenBoer, T. C.: Passive sampling capabilities for ultra-trace quantitation of atmospheric nitric acid (HNO_3) in remote environments, Atmos. Environ., 191, 360–369, doi:10.1016/j.atmosenv.2018.08.030, 2018.

Pusede, S. E., VandenBoer, T. C., Murphy, J. G., Markovic, M. Z., Young, C. J., Veres, P. R., Roberts, J. M., Washenfelder, R. A., Brown, S. S., Ren, X., Tsai, C., Stutz, J., Brune, W. H., Browne, E. C., Wooldridge, P. J., Graham, A. R., Weber, R., Goldstein, A. H., Dusanter, S., Griffith, S. M., Stevens, P. S., Lefer, B. L. and Cohen, R. C.: An atmospheric constraint on the NO_2 dependence of daytime near-surface nitrous acid (HONO), Environ. Sci. Technol., 49(21), 12774–12781, doi:10.1021/acs.est.5b02511, 2015.

Reed, C., Evans, M. J., Crilley, L. R., Bloss, W. J., Sherwen, T., Read, K. A., Lee, J. D. and Carpenter, L. J.: Evidence for renoxification in the tropical marine boundary layer, Atmos. Chem. Phys., 17(6), 4081–4092, doi:10.5194/acp-17-4081-2017, 2017.

Ren, X., Gao, H., Zhou, X., Crounse, J. D., Wennberg, P. O., Browne, E. C., LaFranchi, B. W., Cohen, R. C., McKay, M., Goldstein, A. H. and Mao, J.: Measurement of atmospheric nitrous acid at Bodgett forest during BEARPEX2007, Atmos. Chem. Phys., 10(13), 6283–6294, doi:10.5194/acp-10-6283-2010, 2010.

Ridley, B. A. and Grahek, F. E.: A small, low flow, high sensitivity reaction vessel for NO chemiluminescence detectors, J. Am. Meteorol. Soc., 7, 307–311, 1990.

Ridley, B. A. and Howlett, L. C.: An instrument for nitric oxide measurements in the stratosphere, Rev. Sci. Instrum., 45(6), 742–746, 1974.

Roberts, J. M., Veres, P., Warneke, C., Neuman, J. A., Washenfelder, R. A., Brown, S. S., Baasandorj, M., Burkholder, J. B., Burling, I. R., Johnson, T. J., Yokelson, R. J. and De Gouw, J.: Measurement of HONO, HNCO, and other inorganic acids by negative-ion proton-transfer chemical-ionization mass spectrometry (NI-PT-CIMS): Application to biomass burning emissions, Atmos. Meas. Tech., 3(4), 981–990, doi:10.5194/amt-3-981-2010, 2010.

Rollins, A. W., Rickly, P. S., Gao, R.-S., Ryerson, T. B., Brown, S. S., Peischl, J. and Bourgeois, I.: Single-photon laser-induced fluorescence detection of nitric oxide at sub-parts per trillion mixing ratios, Atmos. Meas. Tech., 13, 2425–2439, doi:10.5194/amt-13-2425-2020, 2020.

Rubio, M. A., Lissi, E., Villena, G., Elshorbany, Y. F., Kleffmann, J., Kurtenbach, R. and Wiesen, P.: Simultaneous measurements of formaldehyde and nitrous acid in dews and gas phase in the atmosphere of Santiago, Chile, Atmos. Environ., 43(38), 6106–6109, doi:10.1016/j.atmosenv.2009.09.017, 2009.

Ryerson, T. B., Huey, L. G., Knapp, K., Neuman, J. A., Parrish, D. D., Sueper, D. T. and Fehsenfeld, F. C.: Design and initial characterization of an inlet for gas-phase NO_y measurements from aircraft, J. Geophys. Res., 104(D5), 5483–5492, 1999.

Sörgel, M., Trebs, I., Serafimovich, A., Moravek, A., Held, A. and Zetzsch, C.: Simultaneous HONO measurements in and above a forest canopy: Influence of turbulent exchange on mixing ratio differences, Atmos. Chem. Phys., 11(2), 841–855, doi:10.5194/acp-11-841-2011, 2011.

Sörgel, M., Trebs, I., Wu, D. and Held, A.: A comparison of measured HONO uptake and release with calculated source strengths in a heterogeneous forest environment, Atmos. Chem. Phys., 15(16), 9237–9251, doi:10.5194/acp-15-9237-2015, 2015.

Spataro, F. and Ianniello, A.: Sources of atmospheric nitrous acid: State of the science, current research needs, and future prospects, J. Air Waste Manag. Assoc., 64(11), 1232–1250, doi:10.1080/10962247.2014.952846, 2014.

Stutz, J., Kim, E. S., Platt, U., Bruno, P., Perrino, C. and Febo, A.: UV-visible absorption cross sections of nitrous acid, J. Geophys. Res. Atmos., 105(D11), 14585–14592, doi:10.1029/2000JD900003, 2000.

Stutz, J., Oh, H. J., Whitlow, S. I., Anderson, C., Dibb, J. E., Flynn, J. H., Rappenglück, B. and Lefer, B.: Simultaneous DOAS and mist-chamber IC measurements of HONO in Houston, TX, Atmos. Environ., 44(33), 4090–4098, doi:10.1016/j.atmosenv.2009.02.003, 2010.

Susaya, J., Kim, K. H., Cho, J. and Parker, D.: The controlling effect of temperature in the application of permeation tube devices in standard gas generation, J. Chromatogr. A, 1225, 8–16, doi:10.1016/j.chroma.2011.12.066, 2012.

Taira, M. and Kanda, Y.: Continuous generation system for low-concentration gaseous nitrous acid, Anal. Chem., 62(6), 630–633, doi:10.1021/ac00205a018, 1990.

Tong, S., Hou, S., Zhang, Y., Chu, B., Liu, Y., He, H., Zhao, P. and Ge, M.: Exploring the nitrous acid (HONO) formation mechanism in winter Beijing: Direct emissions and heterogeneous production in urban and suburban areas, Faraday Discuss., 189, 213–230, doi:10.1039/c5fd00163c, 2016.

Tsai, C., Spolaor, M., Fedele Colosimo, S., Pikelnaya, O., Cheung, R., Williams, E., Gilman, J. B., Lerner, B. M., Zamora, R. J., Warneke, C., Roberts, J. M., Ahmadov, R., De Gouw, J., Bates, T., Quinn, P. K. and Stutz, J.: Nitrous acid formation in a snow-free wintertime polluted rural area, Atmos. Chem. Phys., 18(3), 1977–1996, doi:10.5194/acp-18-1977-2018, 2018.

VandenBoer, T. C., Brown, S. S., Murphy, J. G., Keene, W. C., Young, C. J., Pszenny, A. A. P., Kim, S., Warneke, C., De Gouw, J. A., Maben, J. R., Wagner, N. L., Riedel, T. P., Thornton, J. A., Wolfe, D. E., Dubé, W. P., Öztürk, F., Brock, C. A., Grossberg, N., Lefer, B., Lerner, B., Middlebrook, A. M. and Roberts, J. M.: Understanding the role of the ground surface in HONO vertical structure: High resolution vertical profiles during NACHTT-11, J. Geophys. Res. Atmos., 118(17), 10155–10171, doi:10.1002/jgrd.50721, 2013.

VandenBoer, T. C., Markovic, M. Z., Sanders, J. E., Ren, X., Pusede, S. E., Browne, E. C., Cohen, R. C., Zhang, L., Thomas, J., Brune, W. H. and Murphy, J. G.: Evidence for a nitrous acid (HONO) reservoir at the ground surface in Bakersfield, CA, during CalNex 2010, J. Geophys. Res. Atmos., 119, 9093-9106, doi:10.1002/2013JD020971, 2014.

VandenBoer, T. C., Young, C. J., Talukdar, R. K., Markovic, M. Z., Brown, S. S., Roberts, J. M. and Murphy, J. G.: Nocturnal loss and daytime source of nitrous acid through reactive uptake and displacement, Nat. Geosci., 8(1), 55–60, doi:10.1038/ngeo2298, 2015.

Večeřa, Z. and Dasgupta, P. K.: Measurement of ambient nitrous acid and a reliable calibration source for gaseous nitrous acid, Environ. Sci. Technol., 25(2), 255–260, doi:10.1021/es00014a006, 1991.

Veres, P., Gilman, J. B., Roberts, J. M., Kuster, W. C., Warneke, C., Burling, I. R. and De Gouw, J.: Development and validation of a portable gas phase standard generation and calibration system for volatile organic compounds, Atmos. Meas. Tech., 3(3), 683–691, doi:10.5194/amt-3-683-2010, 2010a.

Veres, P., Roberts, J. M., Burling, I. R., Warneke, C., De Gouw, J. and Yokelson, R. J.: Measurements of gas-phase inorganic and organic acids from biomass fires by negative-ion proton-transfer chemical-ionization mass spectrometry, J. Geophys. Res. Atmos., 115(23), D23302, doi:10.1029/2010JD014033, 2010b.

Veres, P. R., Andrew Neuman, J., Bertram, T. H., Assaf, E., Wolfe, G. M., Williamson, C. J., Weinzierl, B., Tilmes, S., Thompson, C. R., Thames, A. B., Schroder, J. C., Saiz-Lopez, A., Rollins, A. W., Roberts, J. M., Price, D., Peischl, J., Nault, B. A., Møller, K. H., Miller, D. O., Meinardi, S., Li, Q., Lamarque, J. F., Kupc, A., Kjaergaard, H. G., Kinnison, D., Jimenez, J. L., Jernigan, C. M., Hornbrook, R. S., Hills, A., Dollner, M., Day, D. A., Cuevas, C. A., Campuzano-Jost, P., Burkholder, J., Bui, T. P., Brune, W. H., Brown, S. S., Brock, C. A., Bourgeois, I., Blake, D. R., Apel, E. C. and Ryerson, T. B.: Global airborne sampling reveals a previously unobserved dimethyl sulfide oxidation mechanism in the marine atmosphere, Proc. Natl. Acad. Sci. U. S. A., 117(9), 4505–4510, doi:10.1073/pnas.1919344117, 2020.

Volkamer, R., Sheehy, P., Molina, L. T. and Molina, M. J.: Oxidative capacity of the Mexico City atmosphere-Part 1: A radical source perspective, Atmos. Chem. Phys., 10(14), 6969–6991, doi:10.5194/acp-10-6969-2010, 2010.

Wang, L. and Zhang, J.: Detection of nitrous acid by cavity ring-down spectroscopy, Environ. Sci. Technol., 34(19), 4221–4227, doi:10.1021/es0011055, 2000.

Washenfelder, R. A., Roehl, C. M., McKinney, K. A., Julian, R. R. and Wennberg, P. O.: A compact, lightweight gas standards generator for permeation tubes, Rev. Sci. Instrum., 74(6), 3151–3154, doi:10.1063/1.1570949, 2003.

Ye, C., Zhou, X., Pu, D., Stutz, J., Festa, J., Spolaor, M., Tsai, C., Cantrell, C., Mauldin, R. L., Campos, T., Weinheimer, A., Hornbrook, R. S., Apel, E. C., Guenther, A., Kaser, L., Yuan, B., Karl, T., Haggerty, J., Hall, S., Ullmann, K., Smith, J. N., Ortega, J. and Knote, C.: Rapid cycling of reactive nitrogen in the marine boundary layer, Nature, 532(7600), 489–491, doi:10.1038/nature17195, 2016.

Ye, C., Zhou, X., Pu, D., Stutz, J., Festa, J., Spolaor, M., Tsai, C., Cantrell, C., Mauldin III, R. L., Weinheimer, A., Hornbrook, R. S., Apel, E. C., Guenther, A., Kaser, L., Yuan, B., Karl, T., Haggerty, J., Hall, S., Ullmann, K., Smith, J. and Ortega, J.: Tropospheric HONO distribution and chemistry in the southeastern US, Atmos. Chem. Phys., 18, 9107–9120, doi:10.5194/acp-2018-105, 2018.

Young, C. J., Washenfelder, R. A., Roberts, J. M., Mielke, L. H., Osthoff, H. D., Tsai, C., Pikelnaya, O., Stutz, J., Veres, P. R., Cochran, A. K., Vandenboer, T. C., Flynn, J., Grossberg, N., Haman, C. L., Lefer, B., Stark, H., Graus, M., De Gouw, J., Gilman, J. B., Kuster, W. C. and Brown, S. S.: Vertically resolved measurements of nighttime radical reservoirs in Los Angeles and their contribution to the urban radical budget, Environ. Sci. Technol., 46(20), 10965–10973, doi:10.1021/es302206a, 2012.

Young, C. J., Zhou, S., Siegel, J. A. and Kahan, T. F.: Illuminating the dark side of indoor oxidants, Environ. Sci. Process. Impacts, 21(8), 1229–1239, doi:10.1039/c9em00111e, 2019.

Zhang, N., Zhou, X., Shepson, P. B., Gao, H., Alaghmand, M. and Stirm, B.: Aircraft measurement of HONO vertical profiles over a forested region, Geophys. Res. Lett., 36(15), L15820, doi:10.1029/2009GL038999, 2009.

Zhang, W., Tong, S., Ge, M., An, J., Shi, Z., Hou, S., Xia, K., Qu, Y., Zhang, H., Chu, B., Sun, Y. and He, H.: Variations and sources of nitrous acid (HONO) during a severe pollution episode in Beijing in winter 2016, Sci. Total Environ., 648, 253–262, doi:10.1016/j.scitotenv.2018.08.133, 2019.

Zhou, S., Young, C. J., Vandenboer, T. C., Kowal, S. F. and Kahan, T. F.: Time-resolved measurements of nitric oxide, nitrogen dioxide, and nitrous acid in an occupied New York home, Environ. Sci. Technol., 52(15), 8355–8364, doi:10.1021/acs.est.8b01792, 2018.

Zhou, X., He, Y., Huang, G., Thornberry, T. D., Carroll, M. A. and Bertman, S. B.: Photochemical production of nitrous acid on glass sample manifold surface, Geophys. Res. Lett., 29(14), 1681, doi:10.1029/2002gl015080, 2002.

Supporting Information For:

A portable, robust, stable and tunable calibration source for gas-phase nitrous acid (HONO)

M. Lao[1], L. R. Crilley[1], L. Salehpoor[1], T. C. Furlani[1], I. Bourgeois[2,3], J. A. Neuman[2,3], A. W. Rollins[2], P. R. Veres[2], R. A. Washenfelder[2], C. C. Womack[2,3], C. J. Young[1], and T. C. VandenBoer[1, *]

[1] *Department of Chemistry, York University, Toronto, ON*
[2] *NOAA Chemical Sciences Laboratory, Boulder, CO*
[3] *Cooperative Institute for Research in Environmental Sciences, University of Colorado, Boulder, CO*

[*] *Communicating Author: tvandenb@yorku.ca*

S1. Rationale for components selected for custom-built permeation oven

The custom-built permeation oven (Figs. S1-4) is comprised of a bent aluminium bent plate (exact dimensions provided in Fig. S2), temperature controller, solid state relay, custom-built four-channel aluminium heating block, cartridge heater with integrated thermocouple, and PFA tubing connected with Swagelok® fittings. The PFA tubing was interfaced with four 2-way stainless steel valves (SS-43GS6-LL, Swagelok®) to provide gas flow independently to each channel of the oven.

Gas flow to the system is provided by a source of dry compressed air, either from a cylinder or a zero-air generator at 20 psi (138 kPa). The flow can be turned on and off to each of the four permeation channels in the aluminum heating block (20.3x7.7x7.7 cm (8x3x3"); l x w x h, Fig S2) using 2-way Swagelok® valves (Weston Valve & Fitting Ltd., Mississauga, ON). The flow through each channel is regulated by a 50-micron critical orifice (Lenox Laser, Glen Arm, MD; SS-4-VCR-2-50) housed in a ¼" Swagelok® VCR assembly (SS-4-VCR-1, SS-4-VCR-4, and SS-4-VCR-3-4TA) to ~50 sccm. The aluminum heating block (Al-block) houses four ½" PFA tubes to provide inert oven surfaces. Each are mounted within machined holes passing through the center of the short axis of the block. The machined holes are the exact size of the outer diameter of the ½" PFA tubes, resulting in firm contact between the polymer and Al. Permeation devices (PDs) can be placed inside the ½" PFA ovens to emit stable quantities of their chemical contents (Section S.2). From the input of the oven to all downstream applications, Swagelok® or Entegris PFA fittings were used to minimize sorption effects for generated gases.

The thermal system is composed of three critical components: a temperature controller, temperature sensor and a heat source. All components were purchase from either Omega™ Environmental (St. Eustache, QC) or Allied Electronics, Inc. (Fort Worth, TX). The temperature controller regulates the temperature of the system by receiving an input signal (measurement) from the thermocouple to compare to its setpoint value. An output signal will be generated if the input value is below the temperature-control setpoint. The output signal is sent to a solid-state relay which enables the heater function and increases the temperature. A proportional-integral-differential (PID) temperature controller (Omega™; CN 7823) monitors and sets the temperature of the Al block shown in Fig. S4. Using PID mode regulates the temperature of the system automatically by using feedback from the thermocouple and associated heating element to compensate for any changes relative to the set point. The PID controller is programmed to match the appropriate thermocouple (Type K used here). The PID parameters are adjusted by using the *auto tune* function to give the precise control (±0.1 °C) without overshooting the set point. The solid-state relay (Allied; SSR, D1210, Crydom) switches the heating cycle by converting the 5 V DC output from the temperature controller to 120 V AC used to operate the heating element. To dissipate the energy required for switching, the SSR was mounted on an aluminium heat sink (Allied; HS172, Crydom) and protected by a Bussman rectifier fuse (Omega^{TM}; Tron, KAX-10 A) against excess current flow that could result from a latching failure. The fuse holder (Omega^{TM}; FB-1) allows easy replacement of a blown fuse in the circuit. A cartridge heater with an integrated K-type thermocouple housed in a high-temperature incoloy sheath (Omega^{TM}; CIR, 300 W, 120 V) is inserted into a 20.3 cm (8") hole with a 3/8" internal diameter, on the long axis of the Al-block. The heater is a high watt density cartridge with maximum working temperature of 760 ºC and F-type leads with fiberglass insulation. The thermocouple measures temperature by the thermoelectric effect which results in a voltage. A K-type thermocouple consists of chromel (Ni-Cr) and alumel (Ni-Al) alloys that generates an accurate voltage in the temperature range of 0 to 1250 ºC. An upper limit on the temperature controller should be set at 150 °C to prevent thermal degradation of PFA tubing in the Al-block during use.

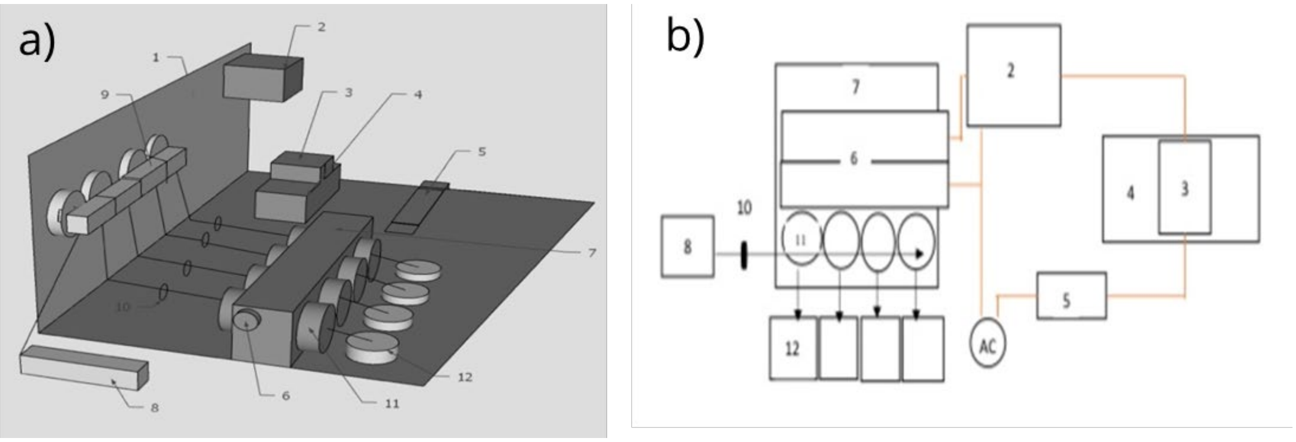

Figure S1. Three (a) and two (b) dimension layout schematics of permeation-oven components on the bent aluminium plate (1), with mounted temperature controller (2), solid state relay (3) and its heat sink (4), electrical fuse (5), cartridge heater with integrated thermocouple (6), aluminum block (7), source of dry compressed air (8), 2-way gas valve (9), critical orifice (10), PFA oven (11), and gaseous output to external system. Black lines represent PFA lines guiding gas flows throughout the system.

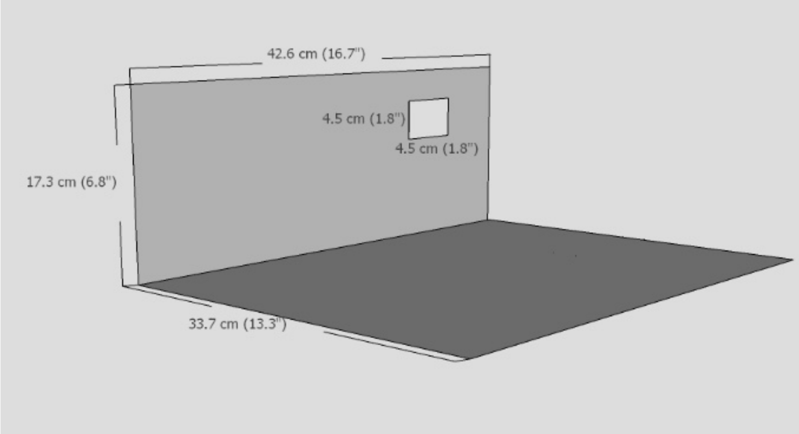

Figure S2. Dimensions of bent aluminium plate and cut-out measurements to mount the temperature controller. Further holes for valves or a holder for the water impinger were created with an electric drill on an as-needed basis.

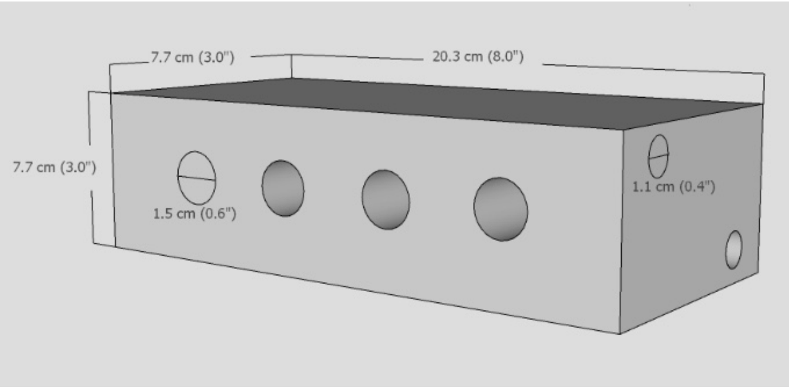

Figure S3. Dimensions and machining specifications of aluminum block oven.

S1.2. Electrical connections for temperature control feedback

Power is supplied to the entire setup from 120 V AC outlet capable of providing up to 15 A of current (Fig. S4). The temperature controller monitors the voltage signal from the thermocouple (here: yellow/+ and red/-; terminals 4 and 5, respectively; Fig. S4). When the thermocouple signal falls below the control setpoint it sends a 5 V signal (terminals 1(-) and 2(+)) to the solid-state relay (3-32 V DC input D(-) and C(+)). The solid-state relay closes the switch to deliver current to the cartridge heater leads from the AC terminals (120 V AC output A(+) and B(-); Fig. S4). The relay and cartridge heater are protected by a fuse. The entire case is grounded, with a ground wire of the power supply fixed to the bent aluminium plate.

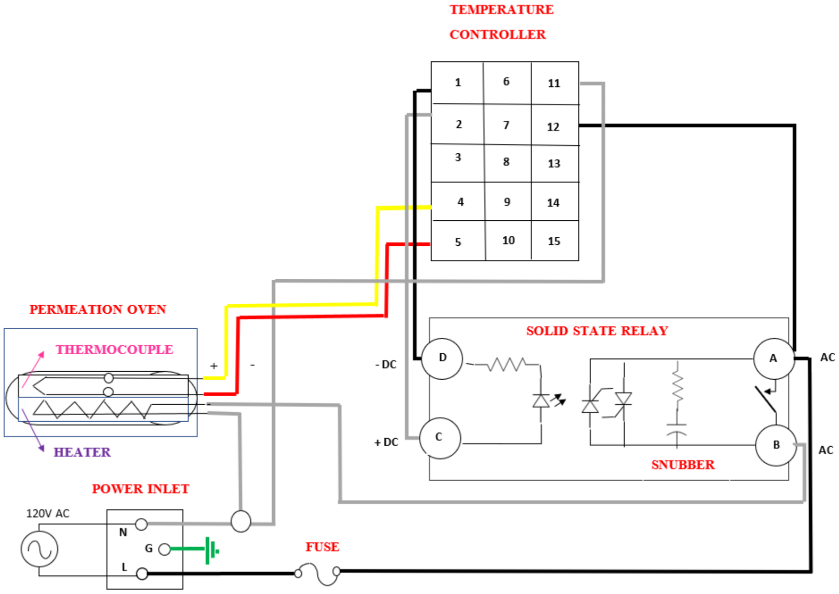

Figure S4. Schematic of the wiring and connections of the custom-built permeation oven. The power supply is distributed from the power inlet into the system through different wires consisting of live wires (black), neutral wires (grey) and a ground wire (green). The temperature controller receives signals by inputs 4 and 5 (yellow and red) connected to the thermocouple. To control the function of the heater, the temperature controller sends a signal from output 1 and 2 to input C and D of the solid-state relay to reach the temperature setpoint.

S2. Rationale and construction of custom permeation devices (PDs)

The purpose of a permeation oven is to obtain a consistent quantity of gaseous analyte via a constant permeation rate, which results in a known mass per unit time delivered to an experimental system or an analytical instrument for calibration purposes. A permeation oven is typically coated or made with inert material to limit surface interactions experienced by the generated gas. The calibration gas permeates by diffusion through the porous polymer according to Fick's second law of diffusion (E1, $m^2 s^{-1}$). If the analyte is in an aqueous solution it is emitted into the oven as a vapor based on its effective Henry's Law constant, which is the product of its acid dissociation constant and volatility (E2, Pa mol m^{-3}; R4) (Mitchell, 2000; Scaringelli et al., 1970). The product of these two properties combine into the overall permeability term (P, Pa mol m^{-1} s^{-1}; E3).

$$D = D_0 e^{-\frac{\Delta E_D}{RT}} \tag{E1}$$

$$S = S_0 e^{-\frac{\Delta H_S}{RT}} \tag{E2}$$

$$P = D \cdot S \tag{E3}$$

$$NO_2^-{}_{(aq)} + H^+_{(aq)} \rightleftharpoons HONO_{(aq)} \rightleftharpoons HONO_{(g)} \tag{R4}$$

Where, S_0, and D_0 are pre-exponential constants of solubility and diffusion. In Equations 1 and 2: E_D is the activation energy for diffusion (J mol^{-1}) and H_S is the enthalpy of solvation (J mol^{-1}), while T is temperature (K) and R is the ideal gas constant (J mol^{-1} K^{-1}). The permeation rate depends on temperature because both diffusion and vapour pressure are exponentially temperature dependent. Therefore, permeation ovens can provide a stable and pure emission rate that can be tuned by adjusting the temperature of the oven.

Clean air moves through the ½" PFA oven tubes, where the vapour emissions from PDs are accumulated, to carry them into the reaction devices, a scrubbing solution, or other instrumentation. High precision of a permeation rate can be obtained by regulating and maintaining constant temperature within ± 0.1 ºC because an increase of 1 ºC of operating temperature results in a 10 % change in sample permeation rate (Lucero, 1971). Adequate precision of our custom-built permeation oven was achieved by choosing the temperature controller, heater, and thermocouple with very strict tolerances. Long-term stability of the system can be ascertained from ion chromatography or real-time measurements (see main manuscript). Also, calibrating the permeation rate of a custom-PD can easily indicate the precision and stability of this custom-built permeation oven.

To construct a custom-PD, a length ¼" PFA tube is filled with analyte solution and the ends are plugged. One end of the tubing is initially made malleable with a heat-gun. Once the tube is sufficiently pliable, a rod of porous PTFE (0.125" diameter, P/N: 84935K64; McMaster-Carr) is carefully inserted with a twisting motion and cut to keep the tubing and rod flush. To ensure an effective seal the two materials are heated further, then compressed and rolled on a flat surface. The open-end of the PD is then filled with analyte solution until it is approximately ½" from the top. The PTFE plugging process is repeated to close the tube. Extra caution during this step should be taken to avoid having the solution boil over or undergoing spontaneous ignition during heating. It is worth noting that the length and quality of the seal around the porous PTFE rod can change the emission rate, where a longer plug may yield a more reliable emission rate. Generally, plugs one centimeter in length were used in this work. If the plug length is too short leakages may arise, resulting in rapid and unstable emission of the contained solution. An alternative that avoids PTFE plugs and associated leaks is to weld the tubing ends. This can be accomplished by heating the end of the tubing with a heat-gun until it is malleable, followed by pinching it with a pair of pliers to create the weld.

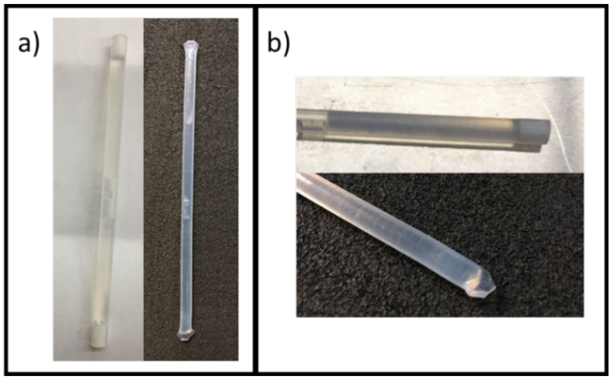

Figure S5. a) Two PDs containing analyte solution fully sealed using the porous PTFE rod (left) and PFA weld (right) techniques. b) Close-up perspective of finished PD ends after sealing by the methods of PTFE rod (top) and PFA weld (bottom).

S3. Additional Supporting Figures and Tables

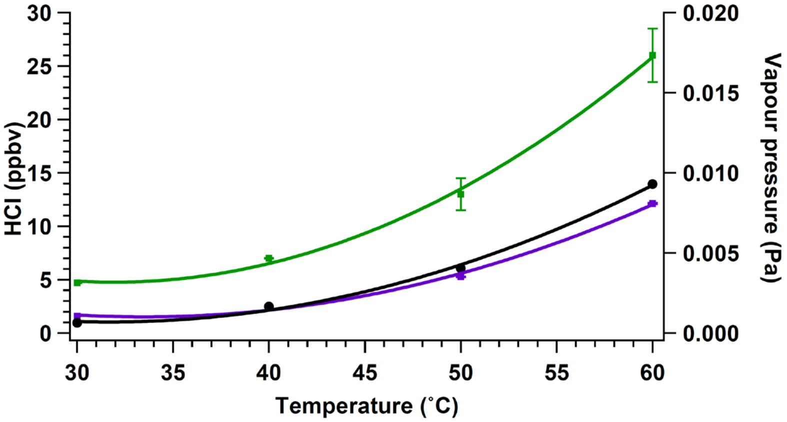

Figure S6. Mixing ratio output of two 6 M HCl PDs as a function of temperature (PD-6b, blue; PD-6c, green). Calculated vapour pressure of 6 M HCl (black) solution using Henry's Law (Sander, 2015). Mean HCl mixing ratios measured for 30 minutes after stable signal was observed by CRDS (1-minute average, see Fig. S7). Error bars denote 1σ standard deviation from the mean.

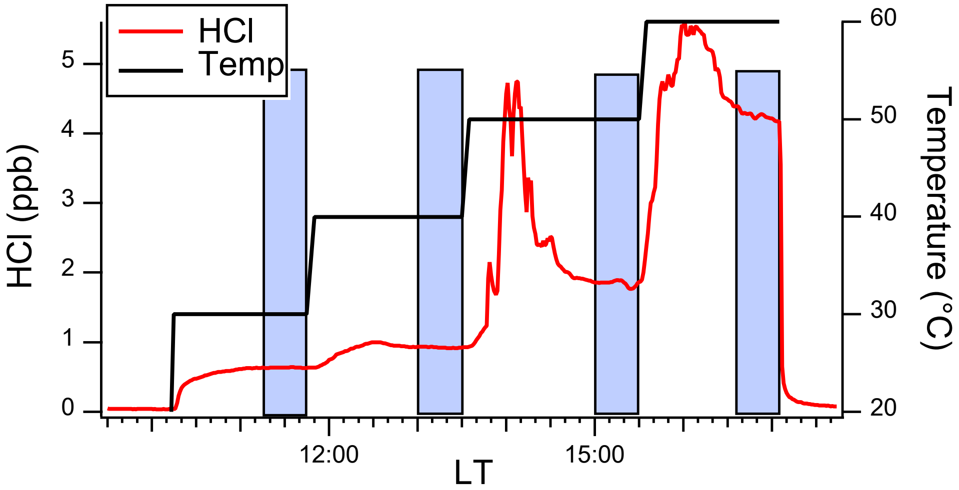

Figure S7: Time series of the measured HCl output from PD-6b using CRDS**, as well as temperature of the oven**. The blue-shaded bars indicate the region where HCl output was considered stable and this data was used to calculate the variance shown in Figure S6.

Table S1. The calculated average HONO (ppbv) output (AVG), standard deviation (SD), and standard error (SE) following the field transport simulations using HCl PD-6a and the same $NaNO_2$ coated device throughout all experiments. The AVG, RSD, and RSE were all calculated from data points collected after two hours of stabilization in each trial run. All experiments were background corrected by linear interpolation using zero air and five experiments had insertions of Na_2CO_3 denuder for further identification of NO_x impurities (*). The NO_x analyzer collected one-minute measurements using a 30 s Kalman filter.

ID	Description of Field Transport Simulation	AVG (ppbv)	SD (ppbv)	SE (ppbv)	Data Points	RSD (%)	RSE (%)
FS1*	Minor shaking for 10 min with the oven off and PD removed overnight	2.51	0.548	0.0537	112	26.6	2.13
FS2*	Transport by cart over rough surfaces for 10 min with the oven off and PD removed overnight	1.81	0.469	0.0342	188	25.9	1.89
FS3*	Transport by cart over rough surfaces for 10 min with the oven off and PD removed overnight	1.68	0.469	0.0308	231	27.8	1.83
FS4*	Minor shaking of stationary setup for 10 min with the oven off and PD removed overnight	2.43	0.447	0.0257	301	18.4	1.06
FS5*	Minor shaking of stationary setup for 10 min with the oven off and PD removed overnight	2.13	0.429	0.0270	253	20.1	1.27

FS6	Oven turned off overnight and Pd kept inside permeation oven	2.04	0.417	0.0240	300	20.5	1.18
FS7	Oven turned off and PD removed overnight	1.73	0.467	0.0340	189	27.0	1.97
FS8	Oven turned off and PD removed overnight	2.21	0.604	0.0454	177	27.3	2.05

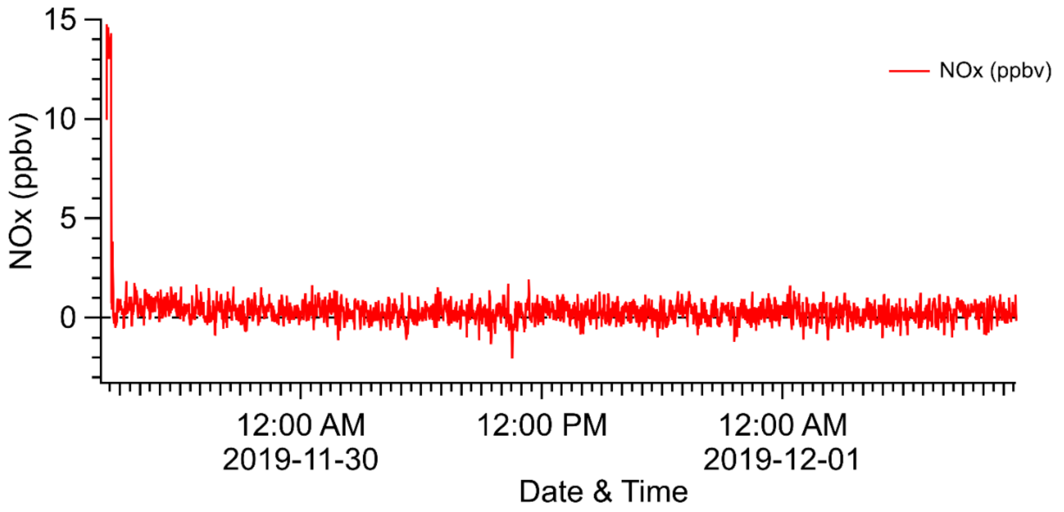

Figure S8. An example of the suitability of nitrogen gas sampled by the NO_x analyzer used for background measurement and subsequent correction of observations.

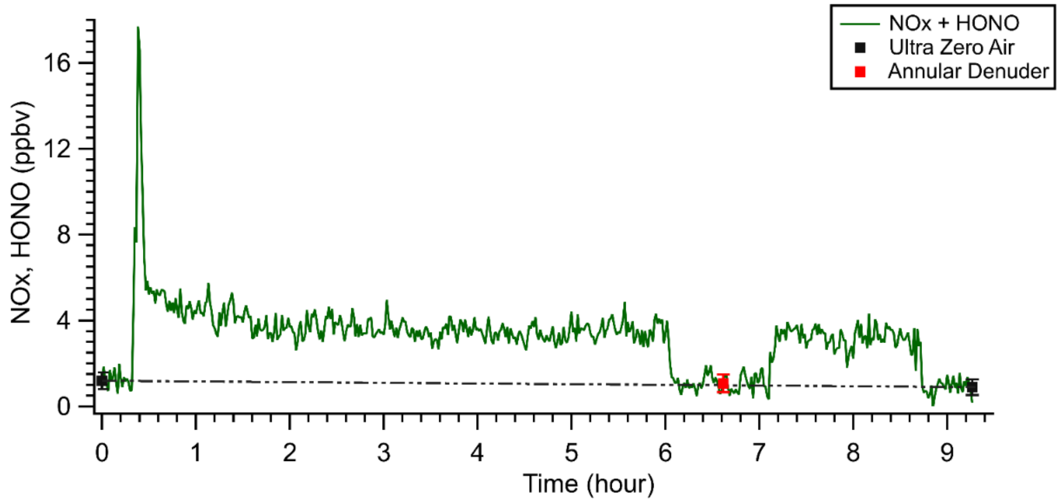

Figure S9. Run FS4 of Table S1 to demonstrate that measured signal from zero air (black square) and HONO passing through the Na_2CO_3 annular denuder (red square) are identical and therefore free of detectable NO_x. These negative controls were combined to create a linearly interpolated background correction over the course of experiments FS1-5 to quantify HONO.

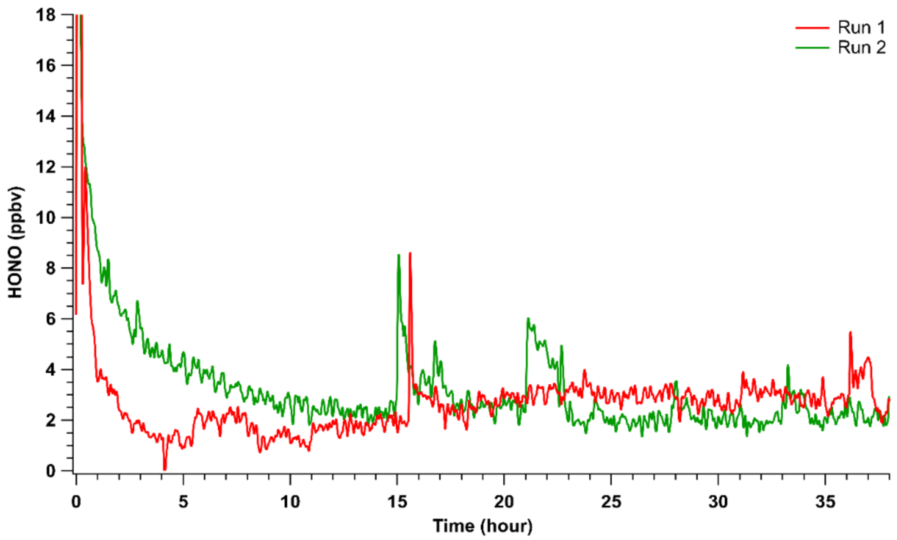

Figure S10. Reproducibility in generating HONO using PD-6b and the same $NaNO_2$ coated device. The red line represents the first trial of using PD-6b followed by a second trial (green) 15 days later. In the intervening time other experiments were performed which involved shutting down and restarting the system with these components. The lag in the second trial results from keeping the PD in the oven while shut down between experiments, resulting in additional HCl that must be reacted in the calibration system before stability is reached. The NO_x analyzer mad one-minute measurements using a Kalman filter of 300 s.

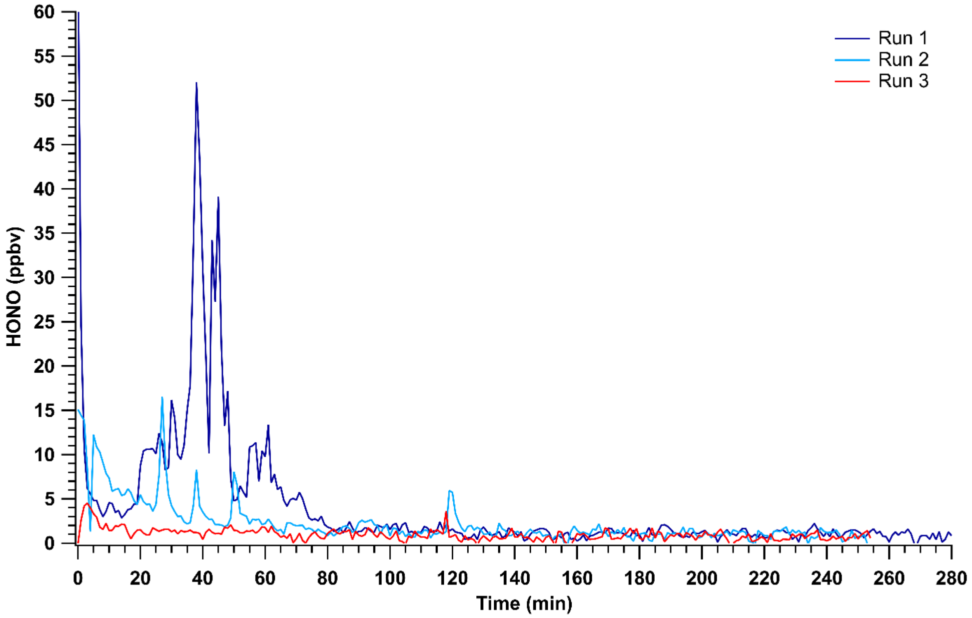

Figure S11. Determining reproducibility in generating HONO (ppbv) against time (min) using PD-1a with a used $NaNO_2$ PFA device.

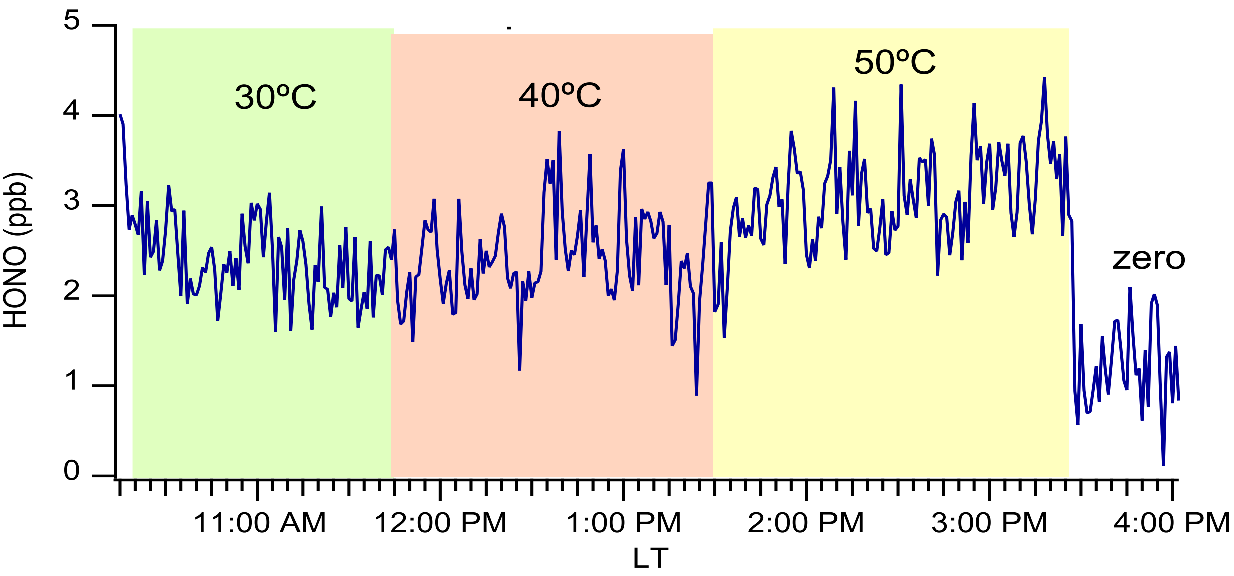

Figure S12. Time series of measured HONO output (ppb) for three different temperatures using HCl PD-6b.

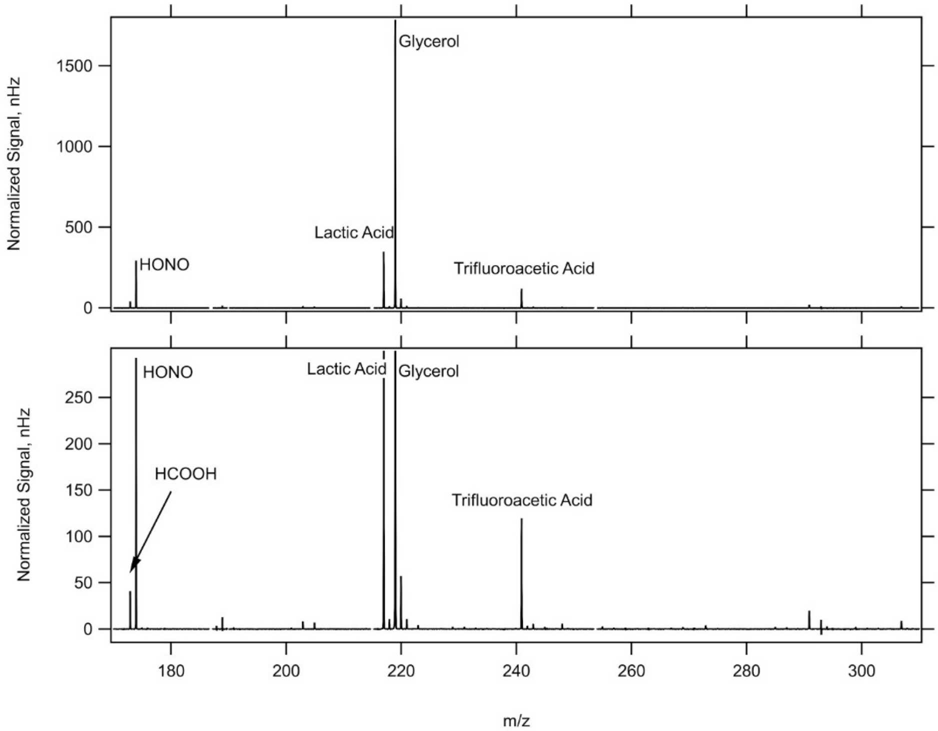

Figure S13. Ion scan of the HONO calibration source output made with the I$^-$-CIMS. Major ions observed in addition to HONO include glycerol from the coating solution, and lactic acid from skin contact with system components. Smaller quantities of formic and trifluoroacetic acids from the plastics used in the instrument assembly were also observed.

References

Lucero, D. P.: Performance Characteristics of Permeation Tubes, Anal. Chem., 43(13), 1744–1749, doi:10.1021/ac60307a005, 1971.

Mitchell, G. D.: A review of permeation tubes and permeators, Sep. Purif. Methods, 29(1), 119–128, doi:10.1081/SPM-100100005, 2000.

Sander, R.: Compilation of Henry's law constants (version 4.0) for water as solvent, Atmos. Chem. Phys., 15(8), 4399–4981, doi:10.5194/acp-15-4399-2015, 2015.

Scaringelli, F. P., O'Keeffe, A. E., Rosenberg, E. and Bell, J. P.: Preparation of Known Concentrations of Gases and Vapors with Permeation Devices Calibrated Gravimetrically, Anal. Chem., 42(8), 871–876, doi:10.1021/ac60290a012, 1970.